JAERI-M
89-214

NEANDC(J)-144/U
INDC(JPN)-131/L

MEASUREMENT OF DOUBLE DIFFERENTIAL NEUTRON EMISSION CROSS SECTIONS AT 14.1 MEV FOR Ca, Mn, Co and W

December 1989

Akito TAKAHASHI*, Yasuhiro SASAKI*
Fujio MAEKAWA* and Hisashi SUGIMOTO*

日本原子力研究所
Japan Atomic Energy Research Institute

JAERI-Mレポートは，日本原子力研究所が不定期に公刊している研究報告書です。
入手の問合わせは，日本原子力研究所技術情報部情報資料課（〒319-11茨城県那珂郡東海村）あて，お申しこしください。なお，このほかに財団法人原子力弘済会資料センター（〒319-11 茨城県那珂郡東海村日本原子力研究所内）で複写による実費頒布をおこなっております。

JAERI-M reports are issued irregularly.
Inquiries about availability of the reports should be addressed to Information Division Department of Technical Information, Japan Atomic Energy Research Institute, Tokai-mura, Naka-gun, Ibaraki-ken 319-11, Japan.

編集兼発行　日本原子力研究所
印　　刷　いばらき印刷㈱

JAERI-M 89-214

Measurement of Double Differential Neutron Emission Cross Sections at 14.1 MeV for Ca, Mn, Co and W

Akito TAKAHASHI*, Yasuhiro SASAKI*, Fujio MAEKAWA*
and Hisashi SUGIMOTO*

Department of Physics
Tokai Research Establishment
Japan Atomic Energy Research Institute
Tokai-mura, Naka-gun, Ibaraki-ken

(Received November 28, 1989)

Using the neutron TOF spectrometer at OKTAVIAN, double differential neutron emission cross sections at 14.1 MeV were measured for Ca, Mn, Co and W which are of interest for shielding and structural material elements of fusion reactors. Data were obtained for 16 angle points from 15 to 160 deg in the LAB system for each element, covering the secondary neutron energy region from 0.5 MeV to 15 MeV. Statistics and energy resolution of obtained data are satisfactory.

The double differential cross sections in the LAB system were once converted to those in the center-of-mass system and integrated over scattering angle to obtain neutron emission spectra. Angle-differential cross sections were obtained for the elastic and discrete-inelastic scatterings whose peaks in DDX spectra could be resolved. The measured DDX data are so numerous that only their graphs are shown in this report. However, the graphs and numerical tables are given for the neutron emission spectra and the angle-differential cross sections.

In the graphs, preliminary comparisons are made with evaluated data (ENDF/B-IV and JENDL-3T). The ENDF/B-IV data for Ca are satisfactory in the high energy region, but overestimate the experimental values in the

---

This report is written by summarizing the study implemented under the Research-in-Trust in 1988 fiscal year from the Japan Atomic Energy Research Institute

* Osaka University

low energy region. The JENDL-3T data for Mn reproduce well the angle-integrated neutron emission spectrum, though underestimation is seen in the 6-13 MeV region. It is noted that ENDF/B-IV underestimates the emission spectrum of Co in the 3-13 MeV region. The ENDF/B-IV data for W do not agree at all with the experimental spectral patterns.

Keywords: Double Differential Neutron Emission Cross Section, 14.1 MeV, TOF Experiment, Ca, Mn, Co, W, JENDL-3T, ENDF/B-IV

Ca，Mn，Co，Wの14.1 MeVにおける中性子放出二重微分断面積の測定

日本原子力研究所東海研究所物理部
高橋　亮人*・佐々木泰裕*・前川　藤夫*・杉本　久司*

（1989年11月28日受理）

中性子遮蔽材及び炉構造材元素として重要なCa，Mn，Co，Wについて，14 MeV中性子入射に対する中性子放出二重微分断面積が阪大オクタビアンのTOF分析装置を用いて測定された。散乱角度は15°から160°にわたり16点である。二次中性子エネルギー範囲は0.5 MeVから15 MeVである。統計精度・エネルギー分解能ともに良好なデータを得られた。

得られた二重微分断面積を重心系に直し，角度積分して中性子放出スペクトルデータが導出された。

二重微分断面積のエネルギースペクトルで，ピークとして分離することができた弾性散乱と離散非弾性散乱については，角度微分断面積が導出された。二重微分断面積は大量のデータとなったので，本報ではグラフのみを与えている。放出スペクトルと角度微分断面積については，グラフと数値表を与えている。

評価核データ（ENDF／B－Ⅳ，JENDL－3T）との予備的比較が行なわれた。その結果，Caについては，低エネルギーではENDF／B－Ⅳの過大評価がみられるが，高エネルギー側では実験を良く再現している。Mnについては，JENDL－3Tは放出スペクトルをかなり良く再現しているが6～13 MeV領域で少し過小評価となっている。Coについては，ENDF／B－Ⅳは3～13 MeVで放出スペクトルを大きく過小評価している。Wについては，ENDF／B－Ⅳのデータは実験とスペクトルパターンが全く一致しない。

本報告書は日本原子力研究所から昭和63年度委託研究で行われた成果をまとめたものである。
東海研究所：〒319－11　茨城県那珂郡東海村白方字白根2－4
＊　大阪大学

Contents

目　　次

1. Introduction

Double differential neutron emission cross sections (DDX) are of importance in fusion applications, namely not only for the neutronics calculations of blankets and shields but also for the calculational estimations of primary knock-on atom spectra and kerma factors. Neutron-induced nuclear reactions with incident energy around 14 MeV generally show the competing process between the direct, the precompound and the compound processes which reflected in the energy spectral shapes of DDX or emission spectrum. The DDX data have been therefore utilized also to the assessment of nuclear model codes for evaluation works.

In this report, measurements and results are described for Ca, Mn, Co and W. The DDX data of Ca are required as fundamental nuclear data for shielding designs using ordinary or low-activation (lime-stone) concrete, due to scarce experimental data. Tungsten is a candidate of the ITER inboard shield, whose available neutron data have large uncertainties and therefore new experimental data are strongly required. The DDX data of medium-heavy nuclei (Mn and Co) are of particular interest to assessing "standard" nuclear model codes. The data of angle-integrated neutron emission spectra and angle differential cross sections which can be obtained from the DDX data are also useful for the evaluation or code-assessing tasks. Therefore, measurements were carried out for a wide range of scattering angles (15-160 deg). Preliminary comparisons are made with a few evaluated nuclear data, e. g., ENDF/B-IV[1] and JENDL-3T[2].

2. Experiment

The details of our experimental method are described elsewhere[3,4]. A brief explanation is as follows: The pulsed D-T neutron source of OKTAVIAN[3] is used with 2 ns pulse width and 1 MHz repetition frequency. A neutron TOF spectrometer has an 8.3 m long collimated flight path fixed in the 85 deg direction against the OKTAVIAN beam line. A 10 inch diam. × 10 cm thick NE213 detector is used as a main neutron detector with two (low- and high-gain) parallel pulse shape discrimination circuits. A scattering sample is set at 17 cm from the center of a TiT target (2 cm diam.) and moved along the 17 cm R arc when we change the

1. Introduction

Double differential neutron emission cross sections (DDX) are of importance in fusion applications, namely not only for the neutronics calculations of blankets and shields but also for the calculational estimations of primary knock-on atom spectra and kerma factors. Neutron-induced nuclear reactions with incident energy around 14 MeV generally show the competing process between the direct, the precompound and the compound processes which reflected in the energy spectral shapes of DDX or emission spectrum. The DDX data have been therefore utilized also to the assessment of nuclear model codes for evaluation works.

In this report, measurements and results are described for Ca, Mn, Co and W. The DDX data of Ca are required as fundamental nuclear data for shielding designs using ordinary or low-activation (lime-stone) concrete, due to scarce experimental data. Tungsten is a candidate of the ITER inboard shield, whose available neutron data have large uncertainties and therefore new experimental data are strongly required. The DDX data of medium-heavy nuclei (Mn and Co) are of particular interest to assessing "standard" nuclear model codes. The data of angle-integrated neutron emission spectra and angle differential cross sections which can be obtained from the DDX data are also useful for the evaluation or code-assessing tasks. Therefore, measurements were carried out for a wide range of scattering angles (15-160 deg). Preliminary comparisons are made with a few evaluated nuclear data, e. g., ENDF/B-IV[1] and JENDL-3T[2].

2. Experiment

The details of our experimental method are described elsewhere[3,4]. A brief explanation is as follows: The pulsed D-T neutron source of OKTAVIAN[3] is used with 2 ns pulse width and 1 MHz repetition frequency. A neutron TOF spectrometer has an 8.3 m long collimated flight path fixed in the 85 deg direction against the OKTAVIAN beam line. A 10 inch diam. × 10 cm thick NE213 detector is used as a main neutron detector with two (low- and high-gain) parallel pulse shape discrimination circuits. A scattering sample is set at 17 cm from the center of a TiT target (2 cm diam.) and moved along the 17 cm R arc when we change the

scattering angle. Incident neutron energy is 14.1 ± 0.2 MeV, which was determined by observing the peak-energies of the elastic scatterings of many elements.

Cylindrical metallic rods are used for the scattering samples. Seven pellets of calcium metal (3 cm diam. × 1 cm thick) are packed with aluminum cooking foil to form the cylindrical sample (7 cm long). The effect of the aluminum foil has been proved to be ignored by background runs with and without the empty aluminum foil at sample position. The sizes of the Mn and W samples are 3 cm diam. × 7 cm long. For Co, a 2.5 cm diam. × 7 cm long metallic cylinder is used.

The calibration of the DDX values is made in usual way; the scattered neutron peaks of H(n, n) reaction are measured with a 1.5 cm diam. × 5 cm long polyethylene sample at the 7 angles (20-50 deg in LAB angle) and peak-area at each angle is normalized to be equal to the corresponding differential cross section of hydrogen.

Data processing procedure is described elsewhere[4] in detail. For multiple scattering correction[5], the DDX data calculated from evaluated nuclear data were used; ENDF/B-IV for Ca, Co and W, and JENDL-3T for Mn. Since the correction is considerably dependent on the spectral shapes of the used nuclear data, we will have to reprocess the Co DDX data using improved data (JENDL-3 final version) when more accurate data are required. For W, the neutron emission spectra by ENDF/B-IV are so different from the measured ones that we can not make correction and have to show the uncorrected data in this report: we may estimate the correction for W to be within 10-15 %.

3. Results

3.1 DDX

Results for Ca are shown in Fig. 1 through Fig. 15. In a spectrum at each angle, we can resolve six discrete inelastic scattering peaks (3.736-3.904 MeV sum peak, 4.492 MeV peak, 6.285 MeV peak, 6.510-7.536 MeV sum peak, 7.760-8.540 MeV sum peak and 9.6 MeV peak) and an elastic scattering peak (the most right-hand peak). Significant angular dependence is seen down to low emission energy where ENDF/B-IV overestimates the measured DDX. In the energy region higher than about 5 MeV, the

scattering angle. Incident neutron energy is 14.1 ± 0.2 MeV, which was determined by observing the peak-energies of the elastic scatterings of many elements.

Cylindrical metallic rods are used for the scattering samples. Seven pellets of calcium metal (3 cm diam. × 1 cm thick) are packed with aluminum cooking foil to form the cylindrical sample (7 cm long). The effect of the aluminum foil has been proved to be ignored by background runs with and without the empty aluminum foil at sample position. The sizes of the Mn and W samples are 3 cm diam. × 7 cm long. For Co, a 2.5 cm diam. × 7 cm long metallic cylinder is used.

The calibration of the DDX values is made in usual way; the scattered neutron peaks of H(n, n) reaction are measured with a 1.5 cm diam. × 5 cm long polyethylene sample at the 7 angles (20-50 deg in LAB angle) and peak-area at each angle is normalized to be equal to the corresponding differential cross section of hydrogen.

Data processing procedure is described elsewhere[4] in detail. For multiple scattering correction[5], the DDX data calculated from evaluated nuclear data were used; ENDF/B-IV for Ca, Co and W, and JENDL-3T for Mn. Since the correction is considerably dependent on the spectral shapes of the used nuclear data, we will have to reprocess the Co DDX data using improved data (JENDL-3 final version) when more accurate data are required. For W, the neutron emission spectra by ENDF/B-IV are so different from the measured ones that we can not make correction and have to show the uncorrected data in this report: we may estimate the correction for W to be within 10-15 %.

3. Results

3.1 DDX

Results for Ca are shown in Fig. 1 through Fig. 15. In a spectrum at each angle, we can resolve six discrete inelastic scattering peaks (3.736-3.904 MeV sum peak, 4.492 MeV peak, 6.285 MeV peak, 6.510-7.536 MeV sum peak, 7.760-8.540 MeV sum peak and 9.6 MeV peak) and an elastic scattering peak (the most right-hand peak). Significant angular dependence is seen down to low emission energy where ENDF/B-IV overestimates the measured DDX. In the energy region higher than about 5 MeV, the

ENDF/B-IV data reproduce the measured spectral patterns though delicate differences are seen.

Results for Mn are shown in Fig. 16 through Fig. 31 compared with JENDL-3T. Three peaks of the discrete inelastic scatterings (0.984, 2.822, and 4.41 MeV levels) and the elastic scattering peak could be resolved.

Results for Co are shown in Fig. 32 through Fig. 47 compared with ENDF/B-IV. We can see the resolved peaks of the elastic scattering and of the two discrete inelastic scatterings (1.099 and 4.086 MeV levels).

Results for W are shown in Fig. 48 through Fig. 63 compared with ENDF/B-IV. Except for the elastic scattering peak, no distinct peaks of the inelastic scatterings are seen at any angle though delicate structures are observed in the 9-13 MeV region.

3.2 Angle-Integrated neutron emission spectra (EDX)

Results for Ca are shown in Fig. 64 and Fig. 65 for the LAB and the CM system, and numerical values for the CM system are given in Table 1(1).

Results for Mn are shown in Fig. 66 and Fig. 67. Numerical values are given in Table 1(2).

Results for Co are shown in Fig. 68 and Fig. 69. Numerical values are given in Table 1(3).

Results for W are shown in Fig. 70 and Fig. 71. Numerical values are given in Table 1(4).

3.3 Angle-differential cross sections (SDX)

Results for Ca are shown in Figs. 72, 73, 74 and 75, together with fitted curves using Legendre polynomials and evaluated curves of ENDF/B-IV. Numerical values are given in Table 2(1) and 2(2).

Results for Mn are shown in Figs. 76, 77 and 78. Fitting with the Legendre polynomials and the JENDL-3T curves are also shown. Numerical values are given in Table 2(3).

Results for Co are shown in Figs. 79 and 80. Numerical values are given in Table 2(4).

Results for W are shown in Figs. 81 and 82, for the elastic scattering, the inelastic continuum (integration of DDX within the 5.5-11

MeV region) and the (n, 2n) neutron emissions. For the (n, 2n) reaction, the DDX values are integrated within the 0-5.5 MeV region. Numerical values are given in Table 2(5).

4. Discussion

4.1 Calcium

As shown in Fig. 1 through Fig. 15, the calculated curves of ENDF/B-IV reproduce the measured DDX curves as a whole. Speaking the local agreements, ENDF/B-IV underestimates the measured values in the 4-11 MeV at forward angles (15-50 deg). Below 3 MeV the measured data show the forward enhancement of the neutron emission while the ENDF/B-IV data give isotropic angular distribution and therefore overestimate the experimental values at the angles greater than 60 deg.

Looking at the angle-integrated neutron emission spectrum in the CM system shown in Fig. 65, the ENDF/B-IV data reproduce very well the measured values in the energy region above 4 MeV while significant (by 30-50 %) overestimation is seen below 4 MeV.

As for the single differential cross sections of the elastic scattering shown in Fig. 72, ENDF/B-IV overestimates 2 times the experimental values at the backward angles (110-150 deg), though the angular distribution resembles one another. For the resolved discrete inelastic scatterings shown in Figs. 73 through 75, the underestimation of ENDF/B-IV is pointed out at the forward angles for the 3.736-3.904 and 4.492 MeV levels.

4.2 Manganese

DDX: As shown in Fig. 16 through 31, the calculated DDXs by JENDL-3T reproduce the overall spectral shapes of the experimental ones but the significant underestimations at the forward angles (15-80 deg) should be pointed out. At the backward angles (90-160 deg), very good agreement is seen except for the elastic scattering peaks at the backward angles (100-160 deg). The angular distribution of the pre-equilibrium neutron emission shall be taken into account to fill the large differences at the forward angles.

MeV region) and the (n, 2n) neutron emissions. For the (n, 2n) reaction, the DDX values are integrated within the 0-5.5 MeV region. Numerical values are given in Table 2(5).

4. Discussion

4.1 Calcium

As shown in Fig. 1 through Fig. 15, the calculated curves of ENDF/B-IV reproduce the measured DDX curves as a whole. Speaking the local agreements, ENDF/B-IV underestimates the measured values in the 4-11 MeV at forward angles (15-50 deg). Below 3 MeV the measured data show the forward enhancement of the neutron emission while the ENDF/B-IV data give isotropic angular distribution and therefore overestimate the experimental values at the angles greater than 60 deg.

Looking at the angle-integrated neutron emission spectrum in the CM system shown in Fig. 65, the ENDF/B-IV data reproduce very well the measured values in the energy region above 4 MeV while significant (by 30-50 %) overestimation is seen below 4 MeV.

As for the single differential cross sections of the elastic scattering shown in Fig. 72, ENDF/B-IV overestimates 2 times the experimental values at the backward angles (110-150 deg), though the angular distribution resembles one another. For the resolved discrete inelastic scatterings shown in Figs. 73 through 75, the underestimation of ENDF/B-IV is pointed out at the forward angles for the 3.736-3.904 and 4.492 MeV levels.

4.2 Manganese

DDX: As shown in Fig. 16 through 31, the calculated DDXs by JENDL-3T reproduce the overall spectral shapes of the experimental ones but the significant underestimations at the forward angles (15-80 deg) should be pointed out. At the backward angles (90-160 deg), very good agreement is seen except for the elastic scattering peaks at the backward angles (100-160 deg). The angular distribution of the pre-equilibrium neutron emission shall be taken into account to fill the large differences at the forward angles.

Seeing the angle-integrated neutron emission spectrum shown in Fig. 67, we can say that the underestimation of JENDL-3T is obvious in the 6-13 MeV region. We see a distinct peak around 9.5 MeV of the measured spectrum, which is attributed to the excitation of one phonon state of octapole vibration (excitation energy 4.41 MeV). A hump at 6-7 MeV may be due to the excitation of the low energy octapole vibration (two phonon state). A shoulder at 11.5 MeV can correspond to the 1.884 MeV level excitation.

For the differential elastic scattering cross sections shown in Fig. 76, the considerable underestimation of JENDL-3T is seen at the forward angles (15-30 deg) while overestimating about twice at the backward angles (100-160 deg). For the 0.984 MeV level excitation, fairly good agreement is seen as shown in Fig. 77 as far as the angle-dependence is concerned. As shown in Fig. 78, the JENDL-3T cross sections for the 2.822 MeV level should be doubled though their shapes of angular distribution curve agree with the measured one. Since the cross section of 4.41 MeV level seems to be large, it is recommended to include this level into the evaluations.

4.3 Cobalt

As shown in Fig. 32 through Fig. 47, the measured spectral shapes and the angular distribution of DDX are very different from those of ENDF/B-IV; especially in the 3-13 MeV region and at the forward angles, the used nuclear models seem to have problems, i. e., the direct collective excitation of the inelastic scattering and the preequilibrium neutron emission are not taken into account or are treated uncorrectly.

The results of the angle-integrated emission spectrum shown in Fig. 69 lead us to a similar conclusion.

The differential cross sections of the elastic scattering are shown in Fig. 79. At the backward angles (70-160 deg), ENDF/B-IV is 2-3 times larger than the experimental values. Overestimation over the whole angle and the difference of the distribution shape may suggest us the necessity of the reestimation of optical parameters. No comparisons with the evaluated curves are made for the 1.099 and 4.086 MeV levels, and the analyses with DWUCK4 are desirable.

4.4 Tungsten

Obviously the drastic underestimation of ENDF/B-IV in the 5-13 MeV region shows the ignorance of the direct and preequilibrium neutron emissions. Basically we can apply the EGNASH[6] + DWUCK4[7] analysis for the evaluation tasks. However, the measured DDX spectra in the 5-13 MeV region show us the existence of so many discrete levels of the direct excitations. Natural tungsten contains 5 isotopes, so that the energy spectrum may be monotonous in this region. In the case of Ta[8] which is mono-isotopic, we have observed the quite similar monotonous spectra of DDX in the corresponding energy region. Therefore we can speculate that the many direct excitations with similar magnitudes are possible for these heavy mass elements (from Ta to W). This situation requires us laborious calculations of the direct process neutron emissions.

The differential cross sections of the elastic scattering are shown in Fig. 81 compared with ENDF/B-IV. The measured data are larger on an average than those of ENDF/B-IV at the backward angles (90-160 deg). As shown in Fig. 82, a slight forward-enhancement of (n, 2n) neutrons is seen and the integrated (n, 2n) cross section of the experiment is about 15 % smaller than that of ENDF/B-IV.

Acknowledgment

The authors appreciate the operation crew of OKTAVIAN. The appreciation is also due to the continuous support of this work by Dr. S. Igarasi, Dr. T. Asami and Dr. Y. Kikuchi of JAERI Nuclear Data Center.

4.4 Tungsten

Obviously the drastic underestimation of ENDF/B-IV in the 5-13 MeV region shows the ignorance of the direct and preequilibrium neutron emissions. Basically we can apply the EGNASH[6] + DWUCK4[7] analysis for the evaluation tasks. However, the measured DDX spectra in the 5-13 MeV region show us the existence of so many discrete levels of the direct excitations. Natural tungsten contains 5 isotopes, so that the energy spectrum may be monotonous in this region. In the case of Ta[8] which is mono-isotopic, we have observed the quite similar monotonous spectra of DDX in the corresponding energy region. Therefore we can speculate that the many direct excitations with similar magnitudes are possible for these heavy mass elements (from Ta to W). This situation requires us laborious calculations of the direct process neutron emissions.

The differential cross sections of the elastic scattering are shown in Fig. 81 compared with ENDF/B-IV. The measured data are larger on an average than those of ENDF/B-IV at the backward angles (90-160 deg). As shown in Fig. 82, a slight forward-enhancement of (n, 2n) neutrons is seen and the integrated (n, 2n) cross section of the experiment is about 15 % smaller than that of ENDF/B-IV.

Acknowledgment

The authors appreciate the operation crew of OKTAVIAN. The appreciation is also due to the continuous support of this work by Dr. S. Igarasi, Dr. T. Asami and Dr. Y. Kikuchi of JAERI Nuclear Data Center.

References

1) ENDF/B Summary Documentation, BNL-NCS-17541 (1975)
2) JENDL compilation Group (Nuclear Data Center, JAERI): JENDL-3T, private communication (1987)
3) Takahashi, A., et al.: J. Nucl. Sci. Technol., 25, 215 (1988)
4) Takahashi, A., et al.: JAERI-M 88-102 (1988)
5) Ichimura, E., Takahashi, A.: OKTAVIAN Rep. A-87-02, Osaka Univ., (1987)
6) Yamamuro, N.,: Proc. Nucl. Data Sci. Tech., 1988, Mito, pp.489 SAIKON Publ., (1988)
7) Kunz, P.O.: "Distorted Wave Code DWUCK4", Univ. Colorado (1974)
8) Takahashi, A., et al.: INDC(JPN) 118L (1989)

Table 1(1) Angle-integrated neutron emission spectrum in the CM system with En = 14.1 MeV, for Ca

```
SUBENTRY        00021003      880201                                    00021003     1
BIB                    2           8                                    00021003     2
COMMENT     TWO DATA SETS ARE GIVEN.                                    00021003     3
            DATA OBTAINED FROM RAW DDX DATA , IN LEFT HAND SIDE.        00021003     4
            DATA OBTAINED FROM CORRECTED DDX DATA WITH MUSCC3 CODE      00021003     5
            IN RIGHT HAND SIDE.                                         00021003     6
REACTION    (20-CA-0(N,SCT),,,DE) SECONDARY NEUTRON SPECTRUM            00021003     7
            IN THE CENTER-OF-MASS SYSTEM                                00021003     8
ENDBIB                 8                                              00021003     9
COMMON                 1           5                                  00021003    10
EN                                                                     00021003    11
MEV                                                                    00021003    12
   14.10000                                                            00021003    13
ENDCOMMON              5                                              00021003    14
DATA                   6          66                                  00021003    15
E-MAX       E-MIN       DATA        DATA-ERR    DATA        DATA-ERR   00021003    16
MEV         MEV         B/MEV       B/MEV       B/MEV       B/MEV      00021003    17
   14.20000    14.00000  9.95E-02    2.98E-03    9.27E-02    2.95E-0300021003    18
   14.00000    13.80000  3.11E-01    3.84E-03    3.01E-01    3.82E-0300021003    19
   13.80000    13.60000  7.14E-01    4.66E-03    7.23E-01    4.71E-0300021003    20
   13.60000    13.40000  1.27E+00    5.27E-03    1.29E+00    5.30E-0300021003    21
   13.40000    13.20000  1.15E+00    4.66E-03    1.16E+00    4.67E-0300021003    22
   13.20000    13.00000  6.07E-01    3.58E-03    6.16E-01    3.56E-0300021003    23
   13.00000    12.80000  2.72E-01    2.70E-03    2.72E-01    2.65E-0300021003    24
   12.80000    12.60000  1.22E-01    2.20E-03    1.22E-01    2.15E-0300021003    25
   12.60000    12.40000  6.19E-02    2.05E-03    6.22E-02    2.00E-0300021003    26
   12.40000    12.20000  3.62E-02    1.93E-03    3.66E-02    1.88E-0300021003    27
   12.20000    12.00000  2.37E-02    1.88E-03    2.40E-02    1.83E-0300021003    28
   12.00000    11.80000  1.57E-02    1.85E-03    1.60E-02    1.79E-0300021003    29
   11.80000    11.60000  1.24E-02    1.78E-03    1.27E-02    1.72E-0300021003    30
   11.60000    11.40000  5.30E-03    1.71E-03    5.46E-03    1.67E-0300021003    31
   11.40000    11.20000  1.96E-03    1.66E-03    2.02E-03    1.62E-0300021003    32
   11.20000    11.00000  1.28E-03    1.61E-03    1.31E-03    1.59E-0300021003    33
   11.00000    10.80000  2.22E-03    1.52E-03    2.24E-03    1.52E-0300021003    34
   10.80000    10.60000  4.43E-03    1.46E-03    4.47E-03    1.46E-0300021003    35
   10.60000    10.40000  9.96E-03    1.42E-03    1.01E-02    1.42E-0300021003    36
   10.40000    10.20000  1.80E-02    1.42E-03    1.82E-02    1.43E-0300021003    37
   10.20000    10.00000  4.09E-02    1.49E-03    4.12E-02    1.50E-0300021003    38
   10.00000     9.80000  8.27E-02    1.65E-03    8.34E-02    1.66E-0300021003    39
    9.80000     9.60000  9.75E-02    1.68E-03    9.80E-02    1.69E-0300021003    40
    9.60000     9.40000  5.65E-02    1.54E-03    5.63E-02    1.53E-0300021003    41
    9.40000     9.20000  3.55E-02    1.45E-03    3.50E-02    1.43E-0300021003    42
    9.20000     9.00000  4.42E-02    1.51E-03    4.01E-02    1.42E-0300021003    43
    9.00000     8.80000  3.94E-02    1.57E-03    2.94E-02    1.27E-0300021003    44
    8.80000     8.60000  2.41E-02    1.55E-03    1.63E-02    1.19E-0300021003    45
    8.60000     8.40000  1.49E-02    1.53E-03    9.96E-03    1.19E-0300021003    46
    8.40000     8.20000  1.60E-02    1.48E-03    1.12E-02    1.23E-0300021003    47
    8.20000     8.00000  2.36E-02    1.51E-03    1.86E-02    1.30E-0300021003    48
    8.00000     7.80000  2.38E-02    1.52E-03    1.84E-02    1.32E-0300021003    49
    7.80000     7.60000  2.12E-02    1.52E-03    1.74E-02    1.37E-0300021003    50
    7.60000     7.40000  2.68E-02    1.54E-03    2.37E-02    1.44E-0300021003    51
    7.40000     7.20000  3.30E-02    1.57E-03    3.01E-02    1.48E-0300021003    52
    7.20000     7.00000  3.21E-02    1.59E-03    2.97E-02    1.49E-0300021003    53
    7.00000     6.80000  4.01E-02    1.64E-03    3.62E-02    1.48E-0300021003    54
    6.80000     6.60000  5.38E-02    1.69E-03    4.74E-02    1.50E-0300021003    55
    6.60000     6.40000  5.00E-02    1.69E-03    4.27E-02    1.45E-0300021003    56
    6.40000     6.20000  3.65E-02    1.66E-03    3.06E-02    1.44E-0300021003    57
    6.20000     6.00000  3.83E-02    1.68E-03    3.37E-02    1.47E-0300021003    58
    6.00000     5.80000  3.97E-02    1.70E-03    3.54E-02    1.51E-0300021003    59
    5.80000     5.60000  3.85E-02    1.70E-03    3.29E-02    1.49E-0300021003    60
    5.60000     5.40000  3.71E-02    1.73E-03    3.29E-02    1.50E-0300021003    61
    5.40000     5.20000  3.96E-02    1.74E-03    3.43E-02    1.47E-0300021003    62
    5.20000     5.00000  3.82E-02    1.74E-03    3.03E-02    1.42E-0300021003    63
    5.00000     4.80000  3.51E-02    1.75E-03    2.59E-02    1.38E-0300021003    64
    4.80000     4.60000  4.08E-02    1.77E-03    3.08E-02    1.39E-0300021003    65
    4.60000     4.40000  4.47E-02    1.76E-03    3.40E-02    1.40E-0300021003    66
    4.40000     4.20000  4.76E-02    1.77E-03    3.73E-02    1.43E-0300021003    67
    4.20000     4.00000  5.09E-02    1.78E-03    3.97E-02    1.44E-0300021003    68
    4.00000     3.80000  5.24E-02    1.77E-03    3.89E-02    1.42E-0300021003    69
    3.80000     3.60000  5.82E-02    1.80E-03    4.36E-02    1.44E-0300021003    70
    3.60000     3.40000  6.10E-02    1.81E-03    4.70E-02    1.47E-0300021003    71
    3.40000     3.20000  6.87E-02    1.85E-03    5.37E-02    1.52E-0300021003    72
    3.20000     3.00000  7.80E-02    1.94E-03    6.29E-02    1.62E-0300021003    73
    3.00000     2.80000  9.41E-02    2.06E-03    7.80E-02    1.73E-0300021003    74
    2.80000     2.60000  1.06E-01    2.20E-03    8.72E-02    1.86E-0300021003    75
    2.60000     2.40000  1.20E-01    2.37E-03    9.43E-02    1.91E-0300021003    76
    2.40000     2.20000  1.52E-01    2.52E-03    1.17E-01    1.97E-0300021003    77
    2.20000     2.00000  1.58E-01    2.71E-03    1.26E-01    2.19E-0300021003    78
    2.00000     1.80000  1.71E-01    2.92E-03    1.43E-01    2.43E-0300021003    79
    1.80000     1.60000  1.79E-01    3.28E-03    1.47E-01    2.70E-0300021003    80
    1.60000     1.40000  1.91E-01    3.92E-03    1.57E-01    3.25E-0300021003    81
    1.40000     1.20000  1.94E-01    5.20E-03    1.61E-01    4.37E-0300021003    82
    1.20000     1.00000  2.43E-01    1.14E-02    1.97E-01    9.39E-0300021003    83
ENDDATA               70                                              00021003    84
ENDSUBENTRY           85                                              00021003999999
ENDENTRY               3                                              00021999999999
```

Table 1(2) Angle-integrated neutron emission spectrum in the CM system with En = 14.1 MeV, for Mn

```
SUBENTRY      00020003     881201                                          00020003     1
BIB                2            8                                        00020003     2
COMMENT       TWO DATA SETS ARE GIVEN.                                    00020003     3
              DATA OBTAINED FROM RAW DDX DATA . IN LEFT HAND SIDE.        00020003     4
              DATA OBTAINED FROM CORRECTED DDX DATA WITH MUSCC3 CODE      00020003     5
              IN RIGHT HAND SIDE.                                         00020003     6
REACTION      (25-MN-55(N,SCT)...DE) SECONDARY NEUTRON SPECTRUM           00020003     7
              IN THE CENTER-OF-MASS SYSTEM                                00020003     8
ENDBIB             8                                                      00020003     9
COMMON             1          5                                           00020003    10
EN                                                                        00020003    11
MEV                                                                       00020003    12
   14.10000                                                               00020003    13
ENDCOMMON          5                                                      00020003    14
DATA               6          68                                          00020003    15
E-MAX         E-MIN         DATA         DATA-ERR     DATA         DATA-ERR 00020003    16
MEV           MEV           B/MEV        B/MEV        B/MEV        B/MEV    00020003    17
   14.60000    14.40000    1.02E-02     6.39E-04     1.23E-02     7.82E-0400020003    18
   14.40000    14.20000    4.75E-02     1.19E-03     0.00E+00     1.36E-0300020003    19
   14.20000    14.00000    2.22E-01     1.98E-03     2.69E-01     2.20E-0300020003    20
   14.00000    13.80000    8.08E-01     2.63E-03     9.91E-01     3.08E-0300020003    21
   13.80000    13.60000    1.59E+00     3.25E-03     1.96E+00     3.91E-0300020003    22
   13.60000    13.40000    1.64E+00     3.18E-03     2.02E+00     3.84E-0300020003    23
   13.40000    13.20000    9.59E-01     2.47E-03     1.17E+00     2.94E-0300020003    24
   13.20000    13.00000    4.12E-01     1.80E-03     4.93E-01     2.08E-0300020003    25
   13.00000    12.80000    2.01E-01     1.44E-03     2.36E-01     1.63E-0300020003    26
   12.80000    12.60000    1.28E-01     1.27E-03     1.52E-01     1.46E-0300020003    27
   12.60000    12.40000    9.07E-02     1.16E-03     1.09E-01     1.35E-0300020003    28
   12.40000    12.20000    6.14E-02     1.07E-03     7.44E-02     1.25E-0300020003    29
   12.20000    12.00000    4.32E-02     1.01E-03     5.24E-02     1.18E-0300020003    30
   12.00000    11.80000    3.81E-02     9.85E-04     4.62E-02     1.16E-0300020003    31
   11.80000    11.60000    3.47E-02     9.51E-04     4.21E-02     1.12E-0300020003    32
   11.60000    11.40000    3.25E-02     9.33E-04     3.94E-02     1.11E-0300020003    33
   11.40000    11.20000    2.81E-02     9.08E-04     3.41E-02     1.08E-0300020003    34
   11.20000    11.00000    2.34E-02     8.87E-04     2.81E-02     1.06E-0300020003    35
   11.00000    10.80000    2.38E-02     8.69E-04     2.86E-02     1.04E-0300020003    36
   10.80000    10.60000    2.53E-02     8.70E-04     3.03E-02     1.04E-0300020003    37
   10.60000    10.40000    2.42E-02     8.54E-04     2.88E-02     1.02E-0300020003    38
   10.40000    10.20000    2.27E-02     8.42E-04     2.71E-02     1.00E-0300020003    39
   10.20000    10.00000    2.41E-02     8.50E-04     2.86E-02     1.01E-0300020003    40
   10.00000     9.80000    2.73E-02     8.67E-04     3.24E-02     1.03E-0300020003    41
    9.80000     9.60000    3.06E-02     8.91E-04     3.63E-02     1.06E-0300020003    42
    9.60000     9.40000    4.36E-02     9.27E-04     5.16E-02     1.11E-0300020003    43
    9.40000     9.20000    4.72E-02     9.51E-04     5.47E-02     1.12E-0300020003    44
    9.20000     9.00000    4.21E-02     9.28E-04     4.28E-02     9.56E-0400020003    45
    9.00000     8.80000    3.75E-02     9.14E-04     3.68E-02     9.38E-0400020003    46
    8.80000     8.60000    3.79E-02     9.21E-04     3.74E-02     9.53E-0400020003    47
    8.60000     8.40000    3.82E-02     9.21E-04     3.92E-02     9.67E-0400020003    48
    8.40000     8.20000    3.76E-02     9.25E-04     3.94E-02     9.82E-0400020003    49
    8.20000     8.00000    4.09E-02     9.29E-04     4.32E-02     9.97E-0400020003    50
    8.00000     7.80000    4.37E-02     9.41E-04     4.66E-02     1.01E-0300020003    51
    7.80000     7.60000    4.83E-02     9.51E-04     5.16E-02     1.03E-0300020003    52
    7.60000     7.40000    5.20E-02     9.53E-04     5.60E-02     1.04E-0300020003    53
    7.40000     7.20000    5.72E-02     9.64E-04     6.16E-02     1.05E-0300020003    54
    7.20000     7.00000    6.03E-02     9.66E-04     6.62E-02     1.06E-0300020003    55
    7.00000     6.80000    6.26E-02     9.66E-04     6.90E-02     1.07E-0300020003    56
    6.80000     6.60000    6.38E-02     9.62E-04     6.99E-02     1.06E-0300020003    57
    6.60000     6.40000    6.72E-02     9.69E-04     7.34E-02     1.07E-0300020003    58
    6.40000     6.20000    6.86E-02     9.62E-04     7.52E-02     1.06E-0300020003    59
    6.20000     6.00000    7.33E-02     9.74E-04     8.06E-02     1.08E-0300020003    60
    6.00000     5.80000    7.59E-02     9.77E-04     8.38E-02     1.09E-0300020003    61
    5.80000     5.60000    7.76E-02     9.84E-04     8.60E-02     1.10E-0300020003    62
    5.60000     5.40000    8.20E-02     9.92E-04     9.12E-02     1.11E-0300020003    63
    5.40000     5.20000    8.78E-02     1.01E-03     9.75E-02     1.13E-0300020003    64
    5.20000     5.00000    9.39E-02     1.02E-03     1.04E-01     1.14E-0300020003    65
    5.00000     4.80000    1.02E-01     1.04E-03     1.13E-01     1.16E-0300020003    66
    4.80000     4.60000    1.09E-01     1.05E-03     1.20E-01     1.17E-0300020003    67
    4.60000     4.40000    1.17E-01     1.07E-03     1.29E-01     1.18E-0300020003    68
    4.40000     4.20000    1.25E-01     1.09E-03     1.39E-01     1.21E-0300020003    69
    4.20000     4.00000    1.36E-01     1.11E-03     1.51E-01     1.23E-0300020003    70
    4.00000     3.80000    1.45E-01     1.15E-03     1.60E-01     1.26E-0300020003    71
    3.80000     3.60000    1.55E-01     1.17E-03     1.70E-01     1.29E-0300020003    72
    3.60000     3.40000    1.67E-01     1.20E-03     1.82E-01     1.31E-0300020003    73
    3.40000     3.20000    1.87E-01     1.25E-03     2.04E-01     1.35E-0300020003    74
    3.20000     3.00000    2.11E-01     1.32E-03     2.28E-01     1.42E-0300020003    75
    3.00000     2.80000    2.45E-01     1.40E-03     2.64E-01     1.50E-0300020003    76
    2.80000     2.60000    2.79E-01     1.49E-03     2.97E-01     1.58E-0300020003    77
    2.60000     2.40000    3.32E-01     1.59E-03     3.39E-01     1.61E-0300020003    78
    2.40000     2.20000    4.01E-01     1.68E-03     4.07E-01     1.68E-0300020003    79
    2.20000     2.00000    4.56E-01     1.78E-03     4.73E-01     1.82E-0300020003    80
    2.00000     1.80000    5.10E-01     1.88E-03     5.34E-01     1.97E-0300020003    81
    1.80000     1.60000    5.92E-01     2.08E-03     6.14E-01     2.16E-0300020003    82
    1.60000     1.40000    6.76E-01     2.38E-03     6.90E-01     2.43E-0300020003    83
    1.40000     1.20000    7.55E-01     2.87E-03     7.58E-01     2.88E-0300020003    84
    1.20000     1.00000    7.93E-01     4.04E-03     7.82E-01     3.99E-0300020003    85
ENDDATA           72                                                      00020003    86
ENDSUBENTRY       87                                                      00020003999999
ENDENTRY           3                                                      00020999999999
```

Table 1(3) Angle-integrated neutron emission spectrum in the CM system with En = 14.1 MeV, for Co

```
SUBENTRY      00019003      881201                                          00019003     1
BIB                2             8                                        00019003     2
COMMENT       TWO DATA SETS ARE GIVEN.                                     00019003     3
              DATA OBTAINED FROM RAW DDX DATA , IN LEFT HAND SIDE.         00019003     4
              DATA OBTAINED FROM CORRECTED DDX DATA WITH MUSCC3 CODE       00019003     5
              IN RIGHT HAND SIDE.                                          00019003     6
REACTION      (27-CO-59(N,SCT),,DE) SECONDARY NEUTRON SPECTRUM             00019003     7
              IN THE CENTER-OF-MASS SYSTEM                                 00019003     8
                                                                           00019003     9
ENDBIB             8                                                       00019003    10
COMMON             1             5                                         00019003    11
EN                                                                         00019003    12
MEV                                                                        00019003    13
   14.10000                                                                00019003    14
ENDCOMMON          5                                                       00019003    15
DATA               6            69                                         00019003    16
E-MAX        E-MIN        DATA         DATA-ERR     DATA         DATA-ERR  00019003    17
MEV          MEV          B/MEV        B/MEV        B/MEV        B/MEV     00019003    17
   14.60000   14.40000   3.90E-02   5.30E-04   3.85E-02   6.51E-04 00019003    18
   14.40000   14.20000   4.33E-02   1.20E-03   5.29E-02   1.32E-03 00019003    19
   14.20000   14.00000   2.66E-01   1.79E-03   3.37E-01   2.17E-03 00019003    20
   14.00000   13.80000   7.81E-01   2.46E-03   1.04E+00   3.16E-03 00019003    21
   13.80000   13.60000   1.41E+00   3.07E-03   1.88E+00   3.98E-03 00019003    22
   13.60000   13.40000   1.22E+00   2.80E-03   1.60E+00   3.57E-03 00019003    23
   13.40000   13.20000   5.66E-01   1.98E-03   7.31E-01   2.45E-03 00019003    24
   13.20000   13.00000   2.28E-01   1.41E-03   2.92E-01   1.69E-03 00019003    25
   13.00000   12.80000   1.14E-01   1.14E-03   1.45E-01   1.36E-03 00019003    26
   12.80000   12.60000   8.63E-02   1.07E-03   1.08E-01   1.29E-03 00019003    27
   12.60000   12.40000   8.15E-02   1.06E-03   1.01E-01   1.29E-03 00019003    28
   12.40000   12.20000   6.67E-02   1.01E-03   8.38E-02   1.25E-03 00019003    29
   12.20000   12.00000   4.64E-02   9.40E-04   5.92E-02   1.17E-03 00019003    30
   12.00000   11.80000   3.09E-02   8.77E-04   4.01E-02   1.09E-03 00019003    31
   11.80000   11.60000   2.15E-02   8.38E-04   2.82E-02   1.04E-03 00019003    32
   11.60000   11.40000   1.69E-02   8.16E-04   2.22E-02   1.02E-03 00019003    33
   11.40000   11.20000   1.21E-02   7.86E-04   1.57E-02   9.85E-04 00019003    34
   11.20000   11.00000   8.89E-03   7.61E-04   1.15E-02   9.55E-04 00019003    35
   11.00000   10.80000   8.15E-03   7.43E-04   1.04E-02   9.31E-04 00019003    36
   10.80000   10.60000   1.17E-02   7.34E-04   1.46E-02   9.20E-04 00019003    37
   10.60000   10.40000   1.10E-02   7.29E-04   1.35E-02   9.15E-04 00019003    38
   10.40000   10.20000   1.41E-02   7.09E-04   1.73E-02   8.87E-04 00019003    39
   10.20000   10.00000   2.15E-02   7.27E-04   2.65E-02   9.06E-04 00019003    40
   10.00000    9.80000   2.99E-02   7.48E-04   3.69E-02   9.32E-04 00019003    41
    9.80000    9.60000   2.69E-02   7.29E-04   3.32E-02   9.08E-04 00019003    42
    9.60000    9.40000   2.45E-02   7.10E-04   3.04E-02   8.83E-04 00019003    43
    9.40000    9.20000   2.68E-02   7.04E-04   3.19E-02   8.54E-04 00019003    44
    9.20000    9.00000   2.83E-02   7.19E-04   2.98E-02   7.84E-04 00019003    45
    9.00000    8.80000   2.80E-02   7.04E-04   2.88E-02   7.66E-04 00019003    46
    8.80000    8.60000   2.66E-02   7.09E-04   2.73E-02   7.78E-04 00019003    47
    8.60000    8.40000   2.87E-02   7.11E-04   3.01E-02   7.88E-04 00019003    48
    8.40000    8.20000   2.94E-02   7.24E-04   3.15E-02   8.07E-04 00019003    49
    8.20000    8.00000   3.06E-02   7.18E-04   3.29E-02   8.09E-04 00019003    50
    8.00000    7.80000   3.02E-02   7.31E-04   3.26E-02   8.26E-04 00019003    51
    7.80000    7.60000   3.03E-02   7.33E-04   3.34E-02   8.33E-04 00019003    52
    7.60000    7.40000   3.16E-02   7.47E-04   3.47E-02   8.50E-04 00019003    53
    7.40000    7.20000   3.43E-02   7.47E-04   3.76E-02   8.52E-04 00019003    54
    7.20000    7.00000   3.67E-02   7.57E-04   4.08E-02   8.63E-04 00019003    55
    7.00000    6.80000   3.88E-02   7.58E-04   4.34E-02   8.61E-04 00019003    56
    6.80000    6.60000   4.25E-02   7.64E-04   4.75E-02   8.66E-04 00019003    57
    6.60000    6.40000   4.41E-02   7.71E-04   4.86E-02   8.72E-04 00019003    58
    6.40000    6.20000   4.67E-02   7.77E-04   5.14E-02   8.80E-04 00019003    59
    6.20000    6.00000   5.15E-02   7.95E-04   5.66E-02   9.00E-04 00019003    60
    6.00000    5.80000   5.41E-02   8.10E-04   5.95E-02   9.18E-04 00019003    61
    5.80000    5.60000   5.80E-02   8.26E-04   6.41E-02   9.30E-04 00019003    62
    5.60000    5.40000   6.32E-02   8.49E-04   6.93E-02   9.49E-04 00019003    63
    5.40000    5.20000   6.90E-02   8.65E-04   7.54E-02   9.63E-04 00019003    64
    5.20000    5.00000   7.52E-02   8.92E-04   8.22E-02   9.86E-04 00019003    65
    5.00000    4.80000   8.17E-02   9.18E-04   8.82E-02   1.00E-03 00019003    66
    4.80000    4.60000   9.10E-02   9.44E-04   9.68E-02   1.02E-03 00019003    67
    4.60000    4.40000   9.74E-02   9.67E-04   1.03E-01   1.04E-03 00019003    68
    4.40000    4.20000   1.05E-01   9.92E-04   1.13E-01   1.08E-03 00019003    69
    4.20000    4.00000   1.13E-01   1.01E-03   1.23E-01   1.10E-03 00019003    70
    4.00000    3.80000   1.18E-01   1.03E-03   1.29E-01   1.13E-03 00019003    71
    3.80000    3.60000   1.27E-01   1.05E-03   1.40E-01   1.16E-03 00019003    72
    3.60000    3.40000   1.37E-01   1.09E-03   1.52E-01   1.21E-03 00019003    73
    3.40000    3.20000   1.51E-01   1.13E-03   1.71E-01   1.29E-03 00019003    74
    3.20000    3.00000   1.68E-01   1.17E-03   1.95E-01   1.35E-03 00019003    75
    3.00000    2.80000   1.91E-01   1.24E-03   2.22E-01   1.44E-03 00019003    76
    2.80000    2.60000   2.17E-01   1.27E-03   2.52E-01   1.48E-03 00019003    77
    2.60000    2.40000   2.49E-01   1.36E-03   2.83E-01   1.55E-03 00019003    78
    2.40000    2.20000   2.96E-01   1.41E-03   3.34E-01   1.59E-03 00019003    79
    2.20000    2.00000   3.34E-01   1.52E-03   3.79E-01   1.72E-03 00019003    80
    2.00000    1.80000   3.93E-01   1.64E-03   4.46E-01   1.87E-03 00019003    81
    1.80000    1.60000   4.64E-01   1.85E-03   5.20E-01   2.08E-03 00019003    82
    1.60000    1.40000   5.38E-01   2.14E-03   5.88E-01   2.35E-03 00019003    83
    1.40000    1.20000   6.19E-01   2.73E-03   6.64E-01   2.92E-03 00019003    84
    1.20000    1.00000   7.41E-01   4.59E-03   7.76E-01   4.77E-03 00019003    85
    1.00000    0.80000   8.85E-01   1.40E-02   9.22E-01   1.45E-02 00019003    86
ENDDATA           73                                                       00019003    87
ENDSUBENTRY       88                                                       00019003999999
ENDENTRY           3                                                       00019999999999
```

Table 1(4) Angle-integrated neutron emission spectrum in the CM system with En = 14.1 MeV, for W

```
SUBENTRY        00023003      890601                                          00023003     1
BIB                    2           8                                          00023003     2
COMMENT     TWO DATA SETS ARE GIVEN.                                          00023003     3
            DATA OBTAINED FROM RAW DDX DATA . IN LEFT HAND SIDE.              00023003     4
            DATA OBTAINED FROM CORRECTED DDX DATA WITH MUSCC3 CODE            00023003     5
            IN RIGHT HAND SIDE.                                               00023003     6
REACTION    (74-W-0(N,SCT),,DE) SECONDARY NEUTRON SPECTRUM                    00023003     7
            IN THE CENTER-OF-MASS SYSTEM                                      00023003     8
ENDBIB                 8                                                      00023003     9
COMMON                 1           5                                          00023003    10
EN                                                                            00023003    11
MEV                                                                           00023003    12
   14.10000                                                                   00023003    13
ENDCOMMON              5                                                      00023003    14
DATA                   6          72                                          00023003    15
E-MAX       E-MIN        DATA        DATA-ERR    DATA        DATA-ERR         00023003    16
MEV         MEV          B/MEV       B/MEV       B/MEV       B/MEV            00023003    17
   15.00000   14.80000   1.83E-10    1.45E-03    6.40E-10    1.99E-0300023003    18
   14.80000   14.60000   3.24E-02    1.06E-03    4.36E-02    1.31E-0300023003    19
   14.60000   14.40000   2.19E-01    1.55E-03    2.95E-01    1.86E-0300023003    20
   14.40000   14.20000   9.09E-01    1.91E-03    1.22E+00    2.38E-0300023003    21
   14.20000   14.00000   2.02E+00    2.42E-03    2.71E+00    3.10E-0300023003    22
   14.00000   13.80000   2.38E+00    2.57E-03    3.12E+00    3.25E-0300023003    23
   13.80000   13.60000   1.50E+00    2.08E-03    1.88E+00    2.50E-0300023003    24
   13.60000   13.40000   6.20E-01    1.45E-03    7.44E-01    1.65E-0300023003    25
   13.40000   13.20000   2.54E-01    1.07E-03    3.02E-01    1.19E-0300023003    26
   13.20000   13.00000   1.45E-01    8.99E-04    1.78E-01    1.04E-0300023003    27
   13.00000   12.80000   9.80E-02    8.17E-04    1.24E-01    9.66E-0400023003    28
   12.80000   12.60000   7.50E-02    7.72E-04    9.53E-02    9.20E-0400023003    29
   12.60000   12.40000   6.01E-02    7.37E-04    7.71E-02    8.92E-0400023003    30
   12.40000   12.20000   5.00E-02    7.07E-04    6.46E-02    8.60E-0400023003    31
   12.20000   12.00000   4.32E-02    6.81E-04    5.49E-02    8.22E-0400023003    32
   12.00000   11.80000   3.94E-02    6.56E-04    4.93E-02    7.87E-0400023003    33
   11.80000   11.60000   3.62E-02    6.30E-04    4.48E-02    7.57E-0400023003    34
   11.60000   11.40000   3.62E-02    6.17E-04    4.45E-02    7.41E-0400023003    35
   11.40000   11.20000   3.70E-02    6.04E-04    4.57E-02    7.32E-0400023003    36
   11.20000   11.00000   3.65E-02    5.95E-04    4.53E-02    7.29E-0400023003    37
   11.00000   10.80000   3.64E-02    5.94E-04    4.52E-02    7.28E-0400023003    38
   10.80000   10.60000   3.66E-02    5.94E-04    4.56E-02    7.34E-0400023003    39
   10.60000   10.40000   3.76E-02    5.99E-04    4.68E-02    7.41E-0400023003    40
   10.40000   10.20000   3.88E-02    6.01E-04    4.86E-02    7.53E-0400023003    41
   10.20000   10.00000   3.85E-02    5.98E-04    4.86E-02    7.52E-0400023003    42
   10.00000    9.80000   3.75E-02    5.96E-04    4.72E-02    7.50E-0400023003    43
    9.80000    9.60000   3.70E-02    5.96E-04    4.60E-02    7.37E-0400023003    44
    9.60000    9.40000   3.61E-02    6.00E-04    2.56E-02    4.49E-0400023003    45
    9.40000    9.20000   3.63E-02    6.09E-04    6.50E-03    1.32E-0400023003    46
    9.20000    9.00000   3.55E-02    6.09E-04    4.46E-03    1.29E-0400023003    47
    9.00000    8.80000   3.55E-02    6.14E-04    5.46E-03    1.59E-0400023003    48
    8.80000    8.60000   3.47E-02    6.16E-04    5.98E-03    1.73E-0400023003    49
    8.60000    8.40000   3.44E-02    6.23E-04    7.40E-03    2.18E-0400023003    50
    8.40000    8.20000   3.50E-02    6.30E-04    8.36E-03    2.39E-0400023003    51
    8.20000    8.00000   3.42E-02    6.36E-04    1.15E-02    3.29E-0400023003    52
    8.00000    7.80000   3.30E-02    6.39E-04    1.49E-02    4.12E-0400023003    53
    7.80000    7.60000   3.31E-02    6.49E-04    1.57E-02    4.27E-0400023003    54
    7.60000    7.40000   3.42E-02    6.54E-04    1.86E-02    4.85E-0400023003    55
    7.40000    7.20000   3.44E-02    6.57E-04    2.18E-02    5.27E-0400023003    56
    7.20000    7.00000   3.43E-02    6.54E-04    2.27E-02    5.30E-0400023003    57
    7.00000    6.80000   3.57E-02    6.55E-04    2.64E-02    5.95E-0400023003    58
    6.80000    6.60000   3.68E-02    6.54E-04    3.07E-02    6.50E-0400023003    59
    6.60000    6.40000   3.68E-02    6.54E-04    3.20E-02    6.56E-0400023003    60
    6.40000    6.20000   3.63E-02    6.63E-04    3.32E-02    7.02E-0400023003    61
    6.20000    6.00000   3.82E-02    6.78E-04    3.65E-02    7.50E-0400023003    62
    6.00000    5.80000   3.87E-02    6.89E-04    3.90E-02    7.88E-0400023003    63
    5.80000    5.60000   3.91E-02    6.99E-04    4.15E-02    8.11E-0400023003    64
    5.60000    5.40000   4.17E-02    7.12E-04    4.56E-02    8.37E-0400023003    65
    5.40000    5.20000   4.47E-02    7.25E-04    4.96E-02    8.63E-0400023003    66
    5.20000    5.00000   4.70E-02    7.37E-04    5.28E-02    8.78E-0400023003    67
    5.00000    4.80000   5.07E-02    7.55E-04    5.80E-02    9.08E-0400023003    68
    4.80000    4.60000   5.62E-02    7.72E-04    6.57E-02    9.45E-0400023003    69
    4.60000    4.40000   6.18E-02    7.87E-04    7.36E-02    9.72E-0400023003    70
    4.40000    4.20000   7.13E-02    8.14E-04    8.61E-02    1.01E-0300023003    71
    4.20000    4.00000   8.10E-02    8.32E-04    9.88E-02    1.04E-0300023003    72
    4.00000    3.80000   9.32E-02    8.56E-04    1.16E-01    1.10E-0300023003    73
    3.80000    3.60000   1.08E-01    8.74E-04    1.36E-01    1.12E-0300023003    74
    3.60000    3.40000   1.28E-01    9.14E-04    1.62E-01    1.18E-0300023003    75
    3.40000    3.20000   1.51E-01    9.57E-04    1.93E-01    1.24E-0300023003    76
    3.20000    3.00000   1.85E-01    1.02E-03    2.40E-01    1.34E-0300023003    77
    3.00000    2.80000   2.23E-01    1.09E-03    2.91E-01    1.45E-0300023003    78
    2.80000    2.60000   2.79E-01    1.20E-03    3.57E-01    1.55E-0300023003    79
    2.60000    2.40000   3.56E-01    1.34E-03    4.52E-01    1.74E-0300023003    80
    2.40000    2.20000   4.52E-01    1.43E-03    5.83E-01    1.87E-0300023003    81
    2.20000    2.00000   5.60E-01    1.57E-03    7.36E-01    2.08E-0300023003    82
    2.00000    1.80000   7.00E-01    1.75E-03    9.24E-01    2.33E-0300023003    83
    1.80000    1.60000   8.82E-01    2.00E-03    1.16E+00    2.65E-0300023003    84
    1.60000    1.40000   1.11E+00    2.36E-03    1.44E+00    3.08E-0300023003    85
    1.40000    1.20000   1.42E+00    3.01E-03    1.81E+00    3.88E-0300023003    86
    1.20000    1.00000   1.84E+00    4.42E-03    2.29E+00    5.54E-0300023003    87
    1.00000    0.80000   2.54E+00    1.05E-02    3.09E+00    1.28E-0200023003    88
    0.80000    0.60000   2.40E+00    4.39E-02    2.79E+00    5.12E-0200023003    89
ENDDATA               76                                                      00023003    90
ENDSUBENTRY           91                                                      00023003999999
ENDENTRY               3                                                      0002399999999
```

Table 2(1) Partial differential cross sections for Ca at En = 14.1 MeV

θ_{LAB} (deg)	elastic		Q= -3.736~3.904 MeV		Q= -4.492 MeV		Q= -6.285 MeV	
	$d\sigma/d\Omega$(b/sr)	error	$d\sigma/d\Omega$(b/sr)	error	$d\sigma/d\Omega$(b/sr)	error	$d\sigma/d\Omega$(b/sr)	error
15	1.06E+0	3.2E-2	7.73E-3	1.2E-3	3.57E-3	7.1E-4	1.81E-3	5.4E-4
20	6.63E-1	2.0E-2	7.53E-3	7.5E-4	3.85E-3	5.8E-4	2.99E-3	4.5E-4
30	1.56E-1	4.7E-3	7.37E-3	5.2E-4	3.67E-3	3.7E-4	3.39E-3	3.4E-4
42.5	3.61E-2	1.1E-3	6.90E-3	3.4E-4	2.90E-3	2.9E-4	3.47E-3	3.5E-4
50	5.94E-2	1.8E-3	7.02E-3	3.5E-4	2.39E-3	2.4E-4	2.74E-3	2.7E-4
60	5.26E-2	1.6E-3	6.88E-3	3.4E-4	2.48E-3	2.5E-4	1.75E-3	2.6E-4
70	2.39E-2	7.2E-4	6.19E-3	3.1E-4	1.74E-3	2.6E-4	9.37E-4	1.9E-4
80	1.49E-2	5.6E-4	4.77E-3	2.9E-4	1.69E-3	2.5E-4	6.46E-4	1.9E-4
90	2.07E-2	6.2E-4	3.79E-3	2.6E-4	1.85E-3	2.8E-4	5.77E-4	2.0E-4
100	2.27E-2	6.8E-4	3.25E-3	2.6E-4	1.42E-3	2.1E-4	7.84E-4	2.0E-4
110	1.49E-2	4.5E-4	2.53E-3	2.3E-4	1.07E-3	2.1E-4	6.73E-4	2.0E-4
120	5.37E-3	3.4E-4	2.60E-3	2.3E-4	7.49E-4	1.9E-4	7.75E-4	1.9E-4
130	3.89E-3	3.3E-4	2.92E-3	2.6E-4	9.46E-4	1.9E-4	1.08E-3	2.2E-4
140	3.85E-3	3.2E-4	2.95E-3	2.7E-4	1.08E-3	2.2E-4	7.65E-4	1.9E-4
150	3.44E-3	4.1E-4	2.92E-3	3.5E-4	8.02E-4	2.8E-4	7.69E-4	2.7E-4
σ_{Total} (barn)	8.96E-1	3.6E-2	5.78E-2	2.9E-3	2.21E-2	3.3E-3	1.71E-2	2.6E-3

Table 2(2) Partial differential cross sections for Ca at En = 14.1 MeV (continued)

θ_{LAB} (deg)	Q= -6.510~7.536 MeV		Q= -7.760~8.540 MeV		Q= -9.6 MeV	
	$d\sigma/d\Omega$(b/sr)	error	$d\sigma/d\Omega$(b/sr)	error	$d\sigma/d\Omega$(b/sr)	error
15	1.76E-3	4.4E-4	1.43E-3	5.7E-4	2.27E-3	6.8E-4
20	2.28E-3	3.4E-4	3.34E-3	6.7E-4	2.59E-3	5.2E-4
30	3.67E-3	3.7E-4	4.26E-3	8.5E-4	2.97E-3	5.9E-4
42.5	3.78E-3	3.8E-4	4.68E-3	9.4E-4	3.31E-3	6.6E-4
50	3.47E-3	3.5E-4	4.35E-3	8.7E-4	3.56E-3	7.1E-4
60	2.77E-3	2.8E-4	2.63E-3	5.3E-4	2.30E-3	4.6E-4
70	2.63E-3	2.6E-4	2.53E-3	5.1E-4	2.56E-3	5.1E-4
80	1.85E-3	2.8E-4	2.89E-3	5.8E-4	2.02E-3	4.0E-4
90	1.82E-3	2.7E-4	2.69E-3	5.4E-4	1.95E-3	3.9E-4
100	1.75E-3	2.6E-4	2.68E-3	5.4E-4	1.74E-3	3.5E-4
110	1.35E-3	2.0E-4	1.97E-3	3.9E-4	1.70E-3	3.4E-4
120	1.57E-3	2.4E-4	2.46E-3	4.9E-4	1.73E-3	3.5E-4
130	1.56E-3	2.3E-4	2.18E-3	4.4E-4	1.67E-3	3.3E-4
140	1.71E-3	2.6E-4	2.28E-3	4.6E-4	1.47E-3	2.9E-4
150	1.95E-3	3.7E-4	2.61E-3	5.2E-4	1.55E-3	4.6E-4
σ_{Total} (barn)	2.73E-2	3.3E-3	3.74E-2	7.5E-3	2.69E-2	5.4E-3

Table 2(3) Partial differential cross sections for Mn at En = 14.1 MeV

θ_{LAB} (deg)	elastic		Q= -0.984 MeV		Q= -2.822 MeV		Q= -4.11 MeV	
	dσ/dΩ(b/sr)	error	dσ/dΩ(b/sr)	error	dσ/dΩ(b/sr)	error	dσ/dΩ(b/sr)	error
15	1.89E+0	5.7E-2	———	———	———	———	———	———
20	1.17E+0	3.5E-2	———	———	———	———	———	———
30	3.14E-1	9.4E-3	———	———	———	———	———	———
40	7.39E-2	2.2E-3	5.62E-3	1.7E-3	2.08E-3	2.1E-4	5.07E-3	3.0E-4
50	5.85E-2	1.8E-3	3.94E-3	7.9E-4	1.95E-3	1.9E-4	4.15E-3	2.5E-4
60	2.56E-2	7.7E-4	4.01E-3	8.0E-4	1.50E-3	1.5E-4	5.13E-3	3.1E-4
70	1.40E-2	4.2E-4	2.59E-3	3.9E-4	1.79E-3	1.8E-4	3.29E-3	2.3E-4
80	2.63E-2	7.9E-4	3.86E-3	5.8E-4	1.12E-3	1.3E-4	2.99E-3	2.1E-4
90	3.04E-2	9.1E-4	3.74E-3	5.6E-4	6.77E-4	1.1E-4	2.98E-3	2.1E-4
100	1.94E-2	5.8E-4	2.48E-3	3.7E-4	6.73E-4	9.4E-5	2.94E-3	2.1E-4
110	1.07E-2	3.2E-4	1.27E-3	1.9E-4	6.95E-4	1.0E-4	2.90E-3	2.0E-4
120	1.04E-2	3.1E-4	1.34E-3	2.7E-4	8.61E-4	1.1E-4	2.21E-3	1.5E-4
130	1.16E-2	3.5E-4	9.29E-4	1.9E-4	———	———	1.67E-3	1.3E-4
140	1.37E-2	4.1E-4	7.10E-4	1.4E-4	———	———	2.68E-3	1.9E-4
150	1.52E-2	4.6E-4	9.51E-4	1.9E-4	———	———	2.21E-3	2.2E-4
160	1.38E-2	5.4E-4	5.49E-4	2.5E-4	———	———	———	———
σ_{Total} (barn)	1.38E+0	2.1E-1	3.42E-2	6.8E-3	1.60E-2	1.9E-3	4.12E-2	2.9E-3

Table 2(4) Partial differential cross sections for Co at En = 14.1 MeV

θ_{LAB} (deg)	elastic		Q= -1.099 MeV		Q= -4.086 MeV	
	$d\sigma/d\Omega$(b/sr)	error	$d\sigma/d\Omega$(b/sr)	error	$d\sigma/d\Omega$(b/sr)	error
15	1.61E+0	4.8E-2	———	———	———	———
20	1.01E+0	3.0E-2	———	———	———	———
30	2.53E-1	7.6E-3	1.95E-2	2.3E-3	2.96E-3	2.4E-4
40	5.52E-2	1.7E-3	1.20E-2	8.4E-4	3.02E-3	2.4E-4
50	3.30E-2	9.9E-4	7.33E-3	2.9E-4	3.50E-3	2.8E-4
60	1.32E-2	3.9E-4	4.05E-3	1.6E-4	2.09E-3	1.9E-4
70	1.21E-2	3.6E-4	4.12E-3	2.1E-4	1.54E-3	1.5E-4
80	2.36E-2	7.1E-4	4.22E-3	2.1E-4	1.11E-3	1.2E-4
90	2.49E-2	7.5E-4	3.32E-3	2.0E-4	1.68E-3	1.8E-4
100	1.11E-2	3.3E-4	2.03E-3	1.6E-4	1.32E-3	1.5E-4
110	6.66E-3	2.0E-4	1.18E-3	1.3E-4	1.25E-3	1.4E-4
120	8.52E-3	2.6E-4	6.66E-4	1.1E-4	1.41E-3	1.6E-4
130	9.19E-3	2.8E-4	7.13E-4	1.1E-4	1.14E-3	1.4E-4
140	8.30E-3	2.5E-4	1.01E-3	1.3E-4	1.40E-3	1.7E-4
150	8.19E-3	2.6E-4	1.05E-3	1.9E-4	1.53E-3	2.3E-4
160	6.80E-3	3.3E-4	1.43E-3	2.4E-4	———	———
σ_{Total} (barn)	1.17E+0	1.8E-1	6.61E-2	5.3E-3	2.23E-2	2.2E-3

Table 2(5) Partial differential cross sections for W at En = 14.1 MeV

θ_{LAB} (deg)	elastic		continuum		(n, 2n)	
	dσ/dΩ(b/sr)	error	dσ/dΩ(b/sr)	error	dσ/dΩ(b/sr)	error
15	2.29E+0	2.3E-1	5.67E-2	4.0E-3	3.68E-1	2.6E-2
20	9.81E-1	9.8E-2	4.44E-2	3.1E-3	3.31E-1	2.3E-2
30	1.54E-1	1.5E-2	3.05E-2	2.1E-3	3.35E-1	2.3E-2
40	2.05E-1	2.1E-2	2.67E-2	1.9E-3	3.13E-1	2.2E-2
50	9.60E-2	9.6E-3	2.45E-2	1.7E-3	3.11E-1	2.2E-2
60	3.07E-2	3.1E-3	1.94E-2	1.4E-3	2.91E-1	2.0E-2
70	3.26E-2	3.3E-3	1.63E-2	1.1E-3	2.94E-1	2.1E-2
80	2.29E-2	2.3E-3	1.43E-2	1.0E-3	2.58E-1	1.8E-2
90	1.15E-2	1.2E-3	1.25E-2	8.8E-4	2.74E-1	1.9E-2
100	9.93E-3	9.9E-4	1.12E-2	7.8E-4	2.54E-1	1.8E-2
110	9.06E-3	9.1E-4	9.48E-3	6.6E-4	2.65E-1	1.9E-2
120	7.36E-3	7.4E-4	7.70E-3	5.4E-4	2.42E-1	1.7E-2
130	4.87E-3	4.9E-4	8.45E-3	5.9E-4	2.51E-1	1.8E-2
140	5.82E-3	5.8E-4	8.06E-3	5.6E-4	2.63E-1	1.8E-2
150	8.07E-3	8.1E-4	8.48E-3	5.9E-4	2.95E-1	2.1E-2
160	6.84E-3	6.8E-4	5.38E-3	6.5E-4	2.84E-1	2.0E-2
σ_{Total} (barn)	1.33E+0	1.3E+0	2.01E-1	1.4E-2	3.50E+0	2.5E-1

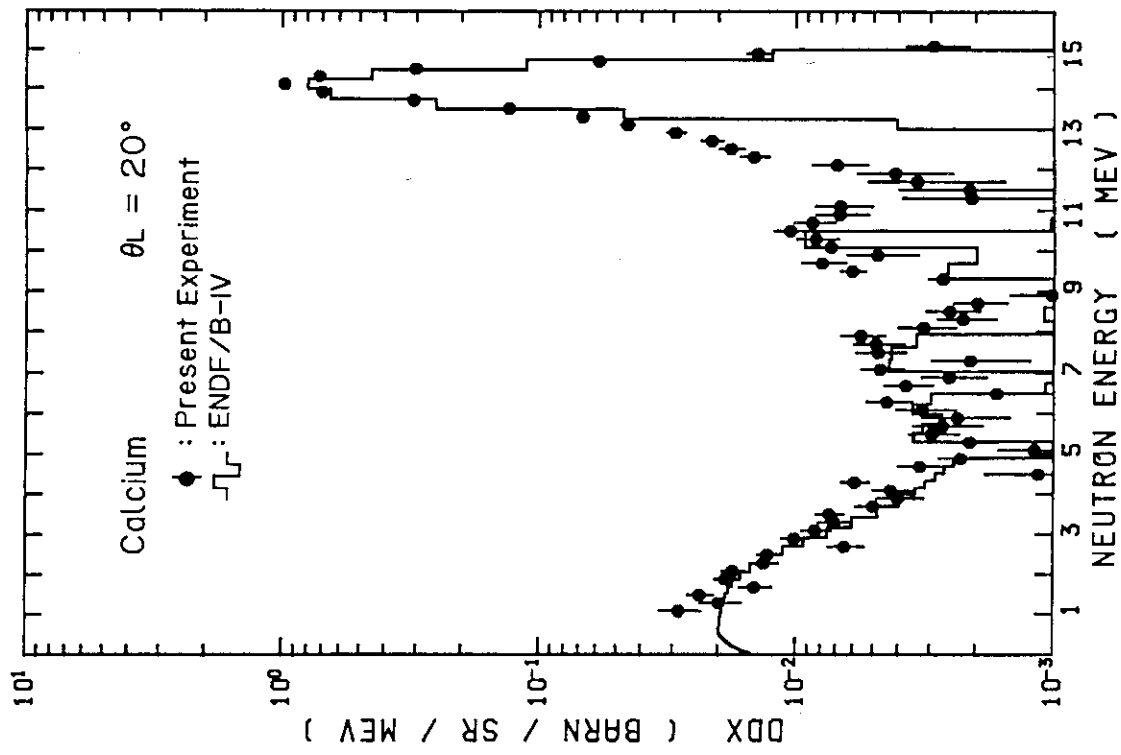

Fig. 2 Double differential neutron emission cross section at 20 deg with En = 14.1 MeV, for Ca

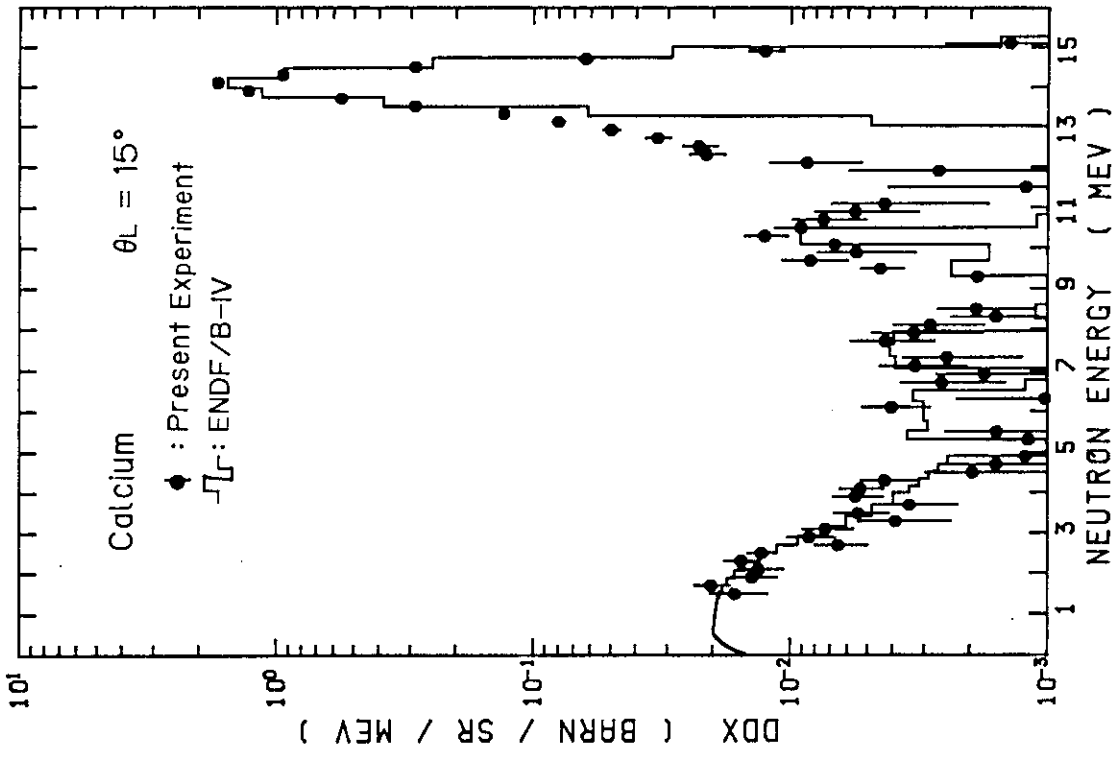

Fig. 1 Double differential neutron emission cross section at 15 deg with En = 14.1 MeV, for Ca

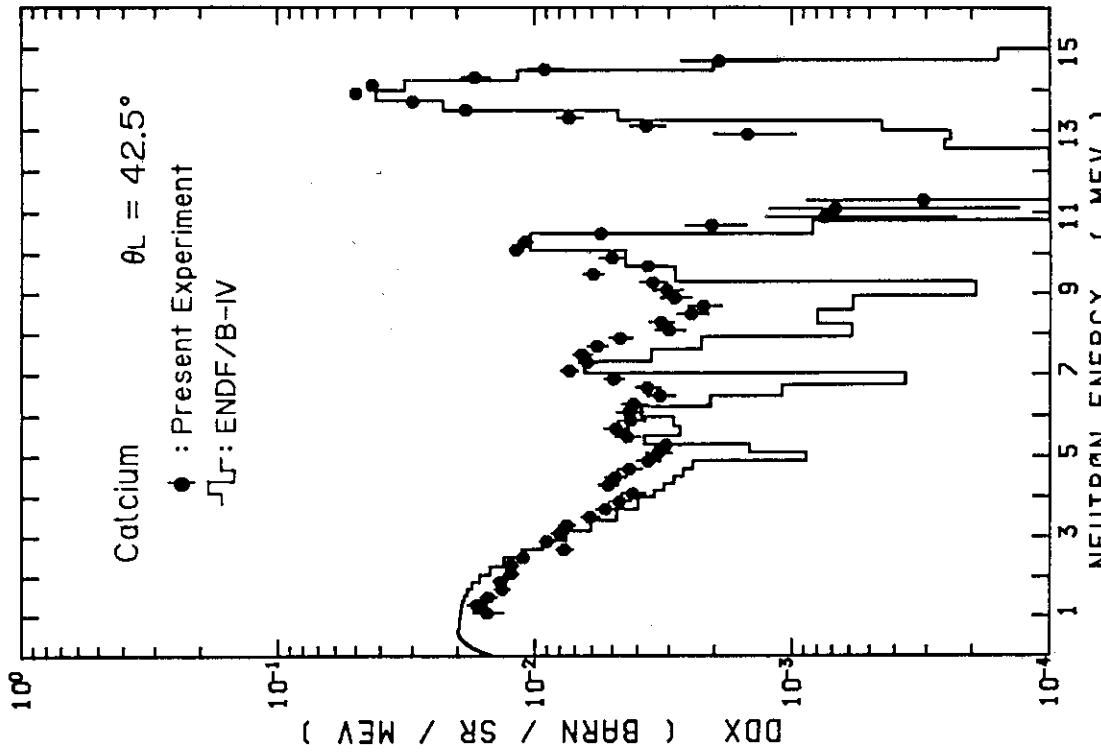

Fig. 4 Double differential neutron emission cross section at 42.5 deg with En = 14.1 MeV, for Ca

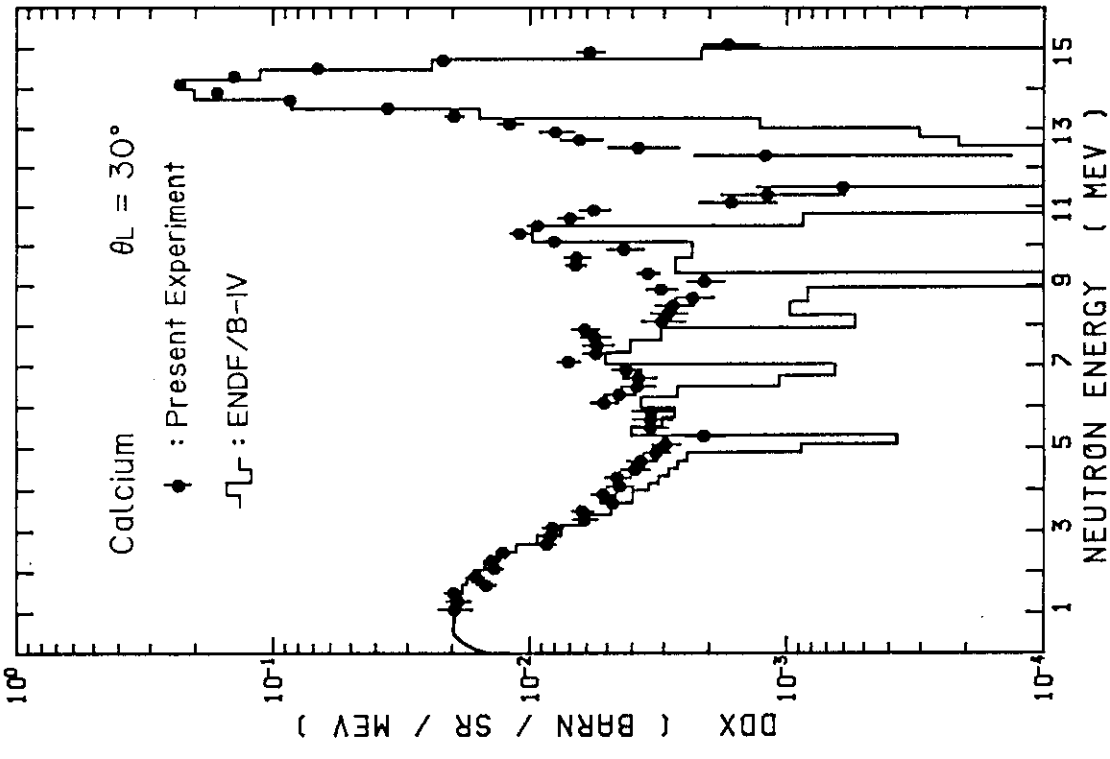

Fig. 3 Double differential neutron emission cross section at 30 deg with En = 14.1 MeV, for Ca

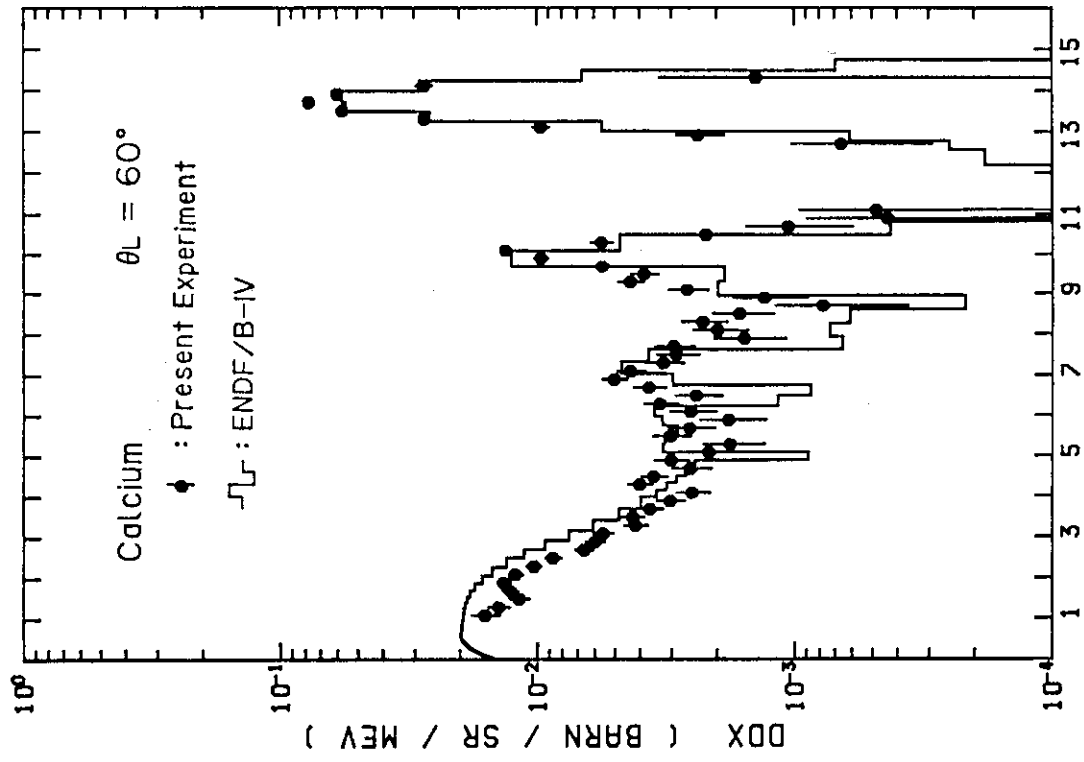

Fig. 6 Double differential neutron emission cross section at 60 deg with En = 14.1 MeV, for Ca

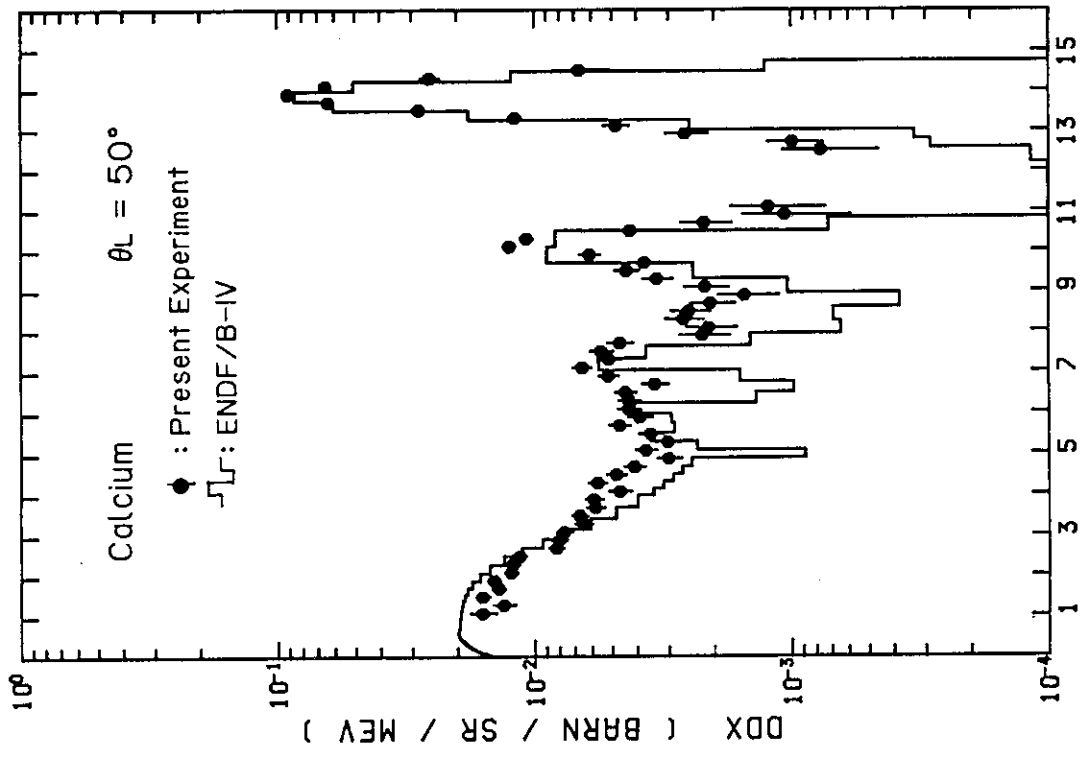

Fig. 5 Double differential neutron emission cross section at 50 deg with En = 14.1 MeV, for Ca

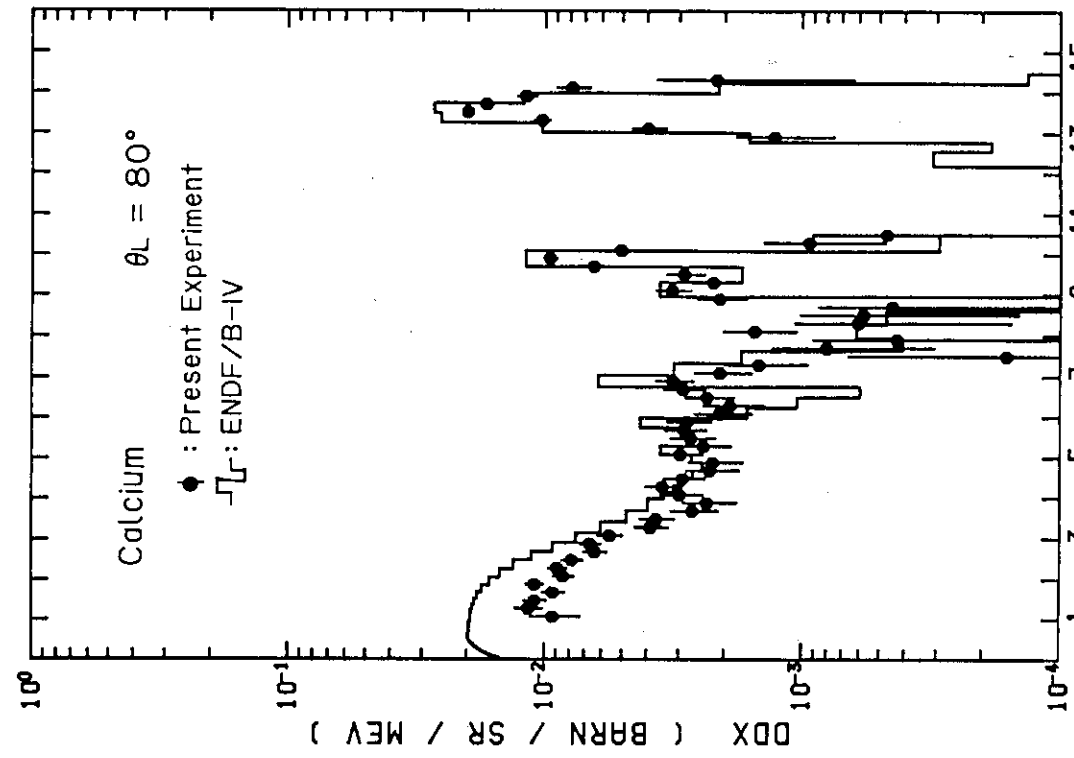

Fig. 8 Double differential neutron emission cross section at 80 deg with En = 14.1 MeV, for Ca

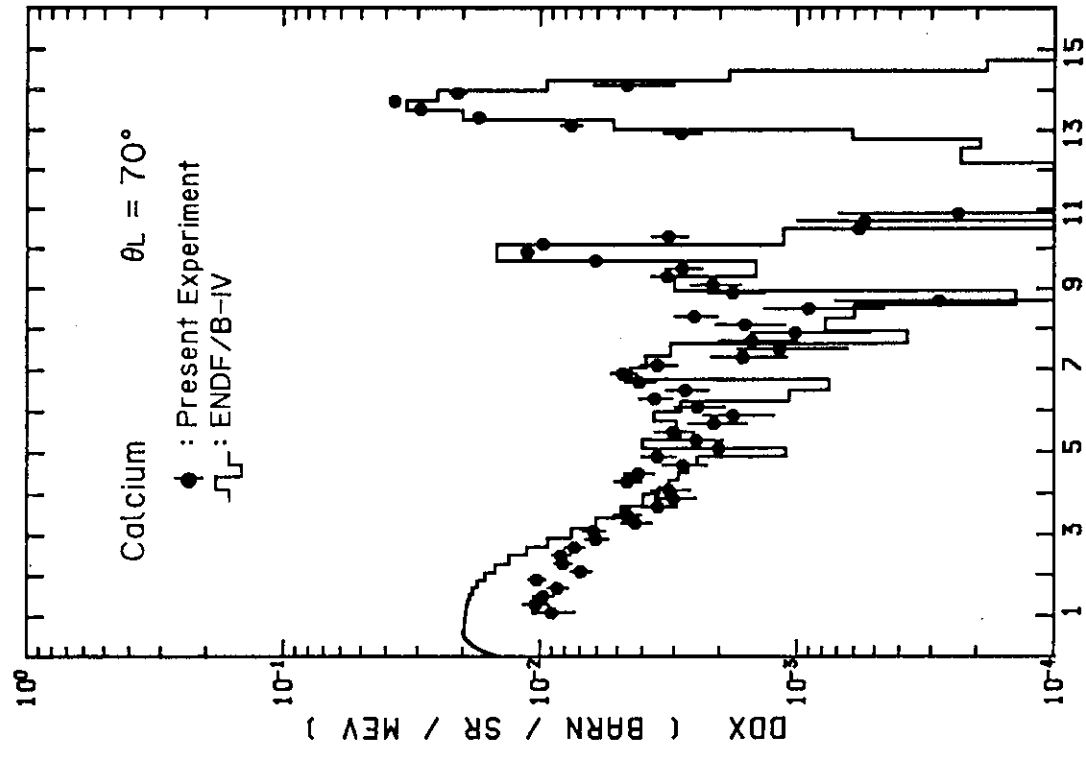

Fig. 7 Double differential neutron emission cross section at 70 deg with En = 14.1 MeV, for Ca

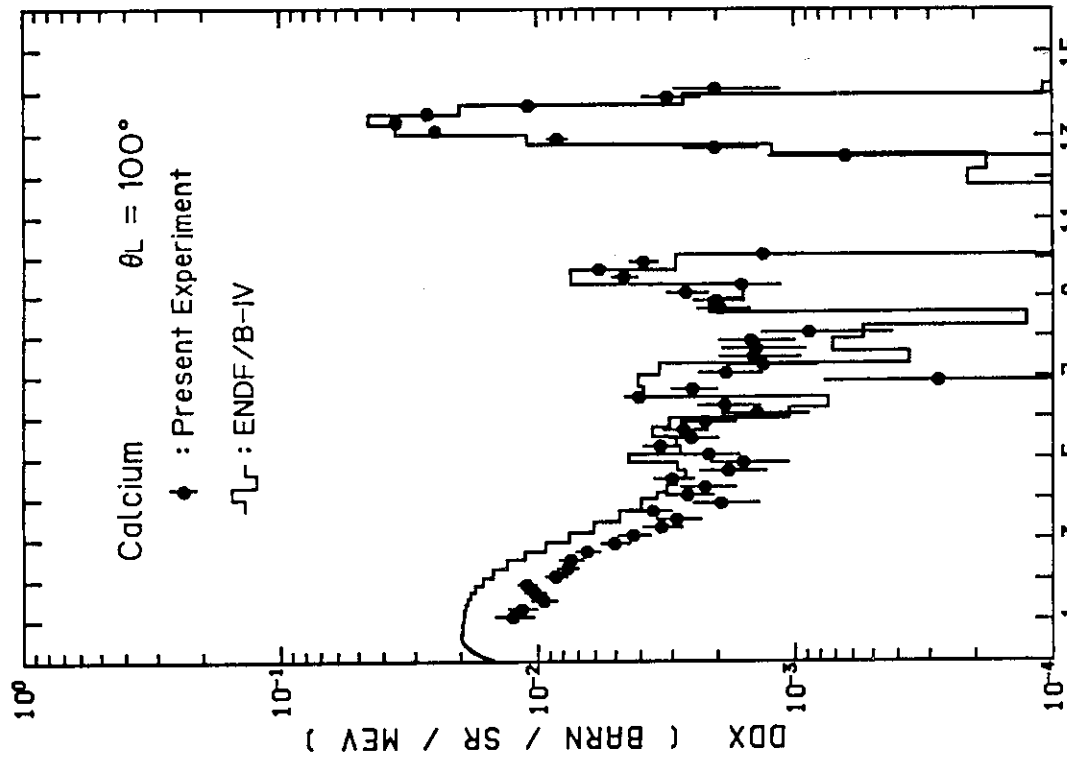

Fig. 10 Double differential neutron emission cross section at 100 deg with En = 14.1 MeV, for Ca

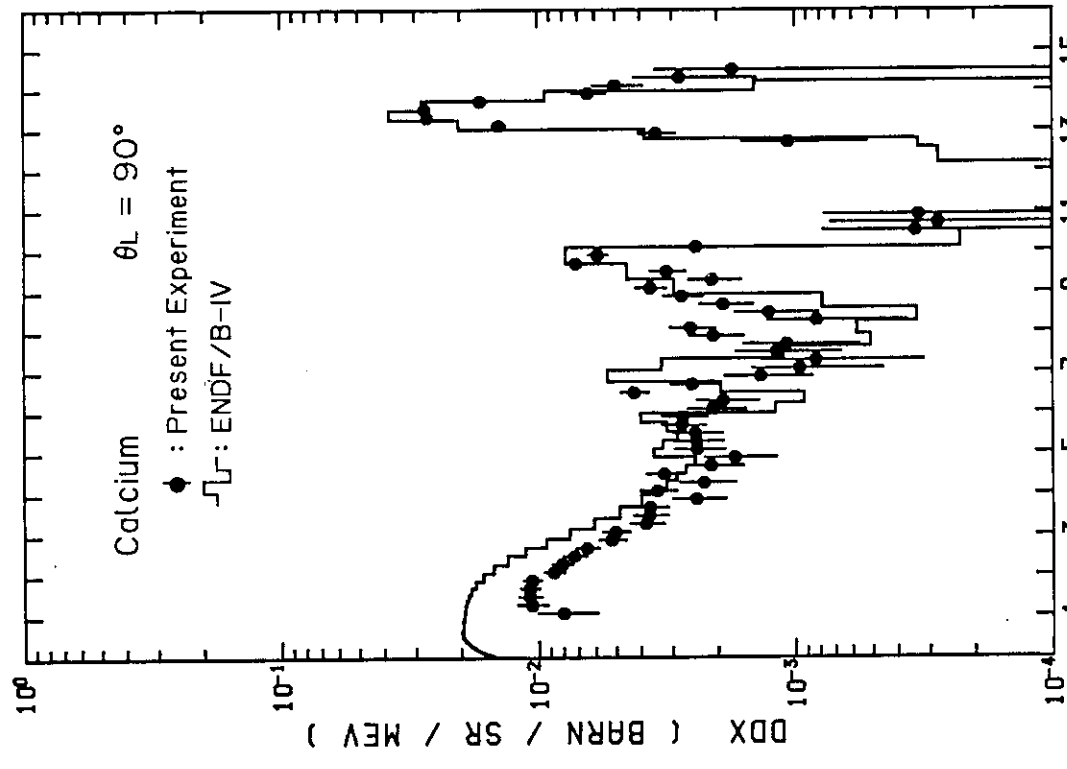

Fig. 9 Double differential neutron emission cross section at 90 deg with En = 14.1 MeV, for Ca

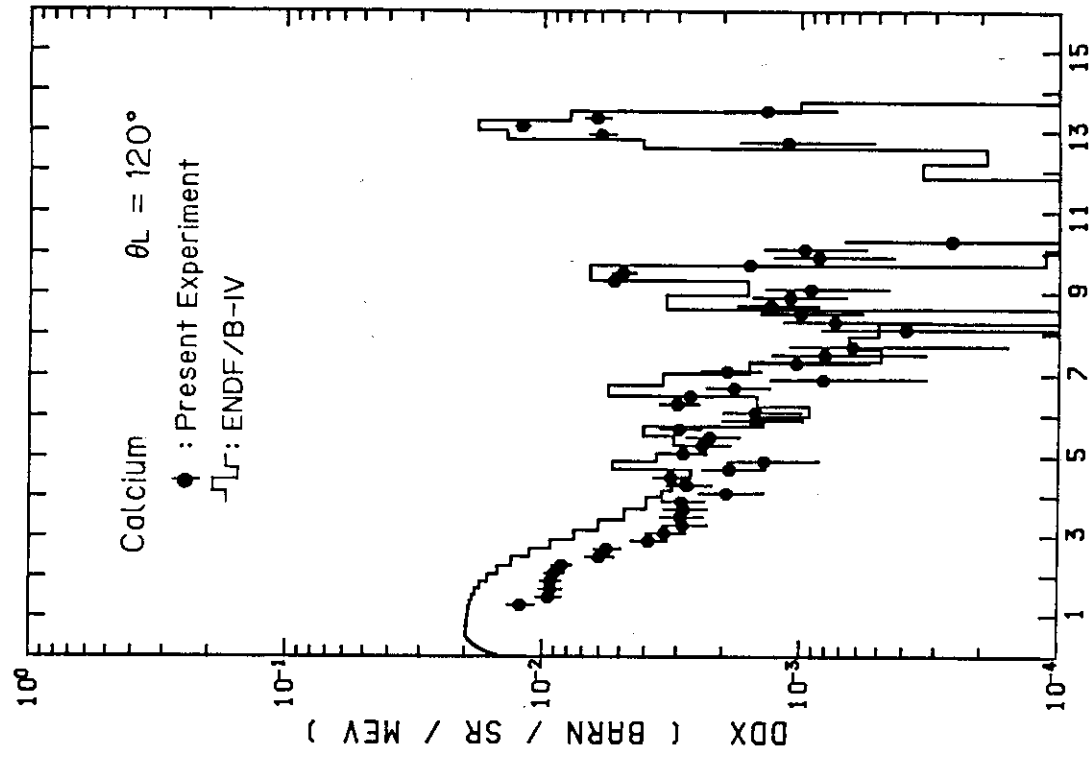

Fig. 12 Double differential neutron emission cross section at 120 deg with En = 14.1 MeV, for Ca

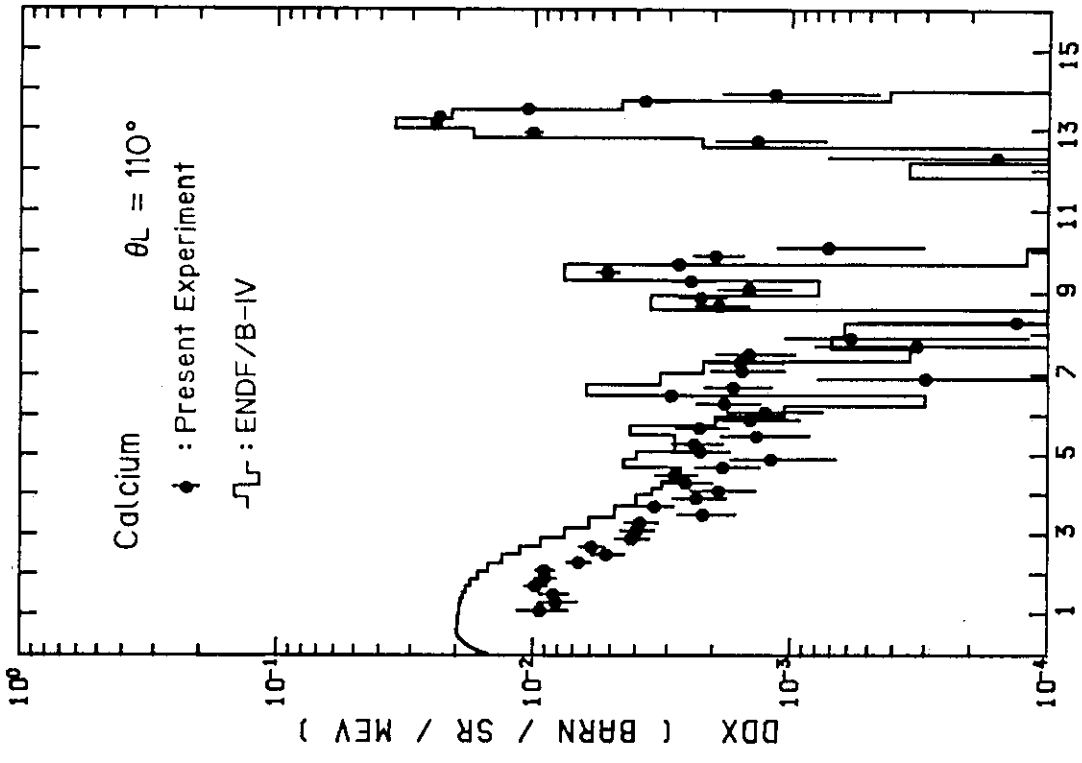

Fig. 11 Double differential neutron emission cross section at 110 deg with En = 14.1 MeV, for Ca

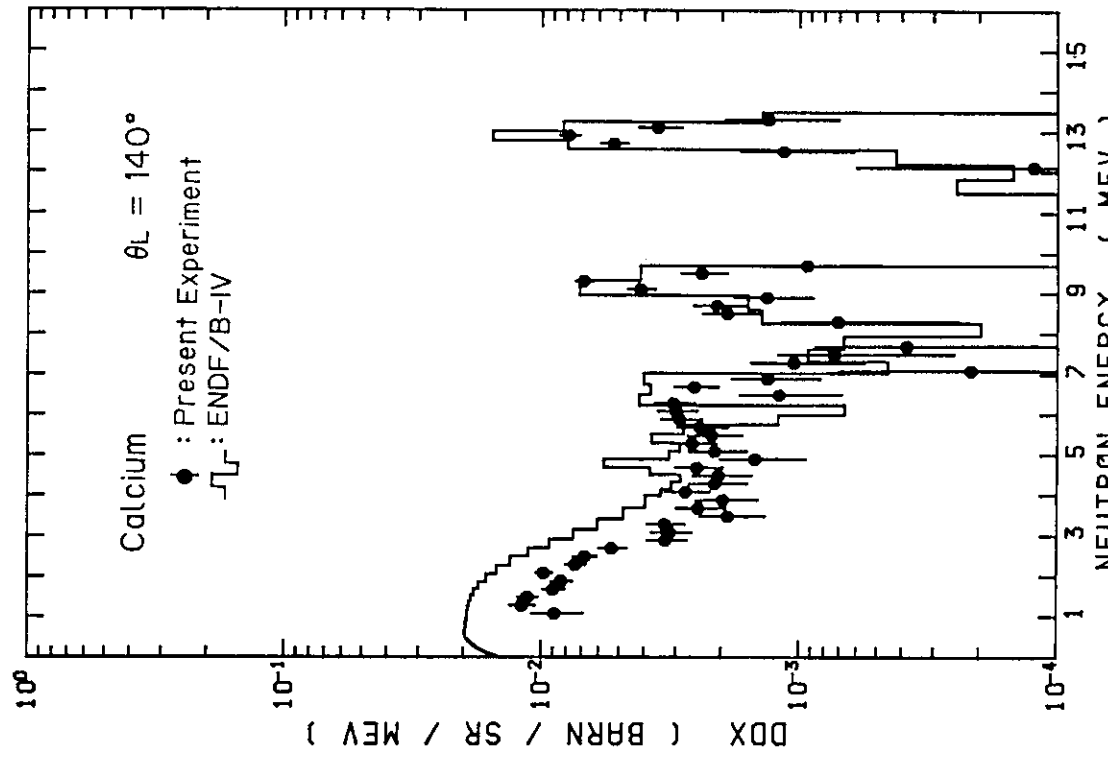

Fig. 14 Double differential neutron emission cross section at 140 deg with En = 14.1 MeV, for Ca

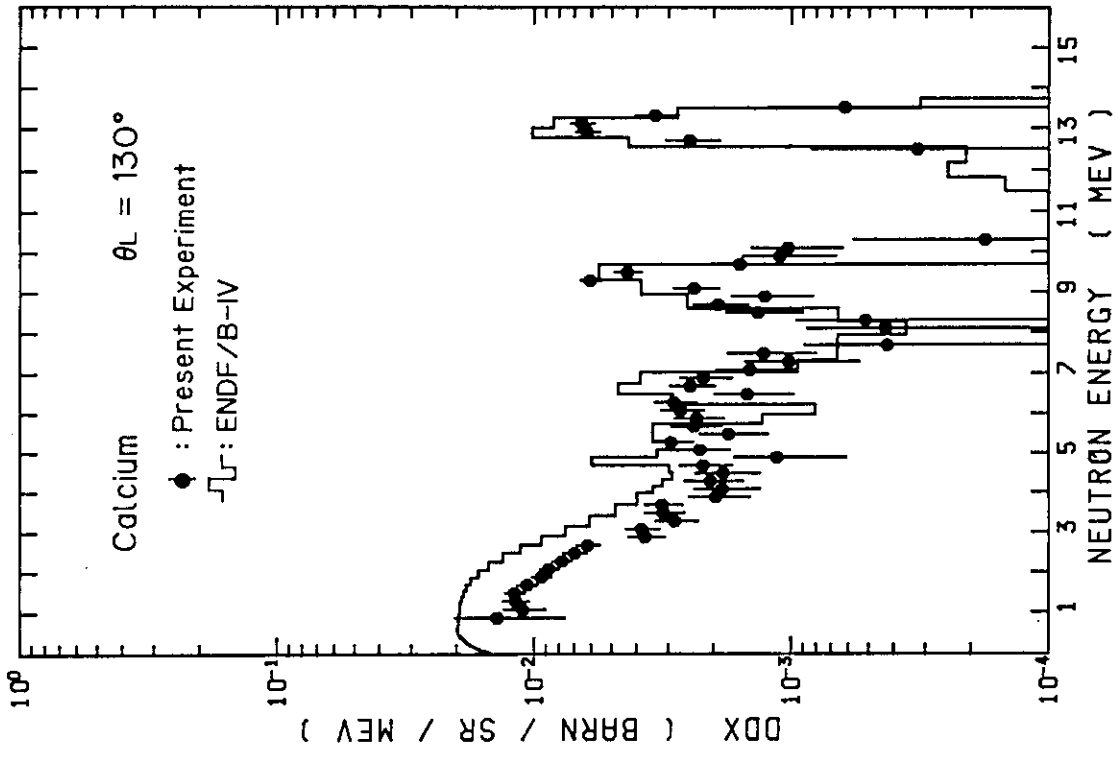

Fig. 13 Double differential neutron emission cross section at 130 deg with En = 14.1 MeV, for Ca

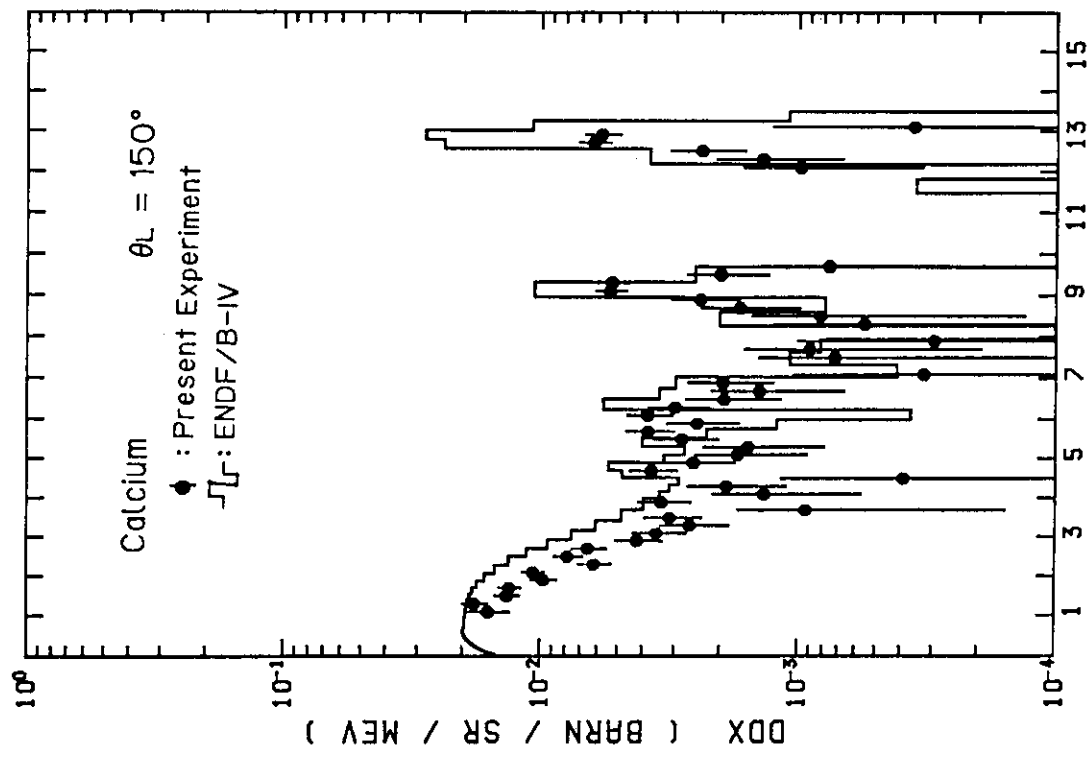

Fig. 15 Double differential neutron emission cross section at 150 deg with En = 14.1 MeV, for Ca

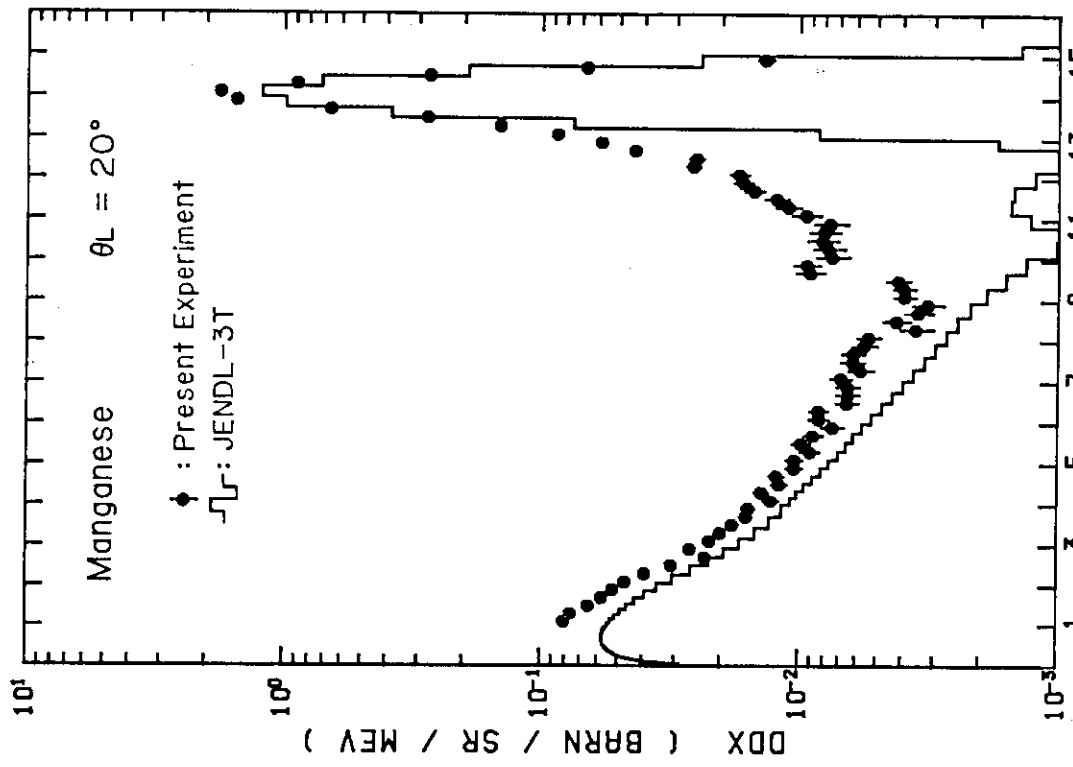

Fig. 17 Double differential neutron emission cross section at 20 deg with En = 14.1 MeV, for Mn

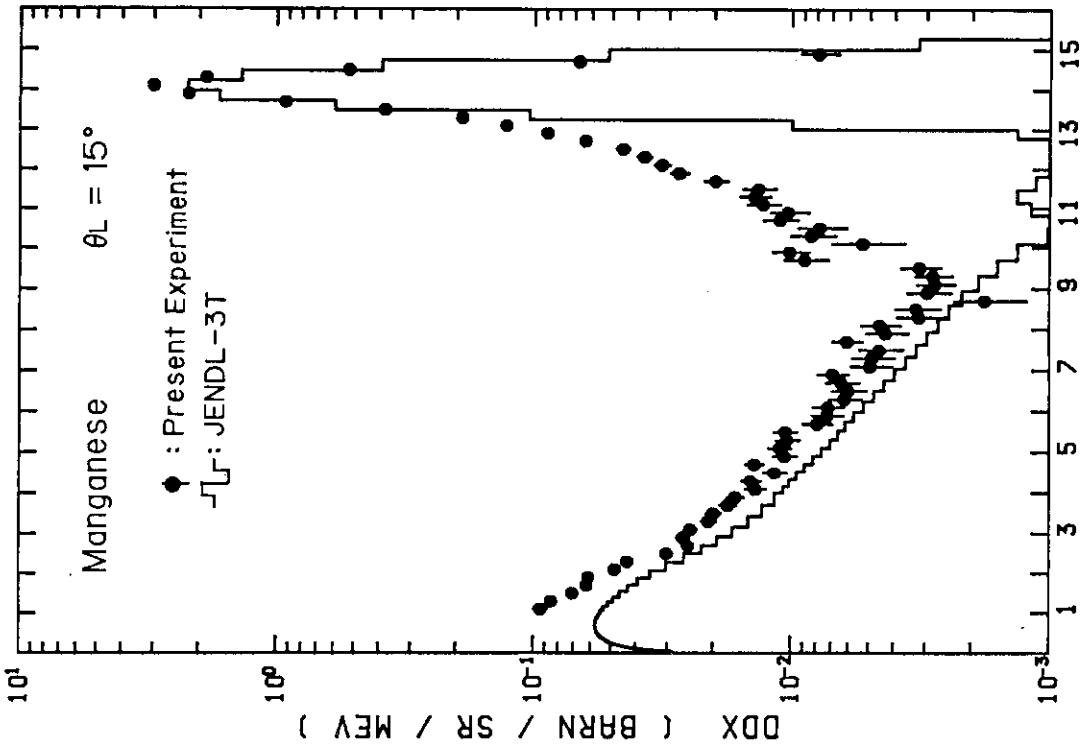

Fig. 16 Double differential neutron emission cross section at 15 deg with En = 14.1 MeV, for Mn

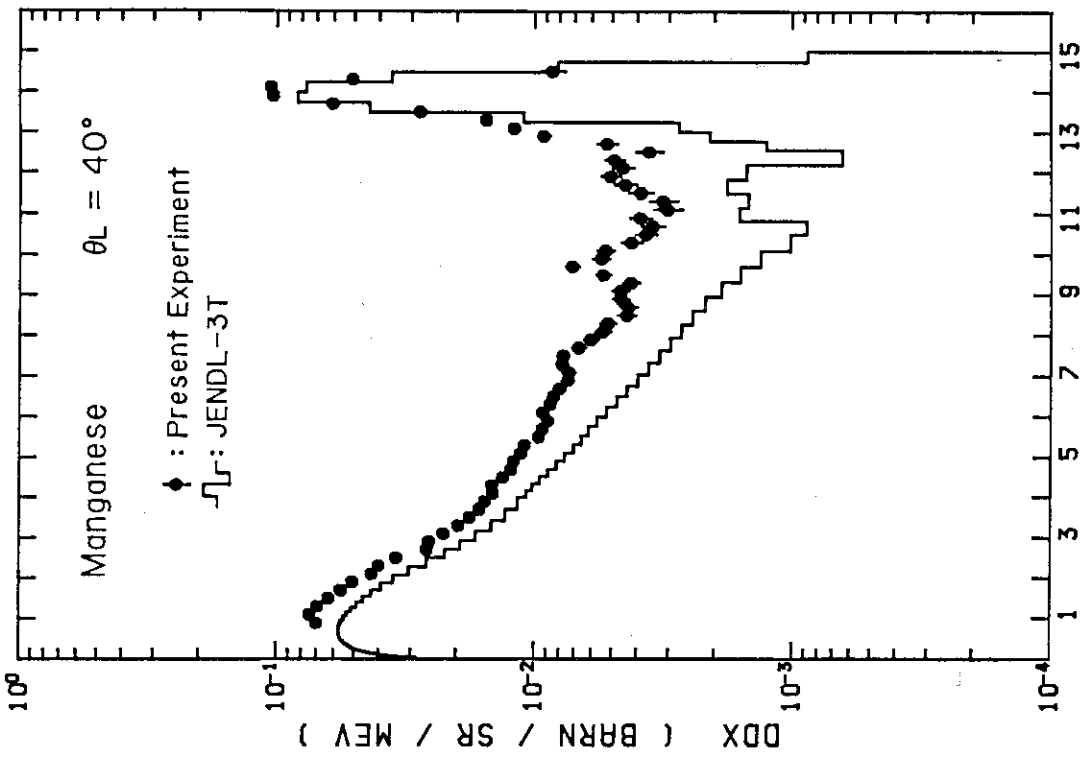

Fig. 19 Double differential neutron emission cross section at 40 deg with En = 14.1 MeV, for Mn

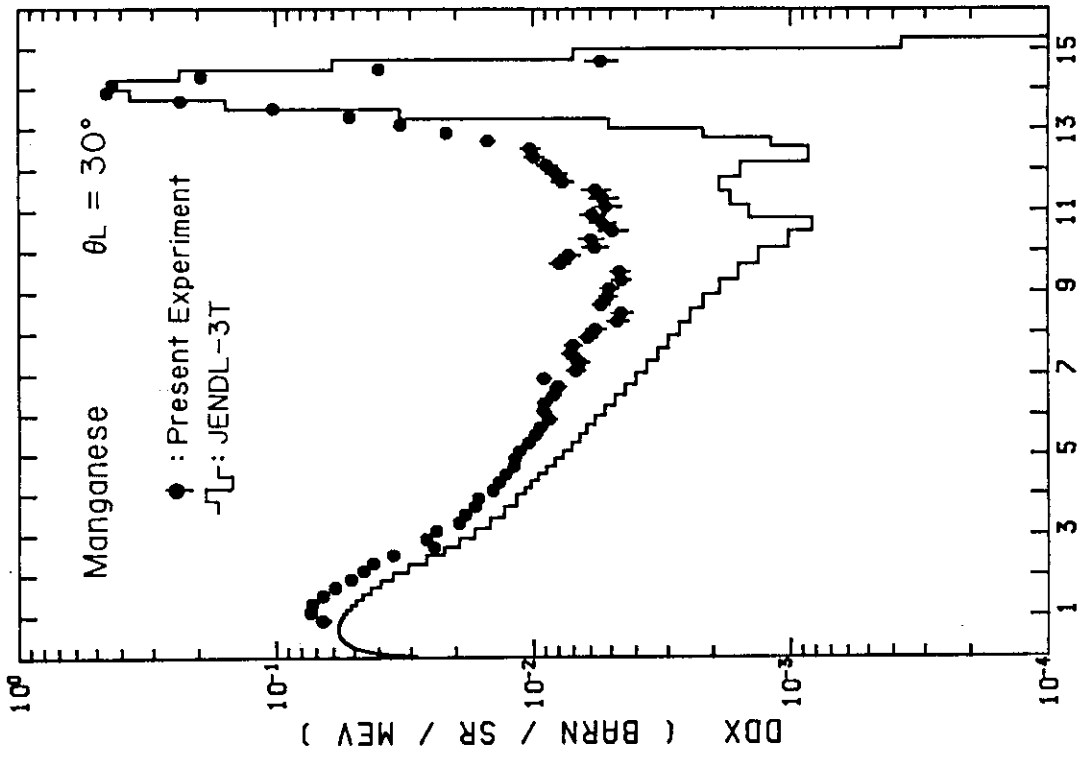

Fig. 18 Double differential neutron emission cross section at 30 deg with En = 14.1 MeV, for Mn

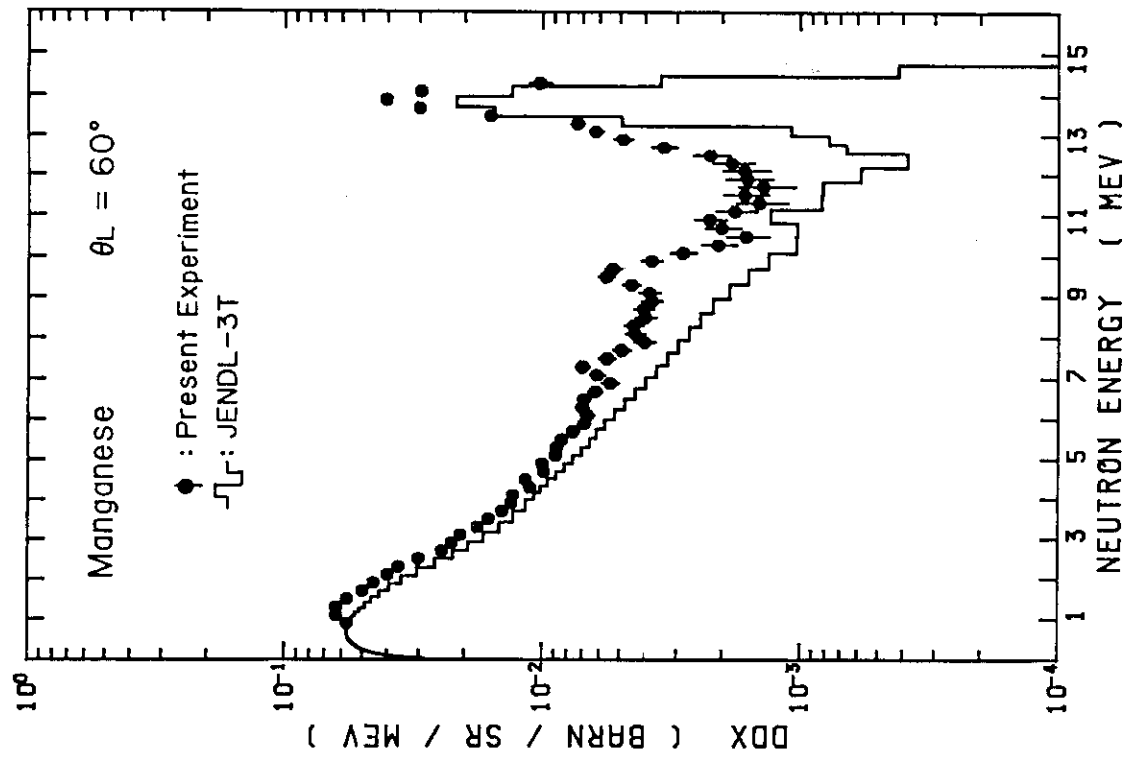

Fig. 21 Double differential neutron emission cross section at 60 deg with En = 14.1 MeV, for Mn

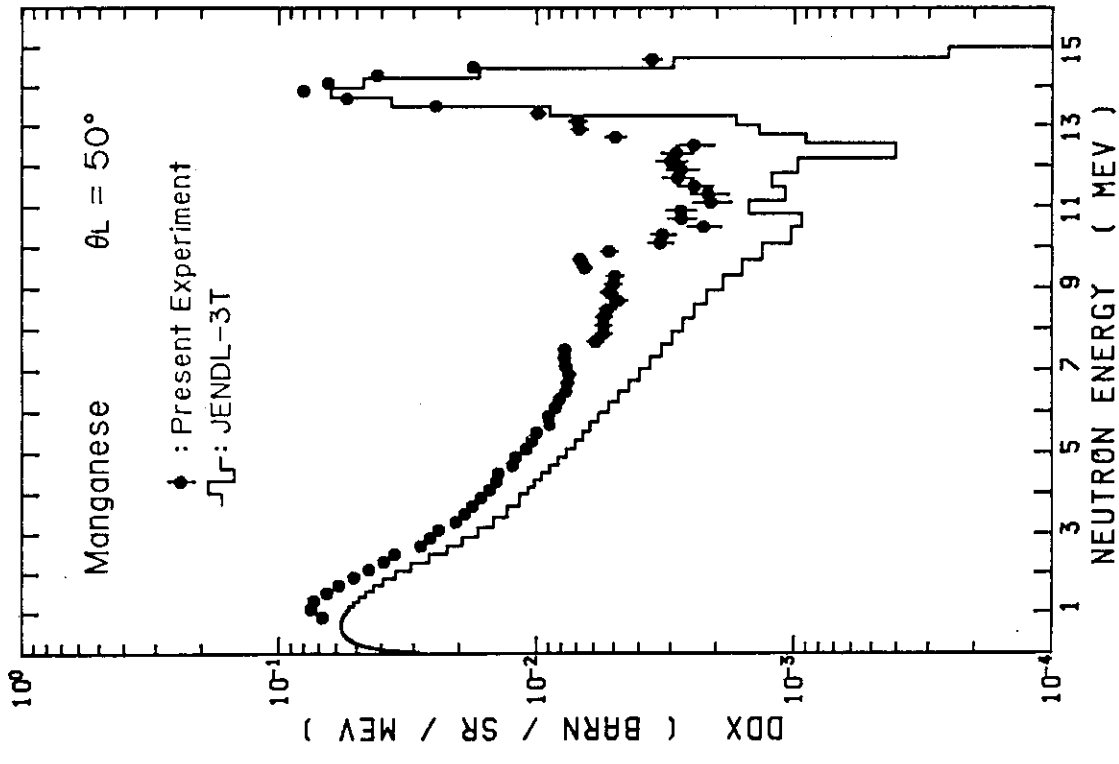

Fig. 20 Double differential neutron emission cross section at 50 deg with En = 14.1 MeV, for Mn

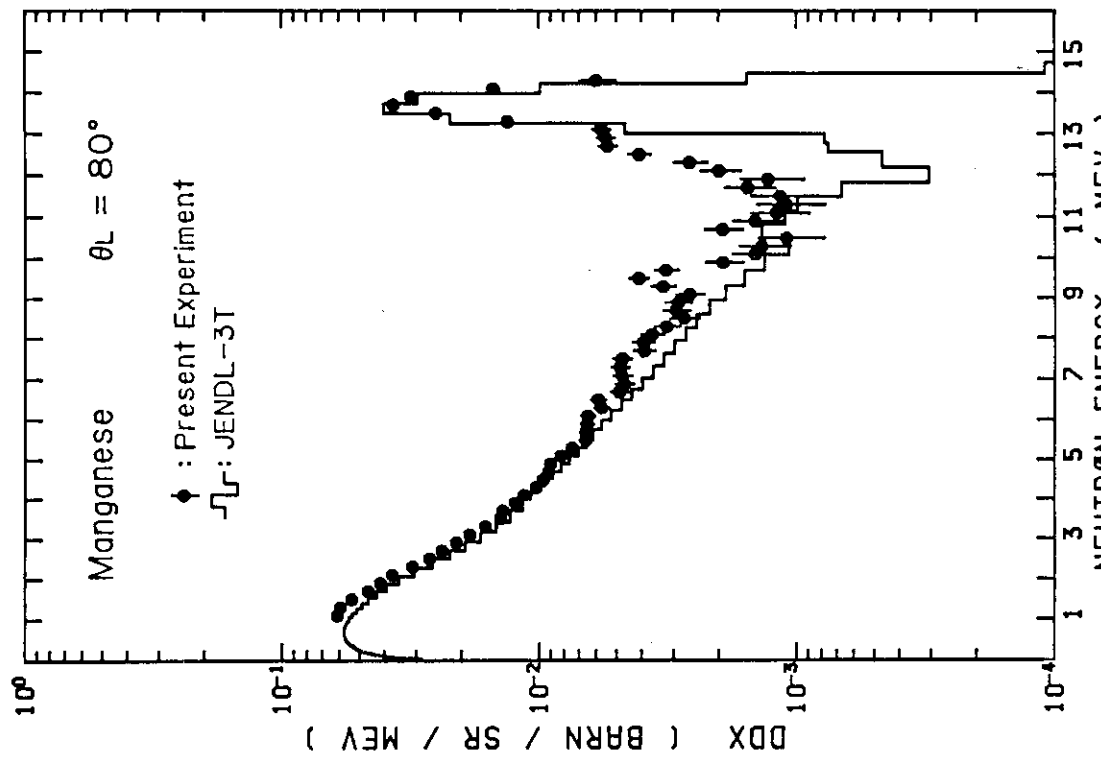

Fig. 23 Double differential neutron emission cross section at 80 deg with En = 14.1 MeV, for Mn

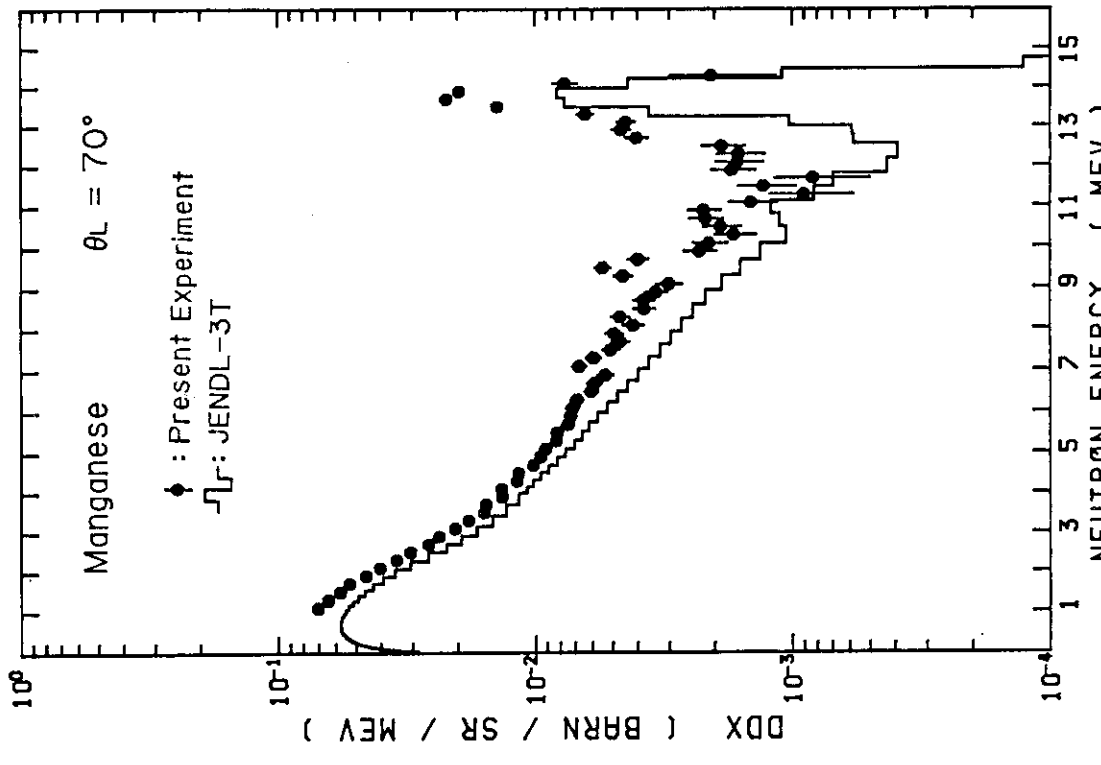

Fig. 22 Double differential neutron emission cross section at 70 deg with En = 14.1 MeV, for Mn

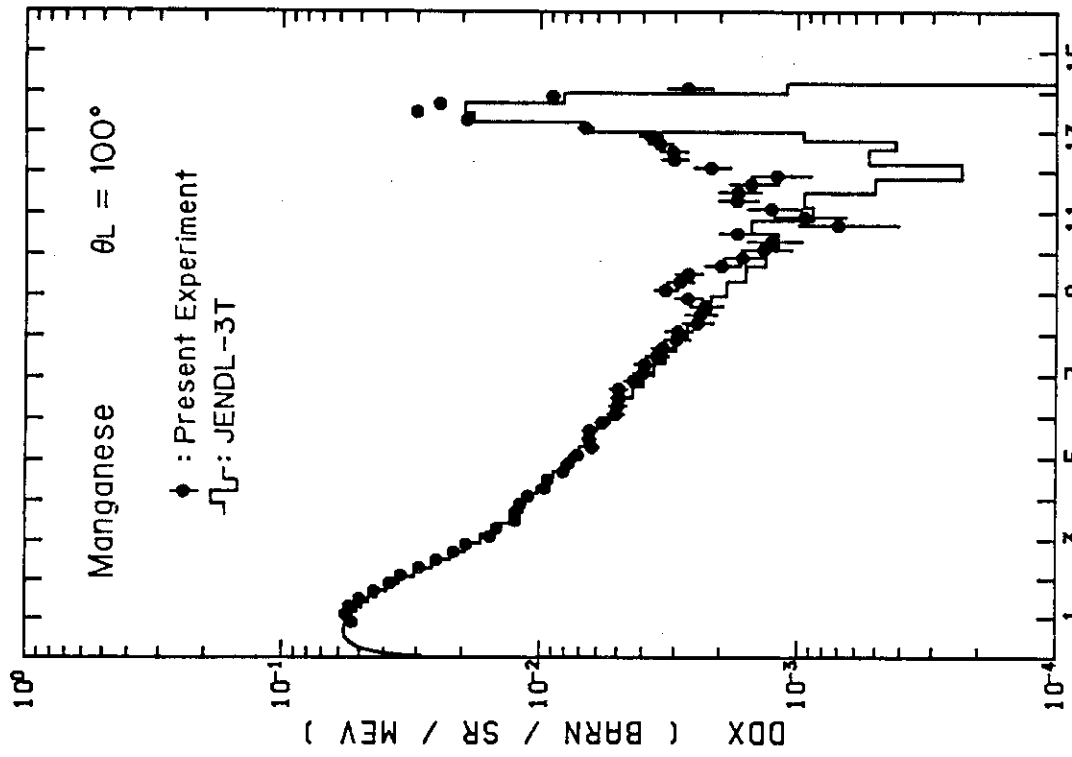

Fig. 25 Double differential neutron emission cross section at 100 deg with En = 14.1 MeV, for Mn

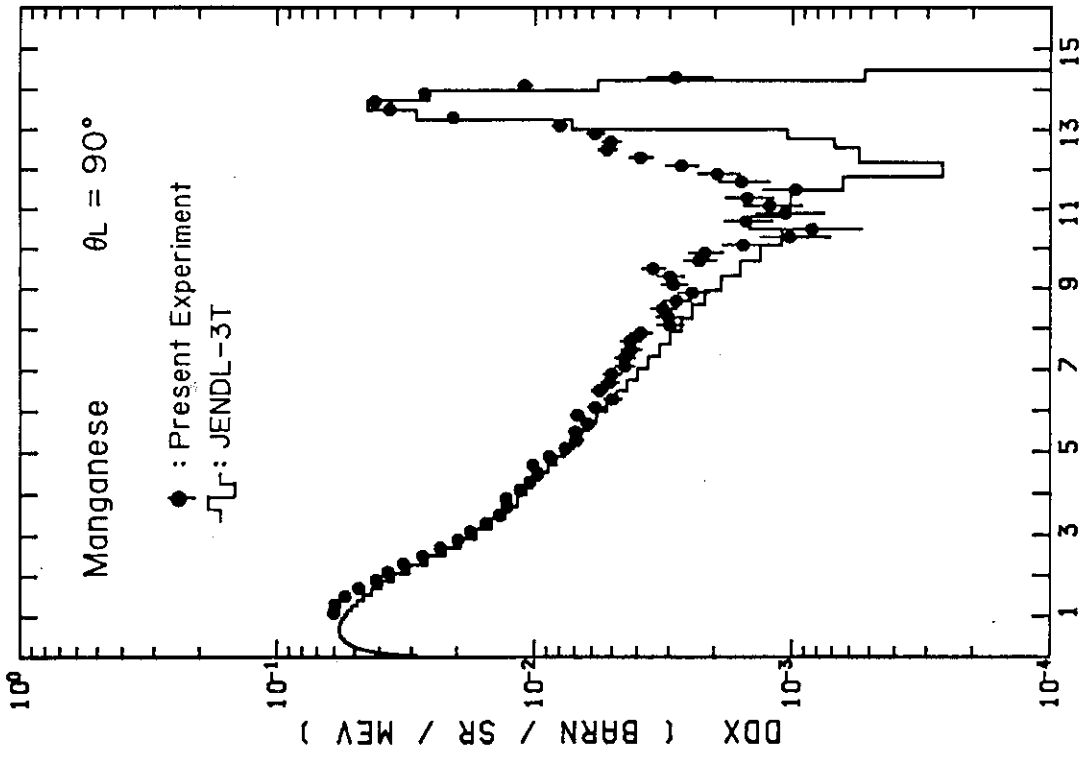

Fig. 24 Double differential neutron emission cross section at 90 deg with En = 14.1 MeV, for Mn

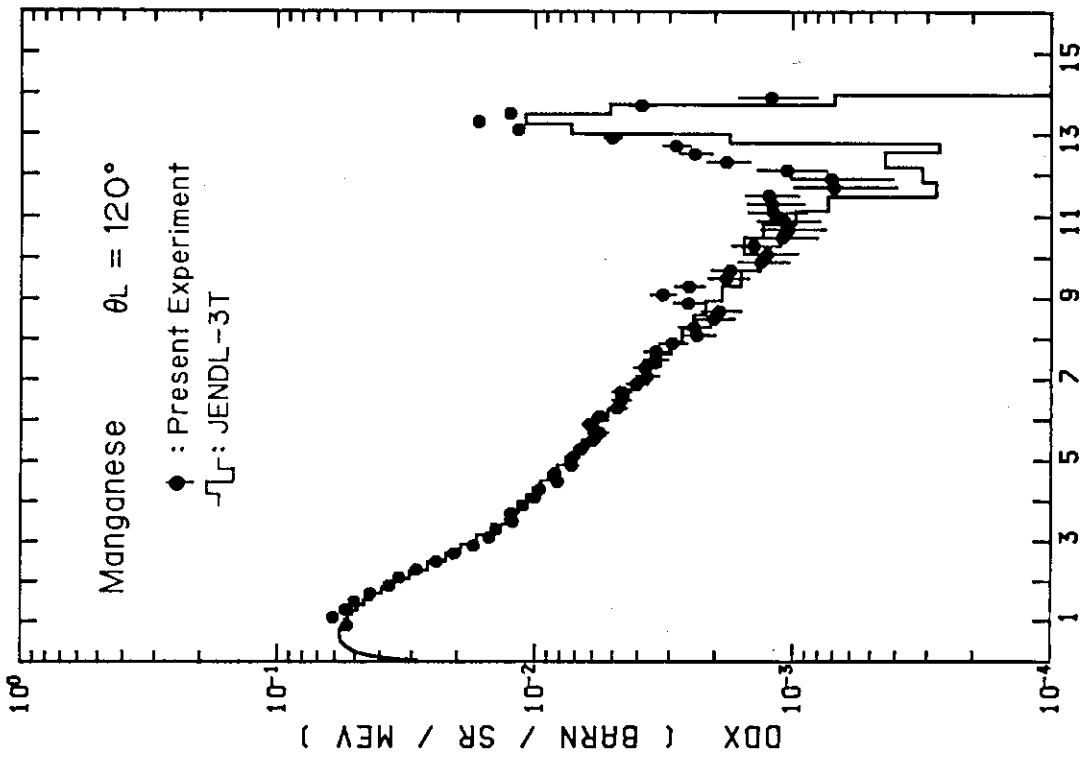

Fig. 27 Double differential neutron emission cross section at 120 deg with En = 14.1 MeV, for Mn

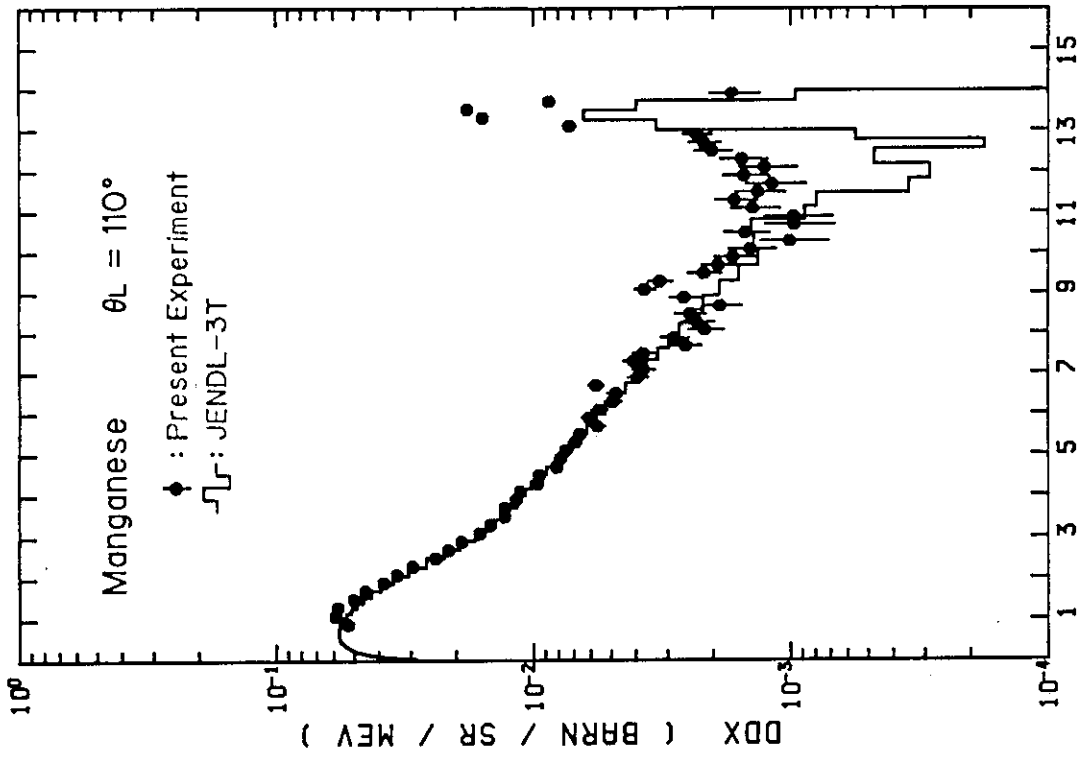

Fig. 26 Double differential neutron emission cross section at 110 deg with En = 14.1 MeV, for Mn

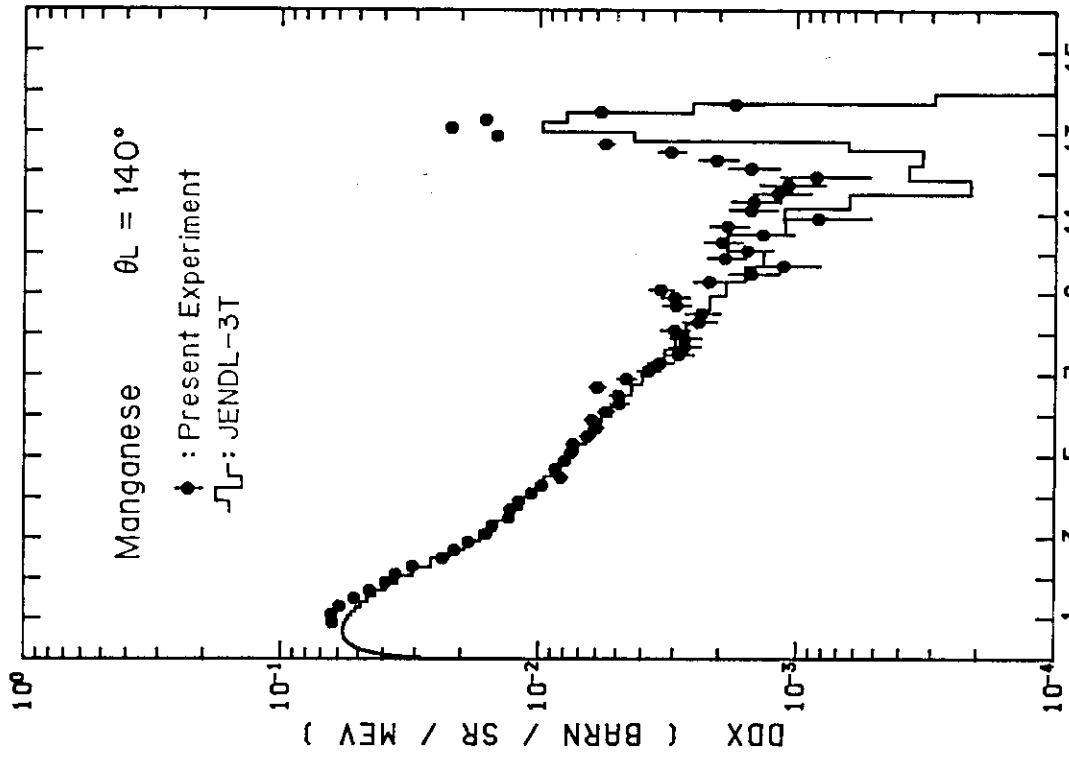

Fig. 29 Double differential neutron emission cross section at 140 deg with En = 14.1 MeV, for Mn

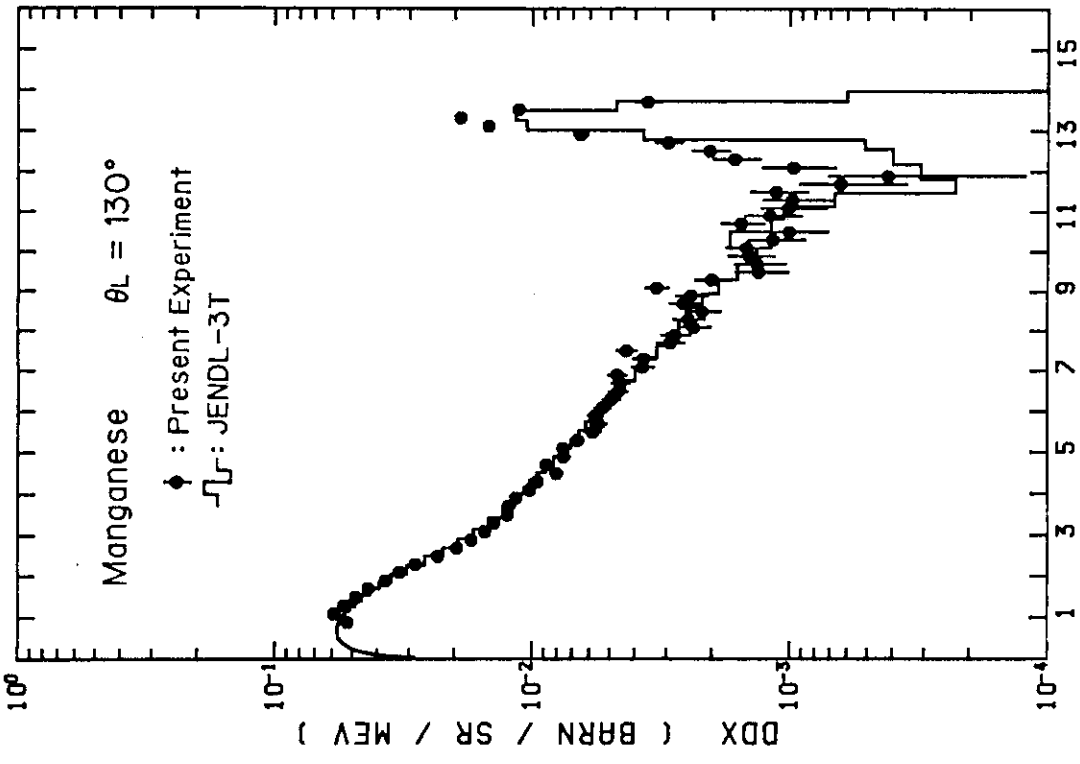

Fig. 28 Double differential neutron emission cross section at 130 deg with En = 14.1 MeV, for Mn

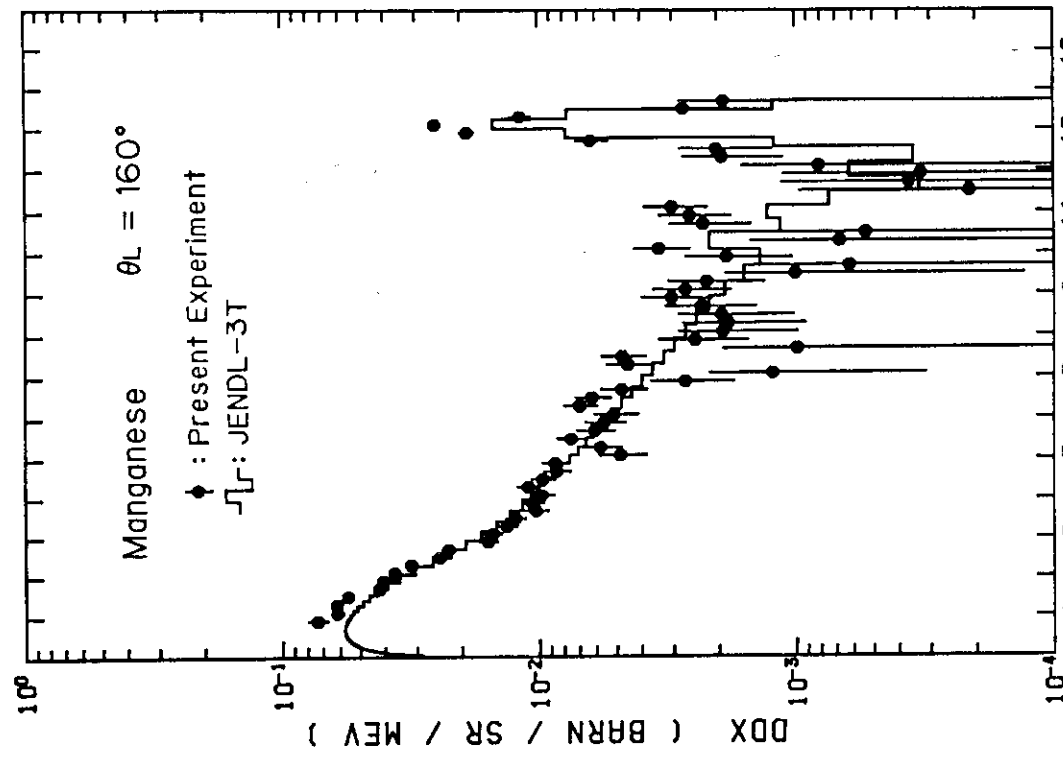

Fig. 31 Double differential neutron emission cross section at 160 deg with En = 14.1 MeV, for Mn

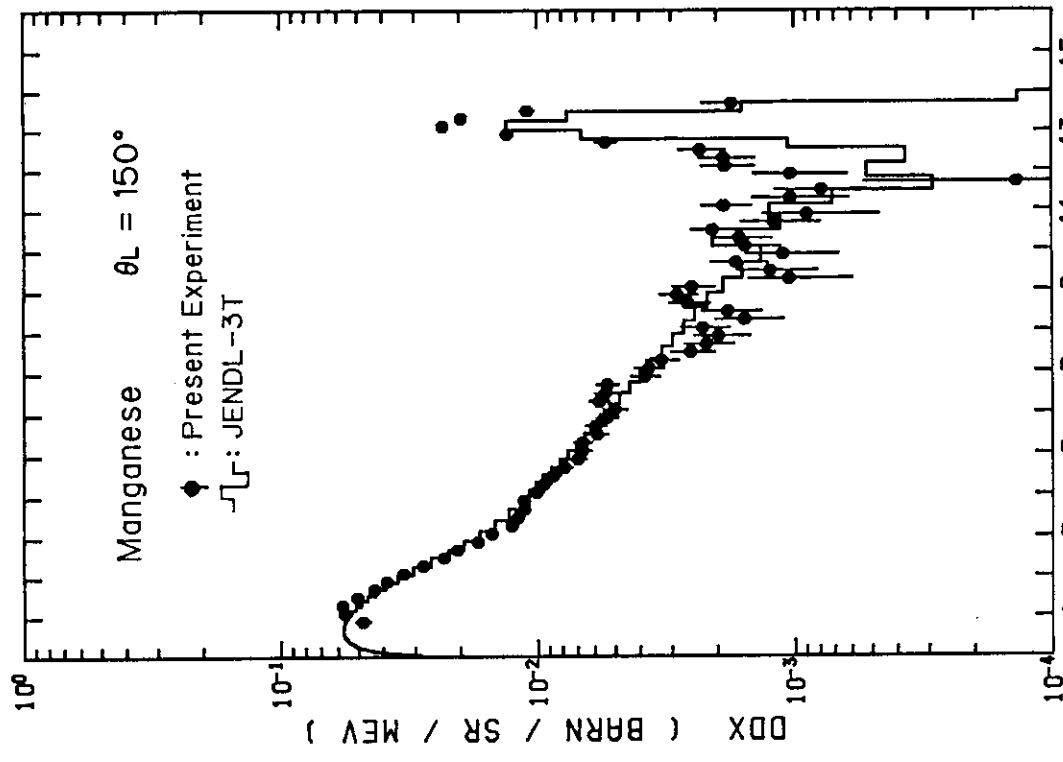

Fig. 30 Double differential neutron emission cross section at 150 deg with En = 14.1 MeV, for Mn

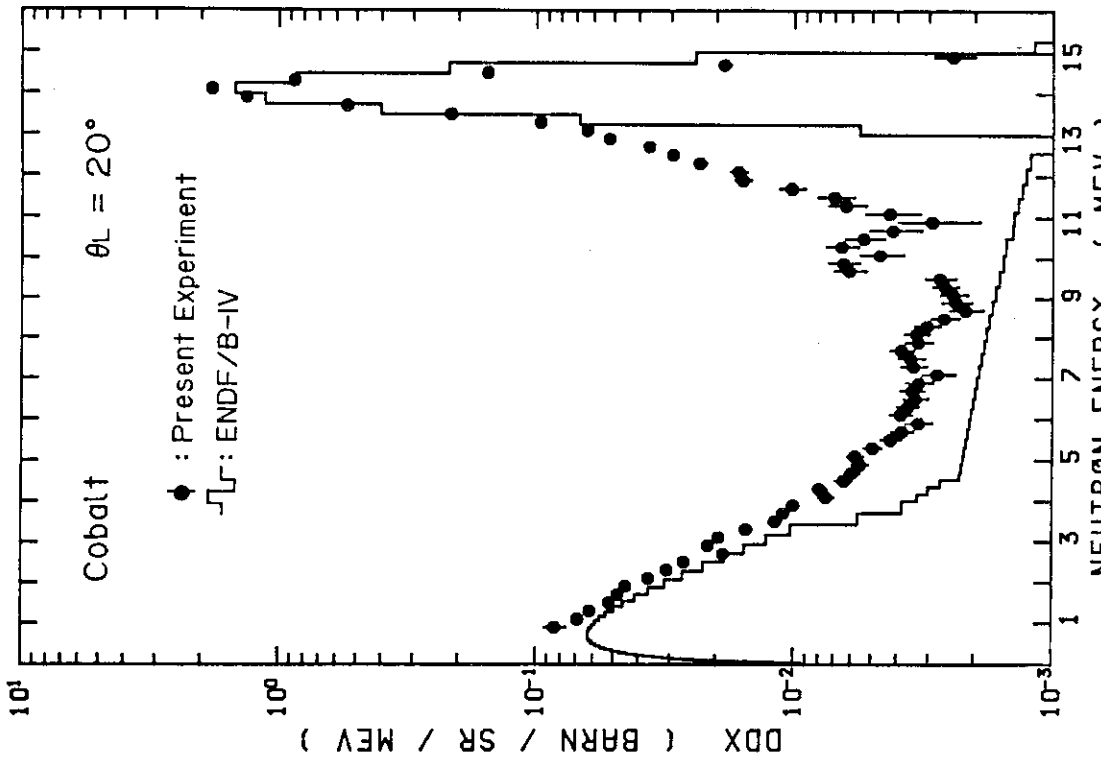

Fig. 33 Double differential neutron emission cross section at 20 deg with En = 14.1 MeV, for Co

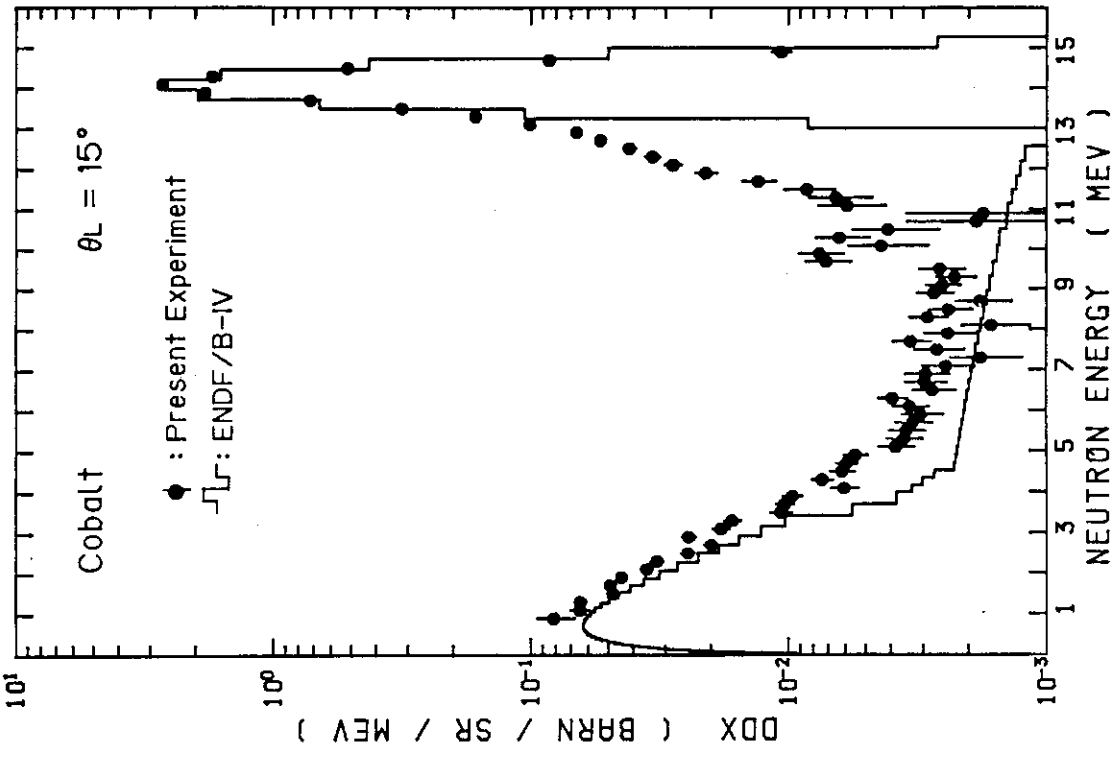

Fig. 32 Double differential neutron emission cross section at 15 deg with En = 14.1 MeV, for Co

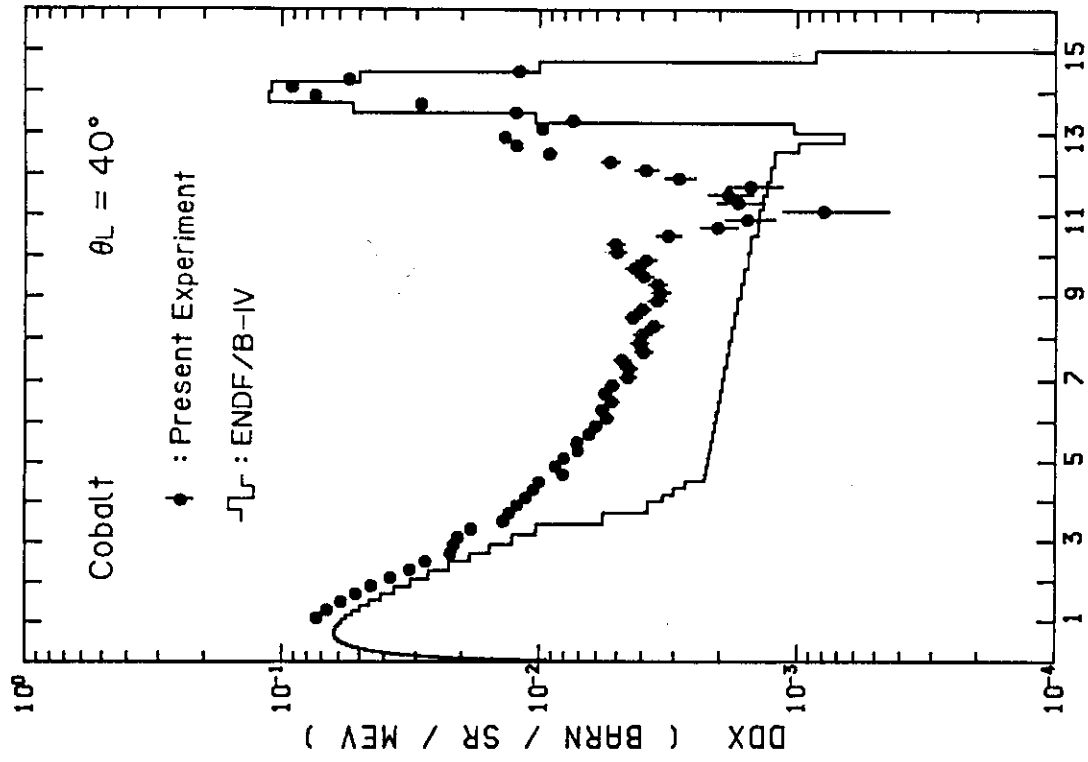

Fig. 35 Double differential neutron emission cross section at 40 deg with En = 14.1 MeV, for Co

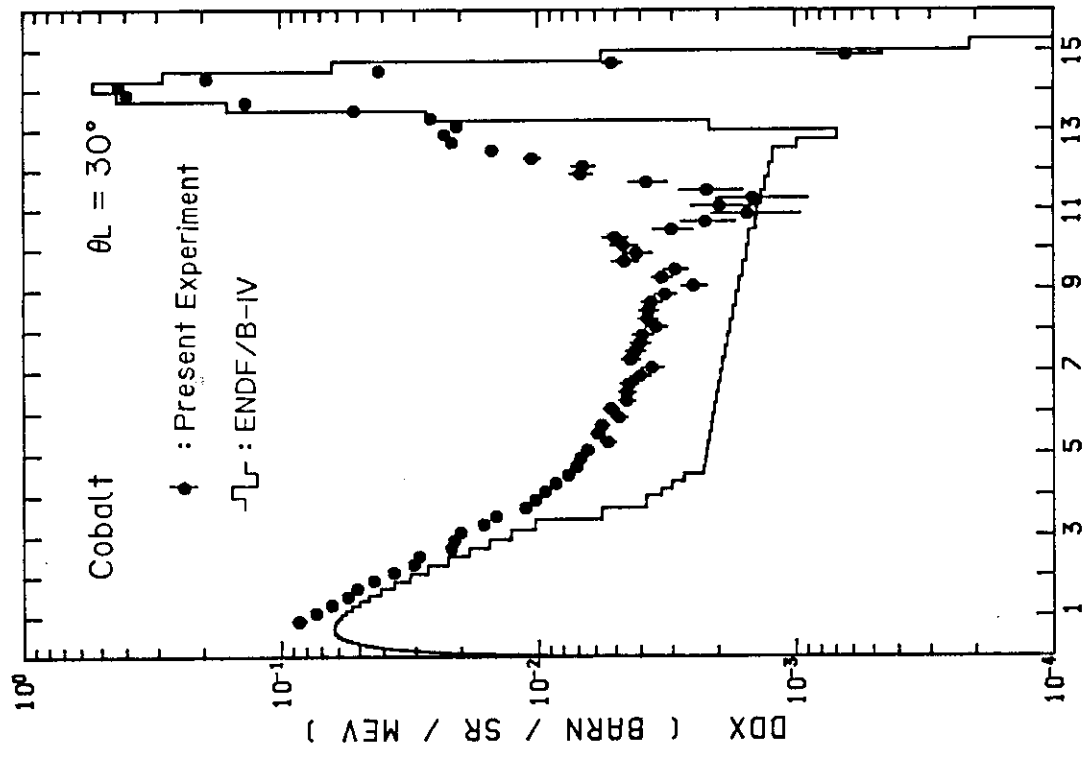

Fig. 34 Double differential neutron emission cross section at 30 deg with En = 14.1 MeV, for Co

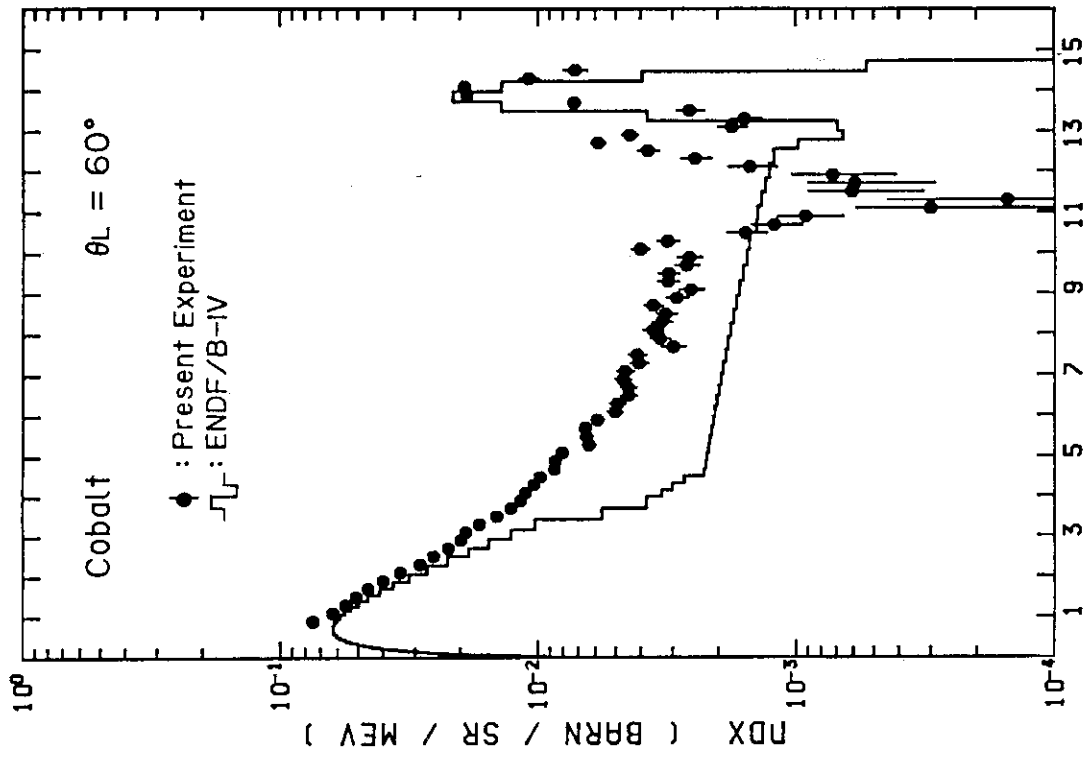

Fig. 37 Double differential neutron emission cross section at 60 deg with En = 14.1 MeV, for Co

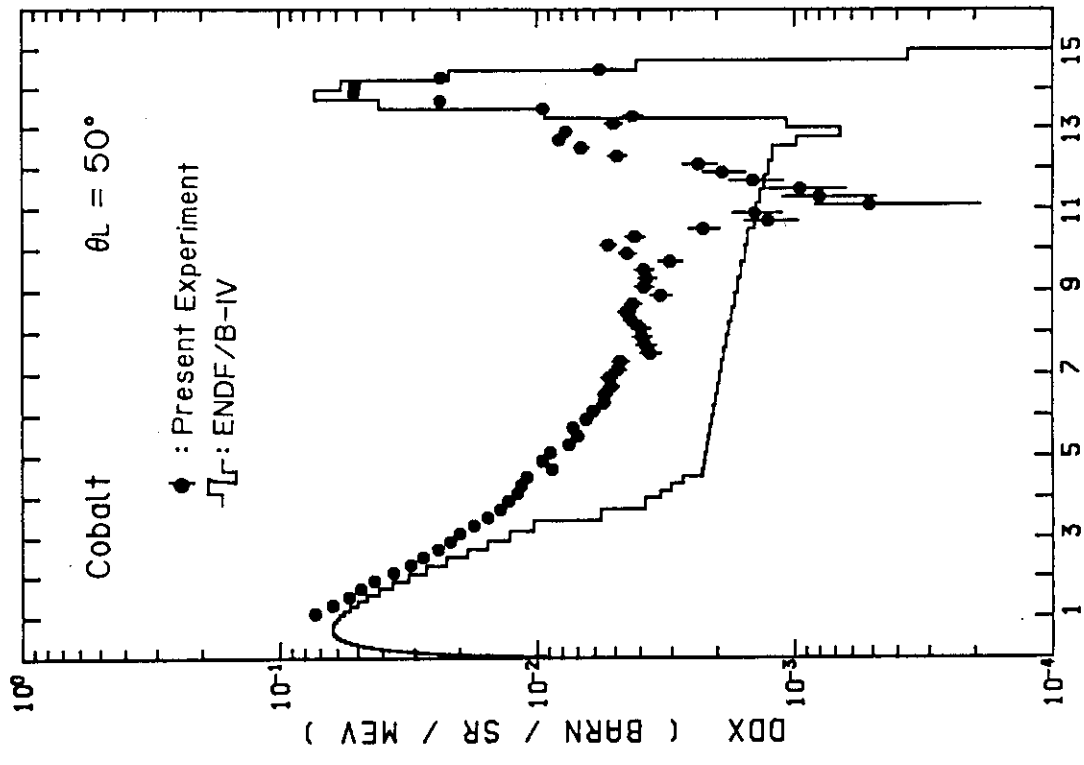

Fig. 36 Double differential neutron emission cross section at 50 deg with En = 14.1 MeV, for Co

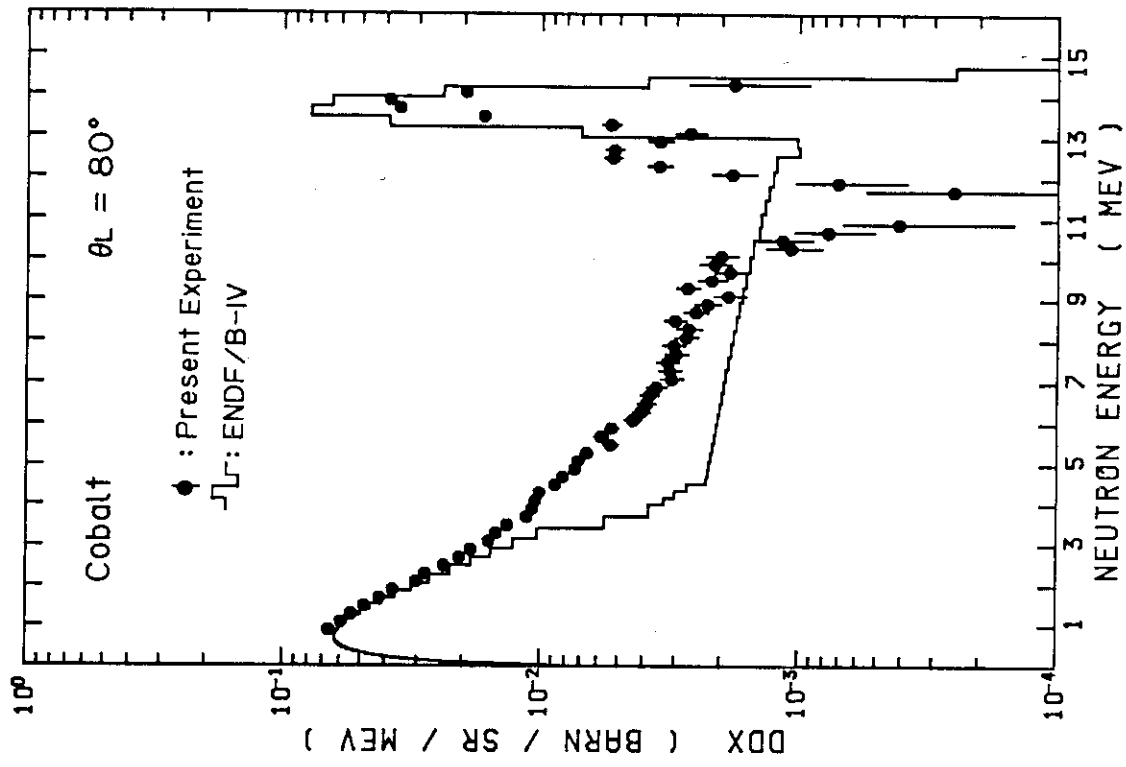

Fig. 39 Double differential neutron emission cross section at 80 deg with En = 14.1 MeV, for Co

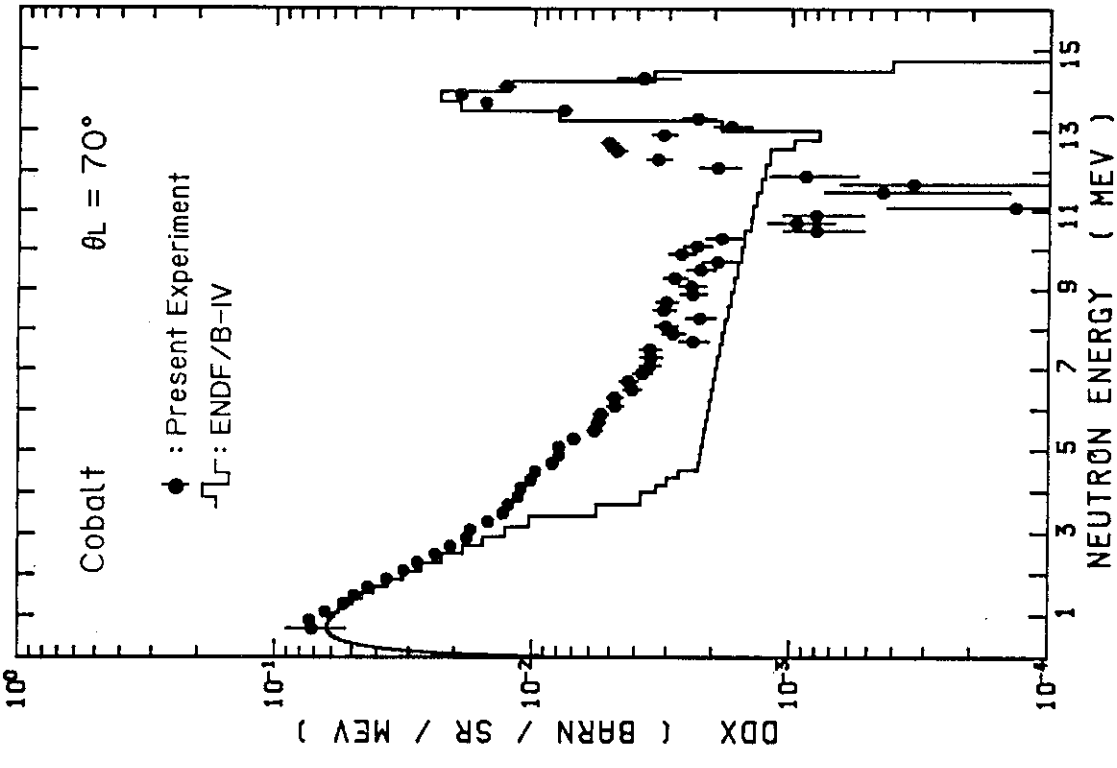

Fig. 38 Double differential neutron emission cross section at 70 deg with En = 14.1 MeV, for Co

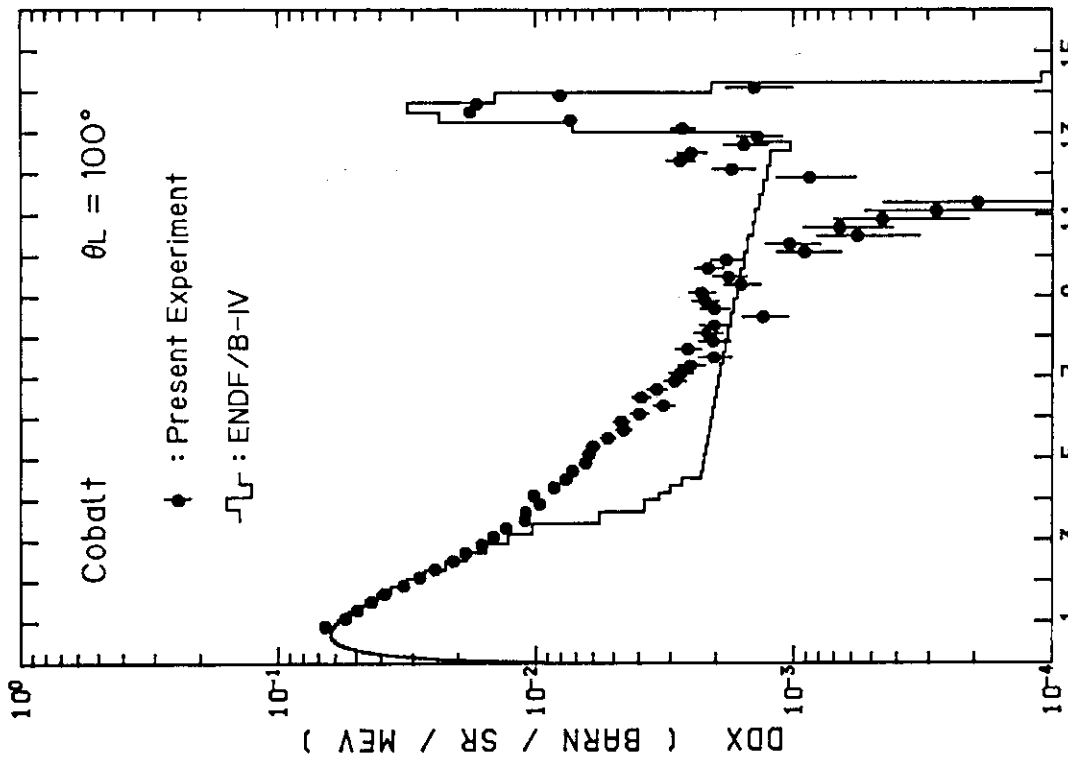

Fig. 41 Double differential neutron emission cross section at 100 deg with En = 14.1 MeV, for Co

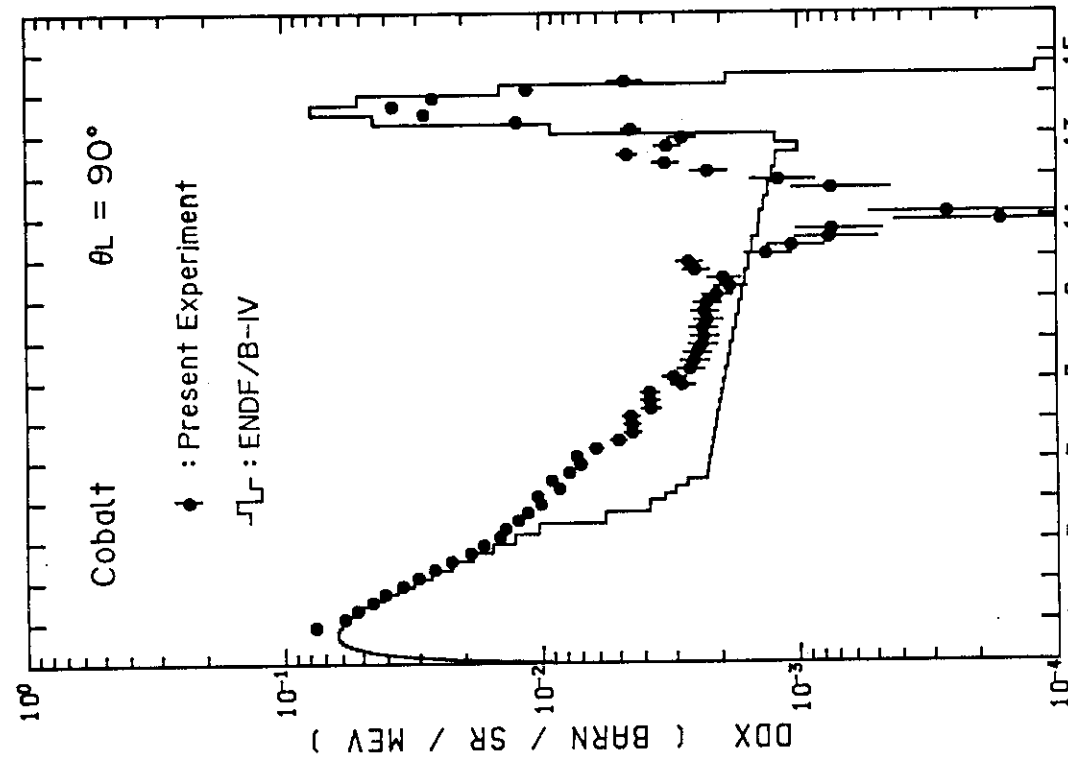

Fig. 40 Double differential neutron emission cross section at 90 deg with En = 14.1 MeV, for Co

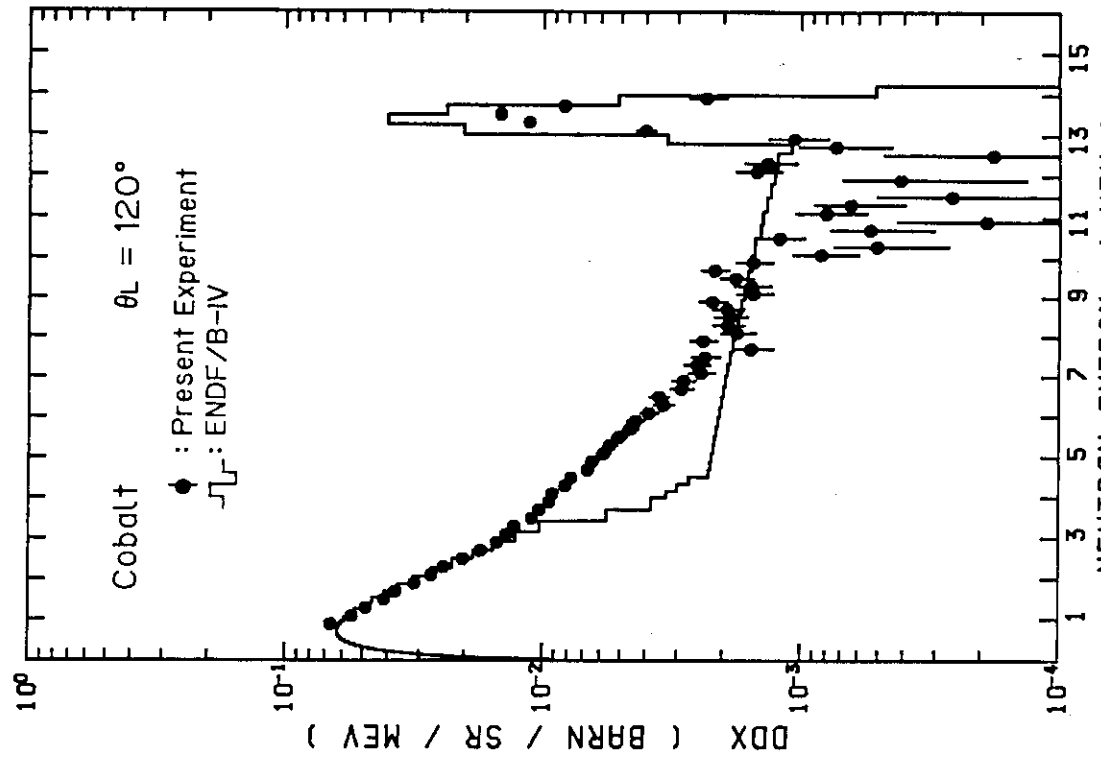

Fig. 43 Double differential neutron emission cross section at 120 deg with En = 14.1 MeV, for Co

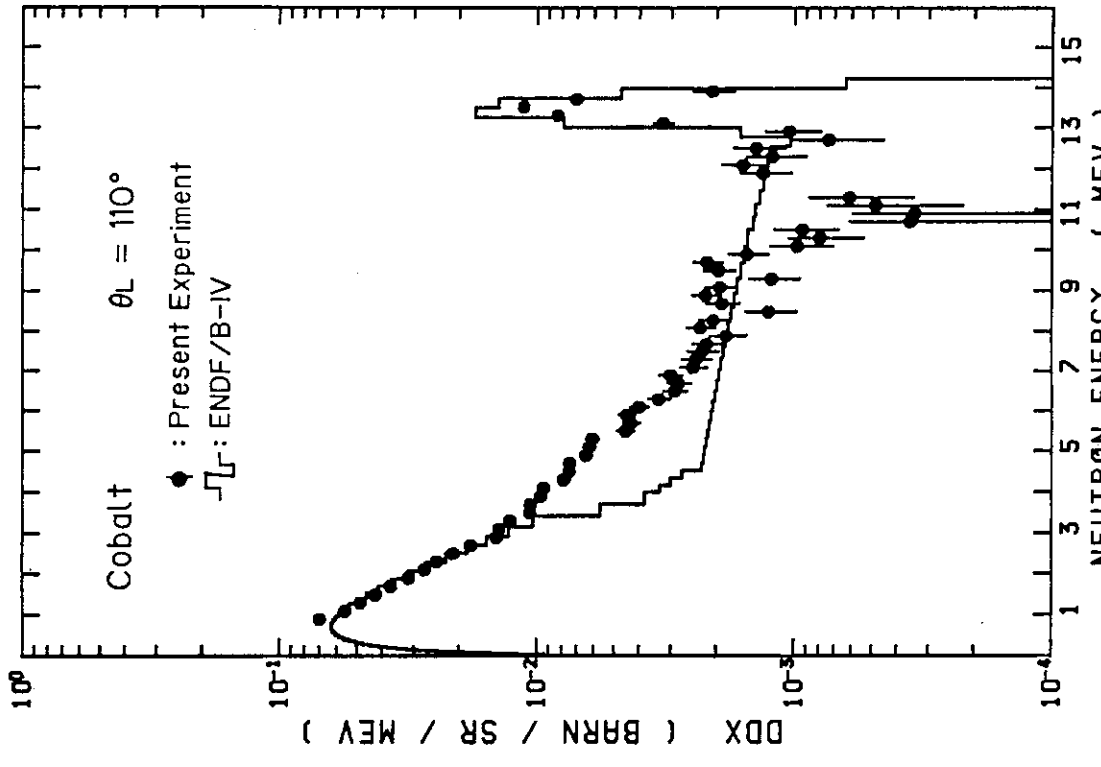

Fig. 42 Double differential neutron emission cross section at 110 deg with En = 14.1 MeV, for Co

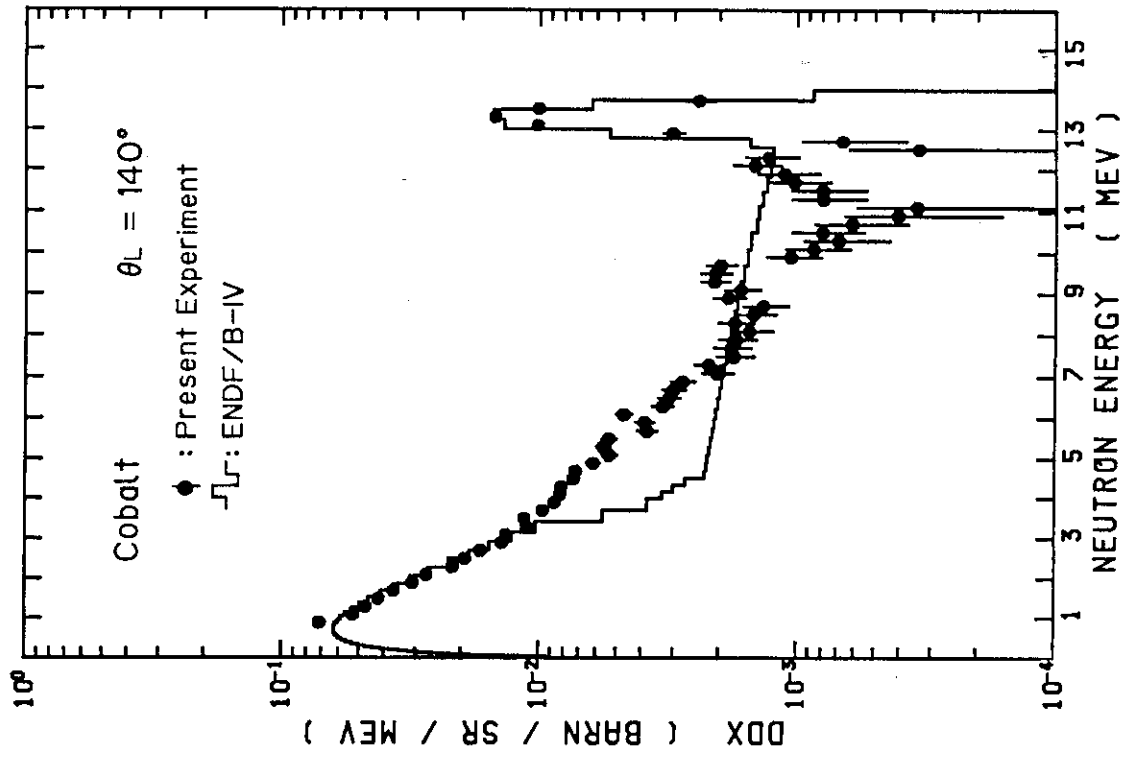

Fig. 45 Double differential neutron emission cross section at 140 deg with En = 14.1 MeV, for Co

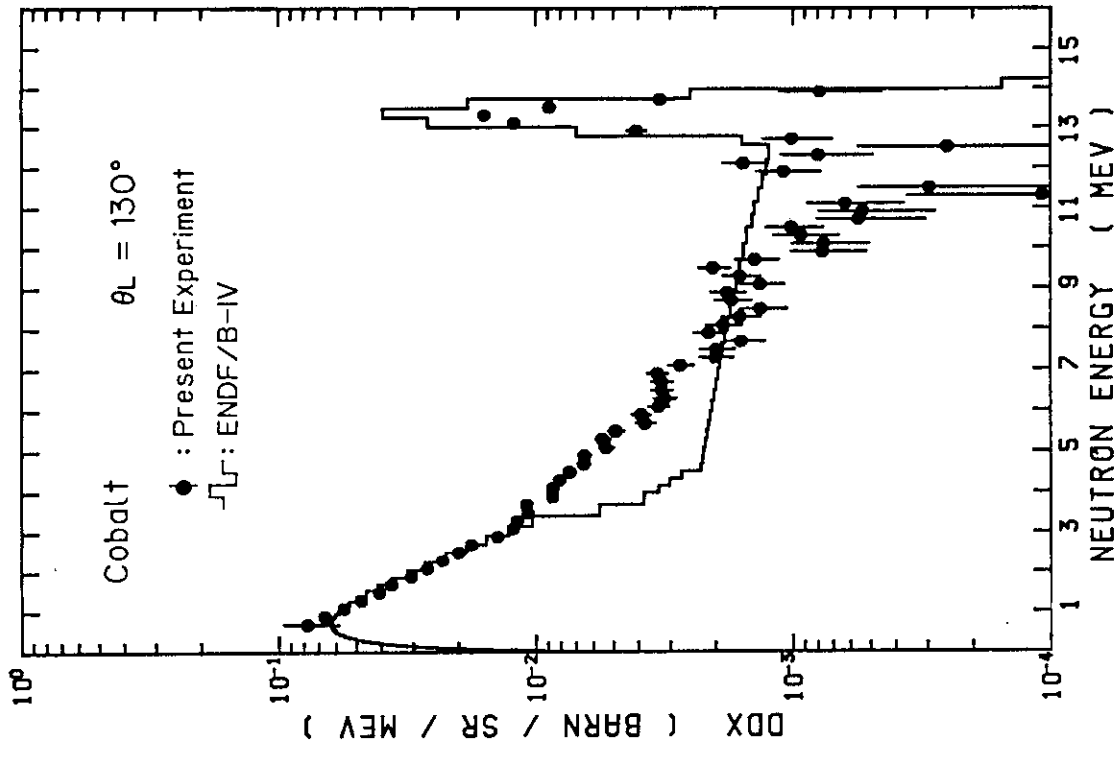

Fig. 44 Double differential neutron emission cross section at 130 deg with En = 14.1 MeV, for Co

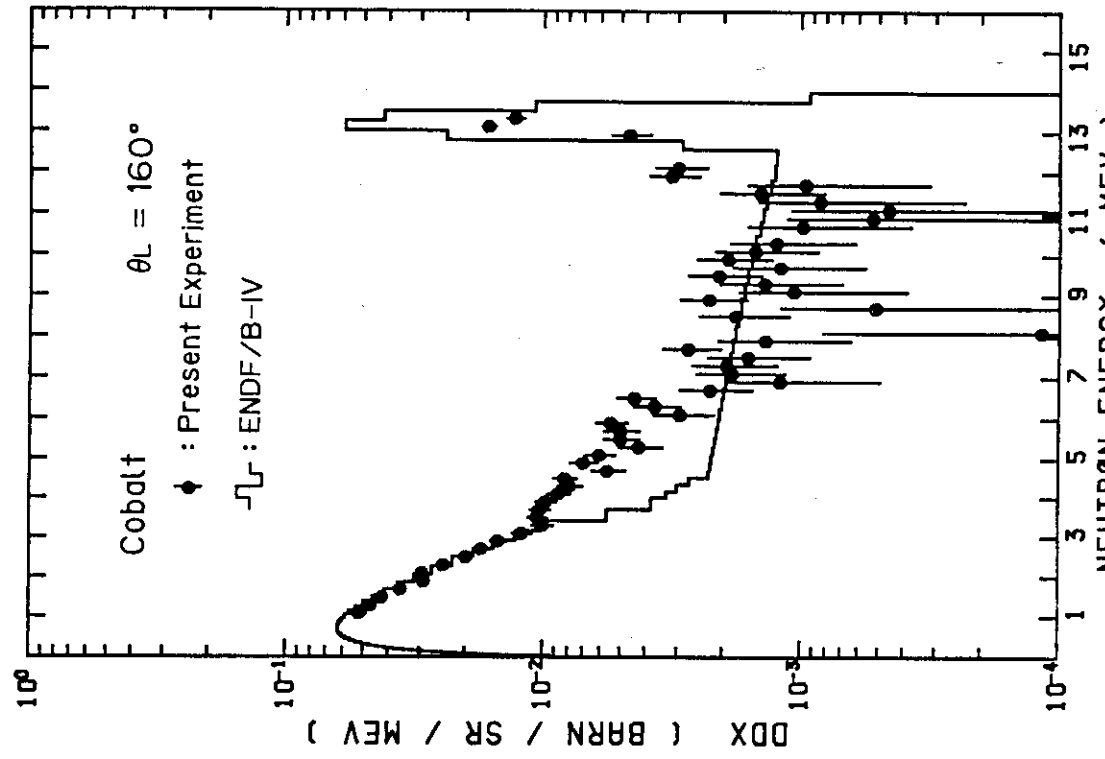

Fig. 47 Double differential neutron emission cross section at 160 deg with En = 14.1 MeV, for Co

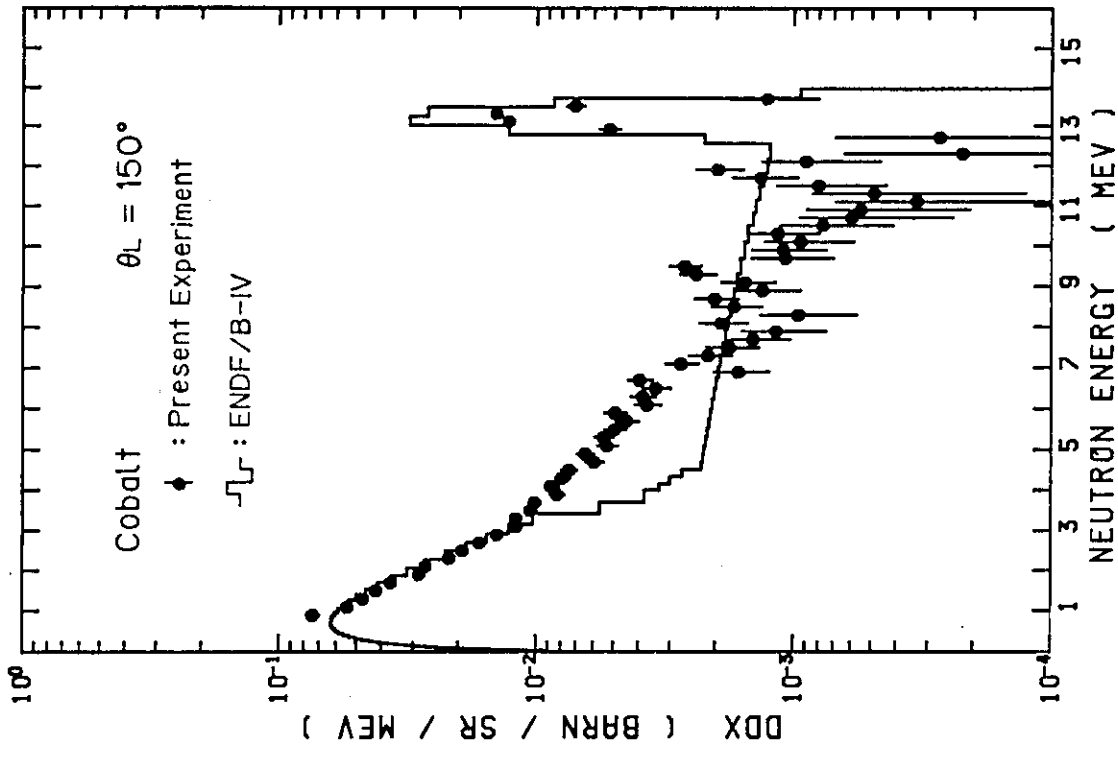

Fig. 46 Double differential neutron emission cross section at 150 deg with En = 14.1 MeV, for Co

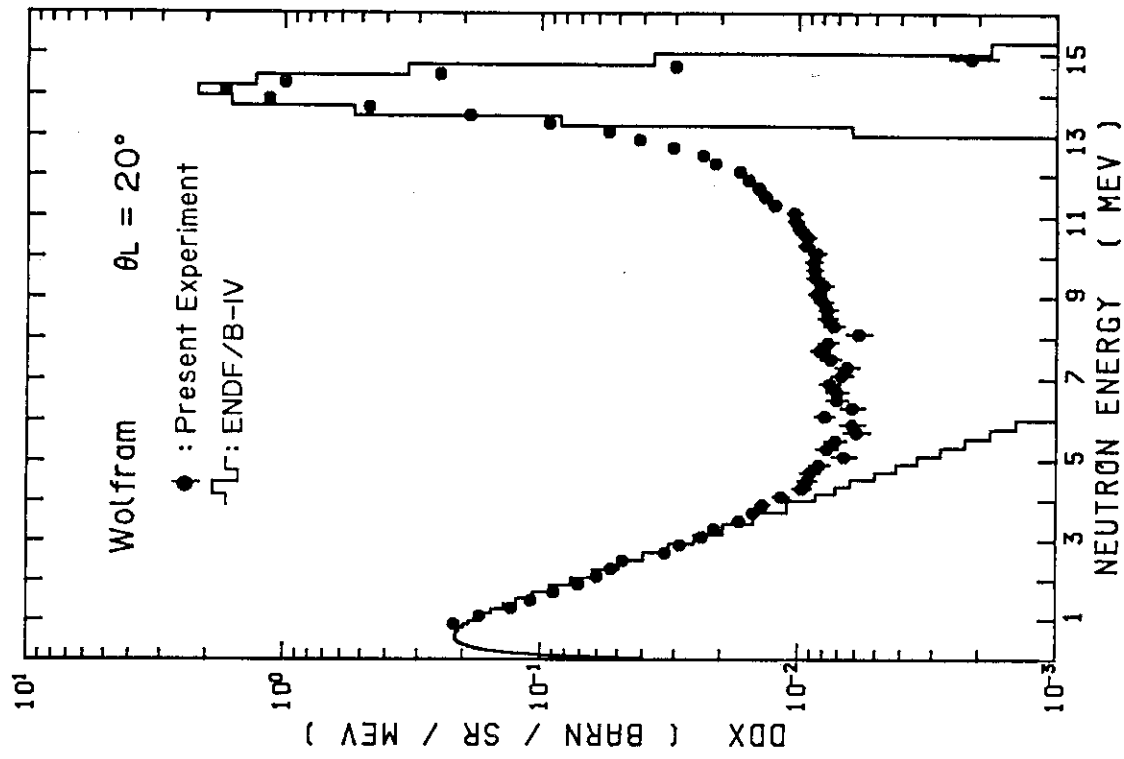

Fig. 49 Double differential neutron emission cross section at 20 deg with En = 14.1 MeV, for W

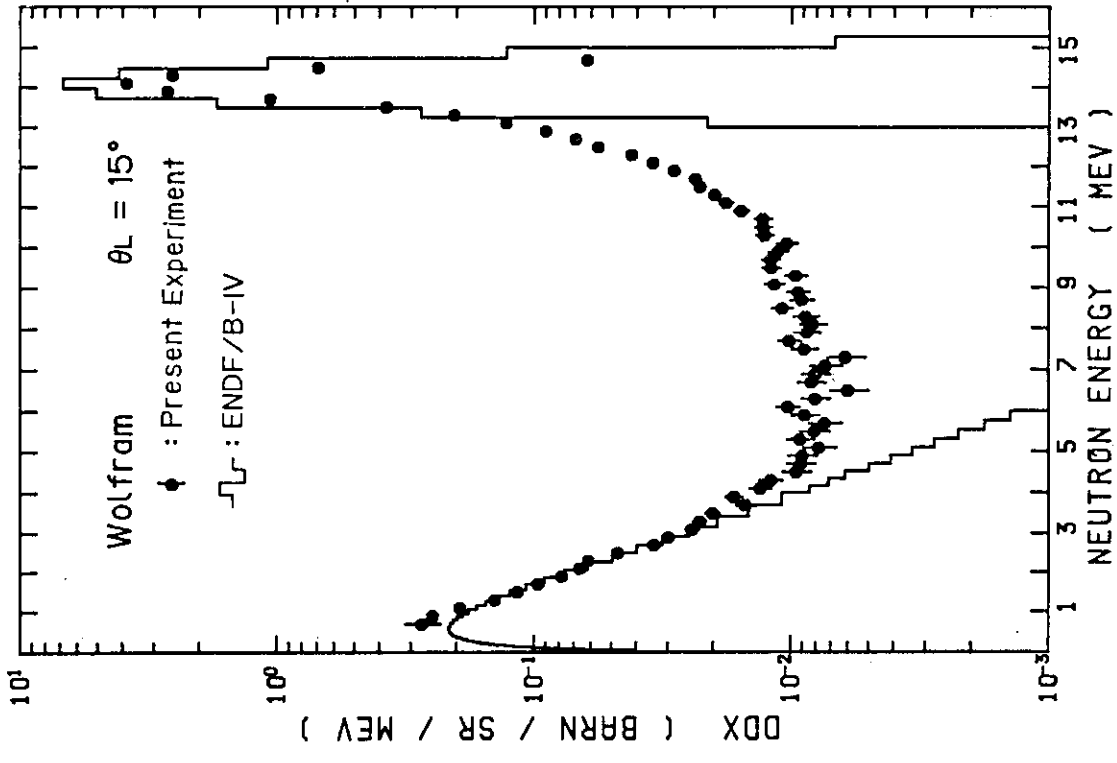

Fig. 48 Double differential neutron emission cross section at 15 deg with En = 14.1 MeV, for W

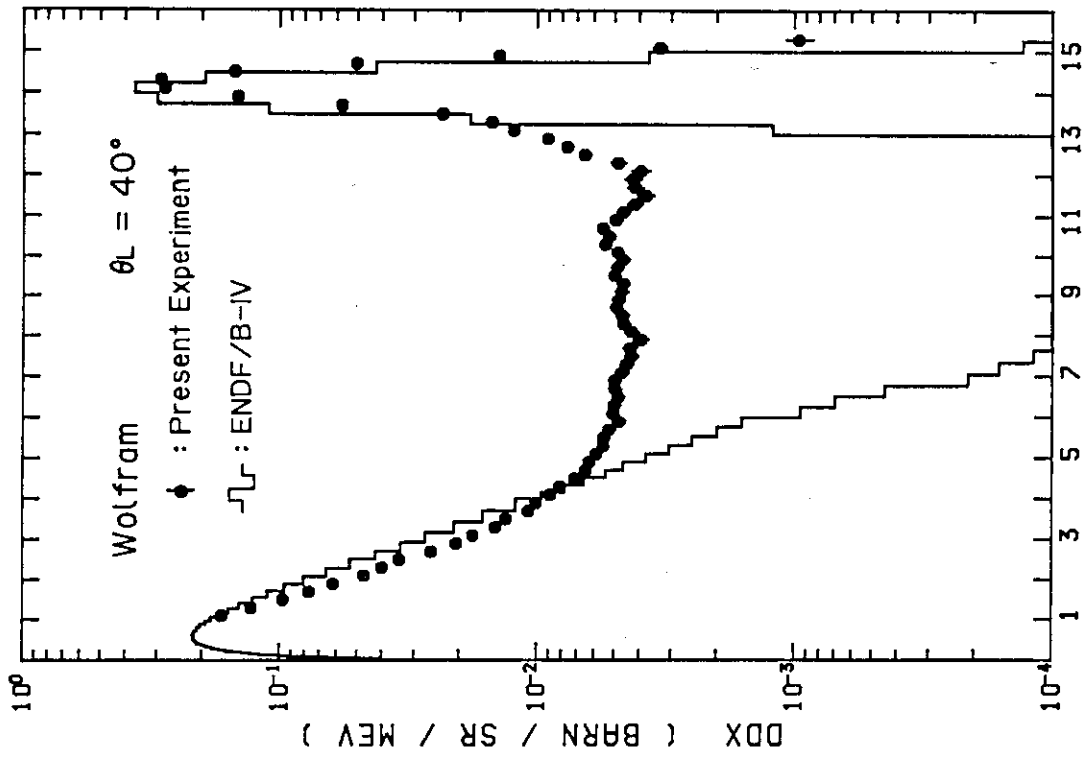

Fig. 51 Double differential neutron emission cross section at 40 deg with En = 14.1 MeV, for W

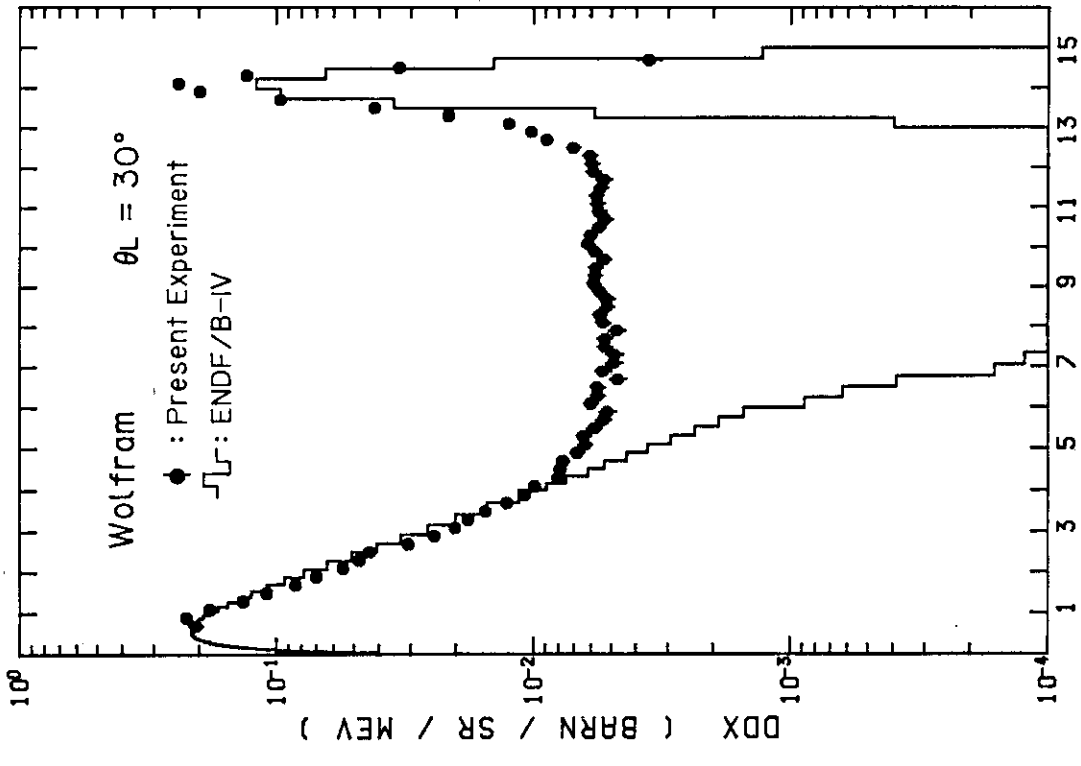

Fig. 50 Double differential neutron emission cross section at 30 deg with En = 14.1 MeV, for W

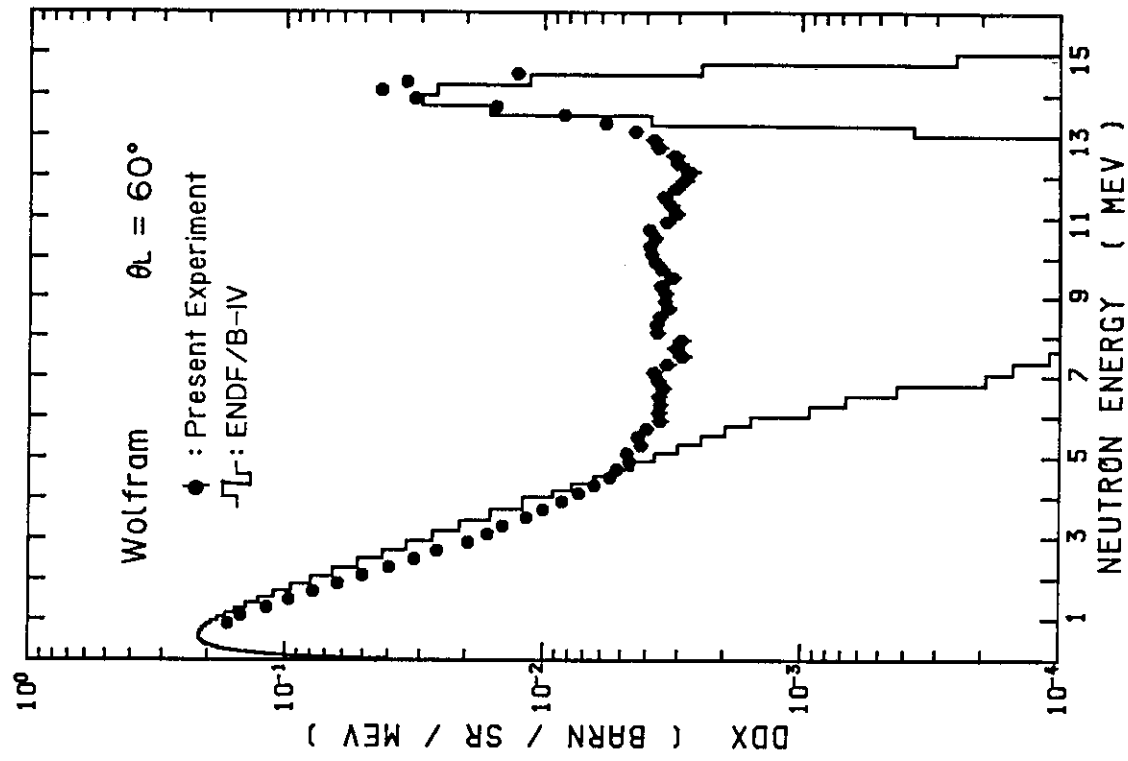

Fig. 53 Double differential neutron emission cross section at 60 deg with En = 14.1 MeV, for W

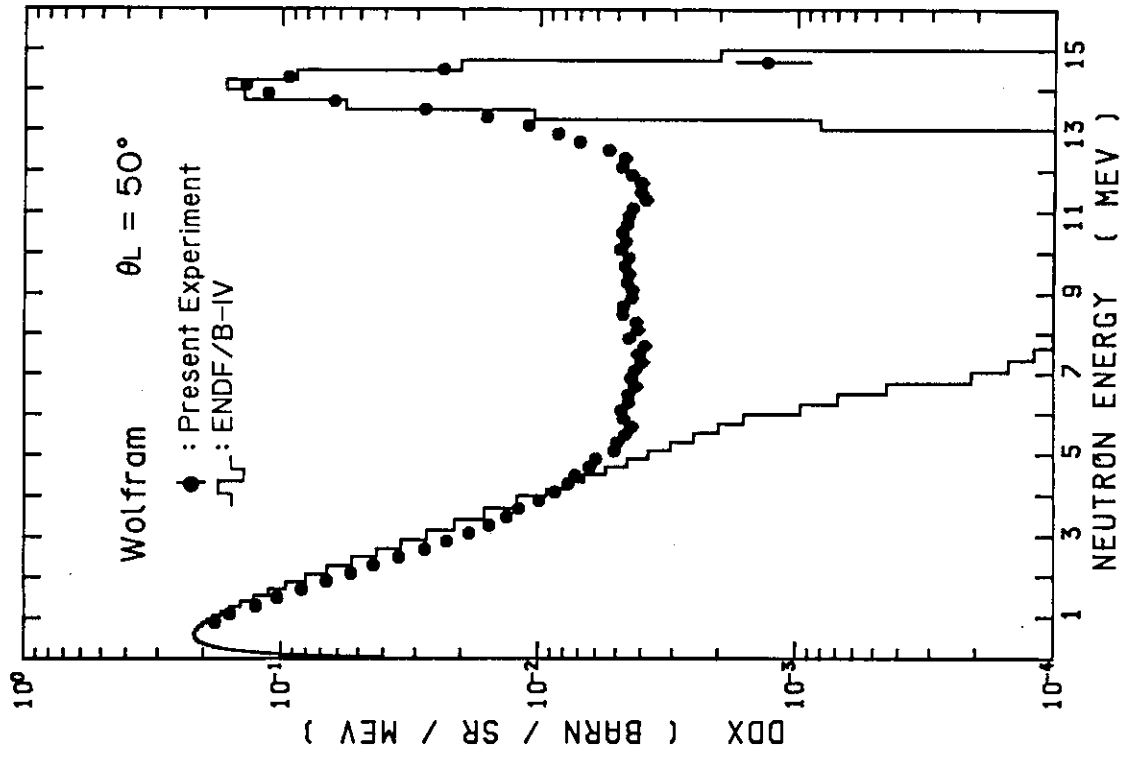

Fig. 52 Double differential neutron emission cross section at 50 deg with En = 14.1 MeV, for W

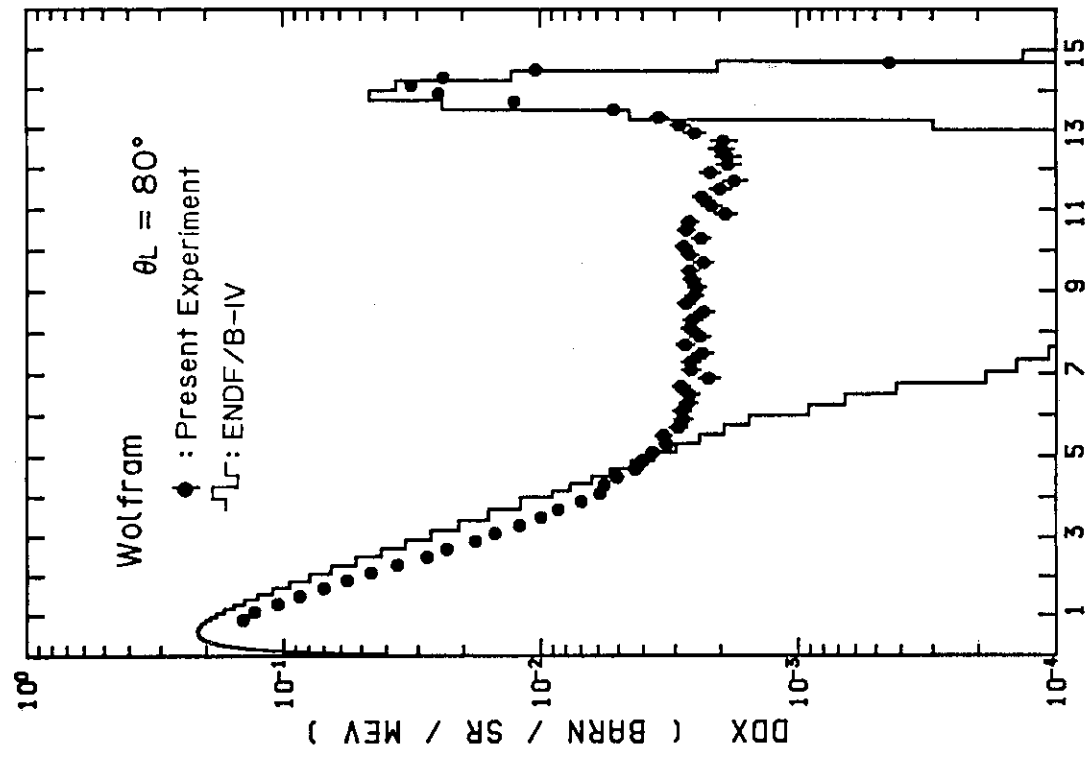

Fig. 55 Double differential neutron emission cross section at 80 deg with En = 14.1 MeV, for W

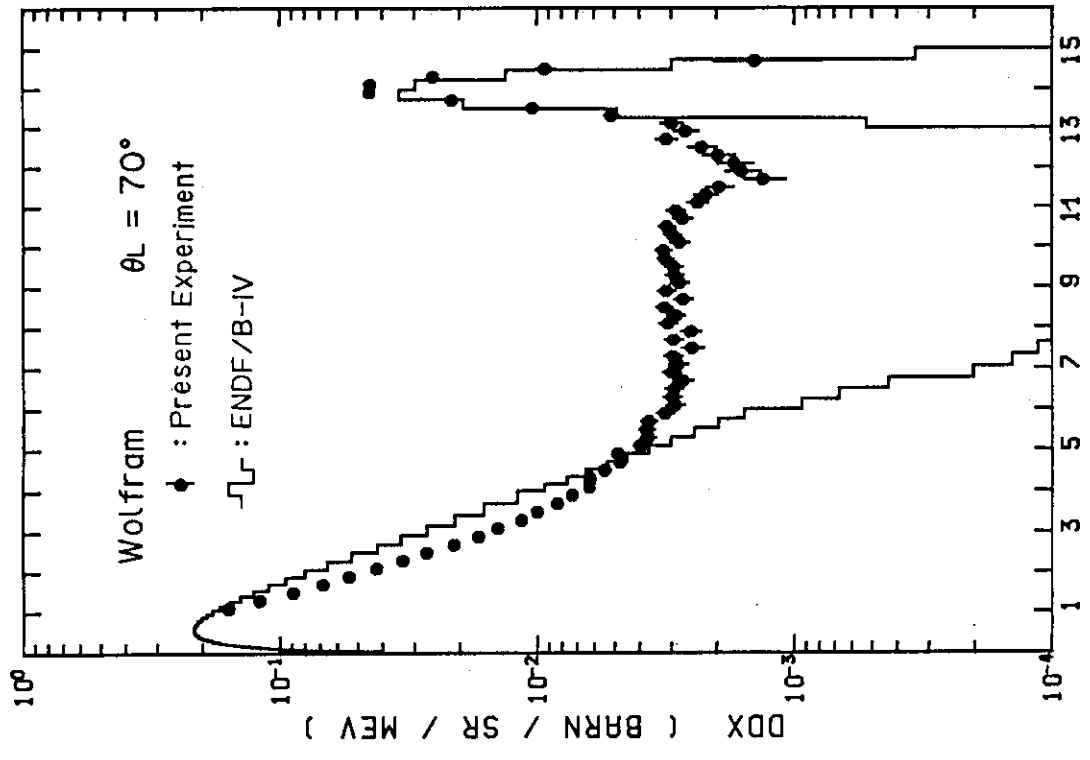

Fig. 54 Double differential neutron emission cross section at 70 deg with En = 14.1 MeV, for W

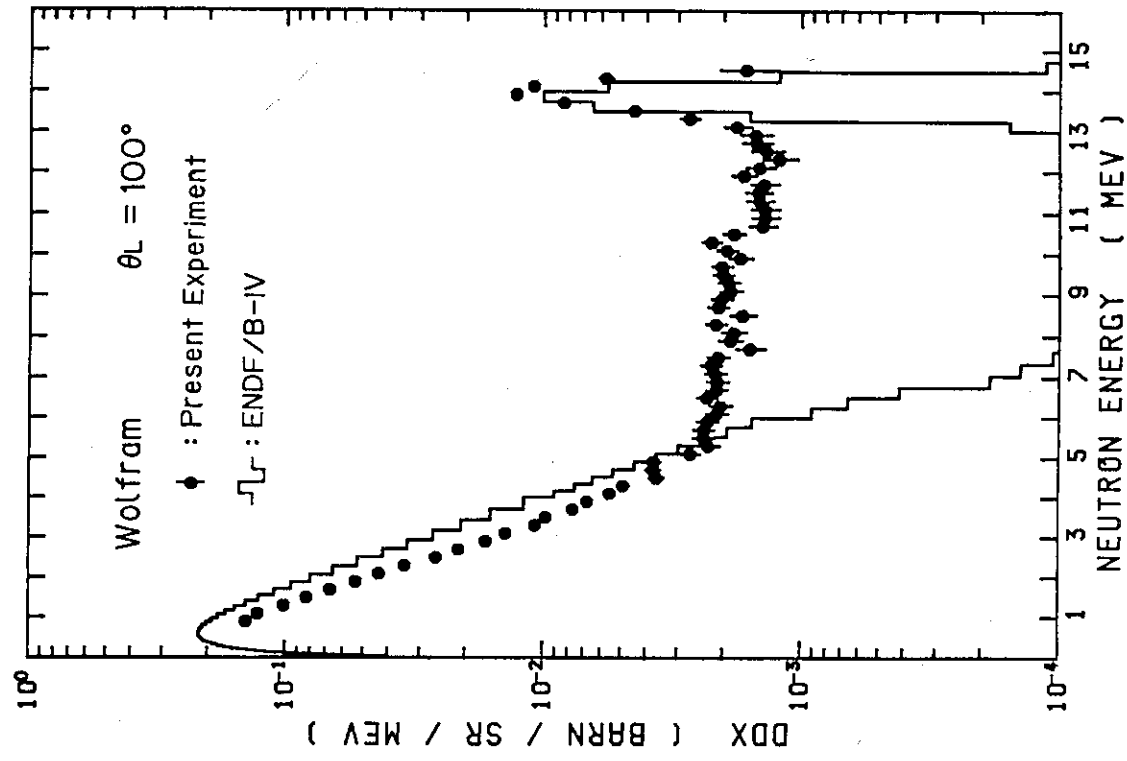

Fig. 57 Double differential neutron emission cross section at 100 deg with En = 14.1 MeV, for W

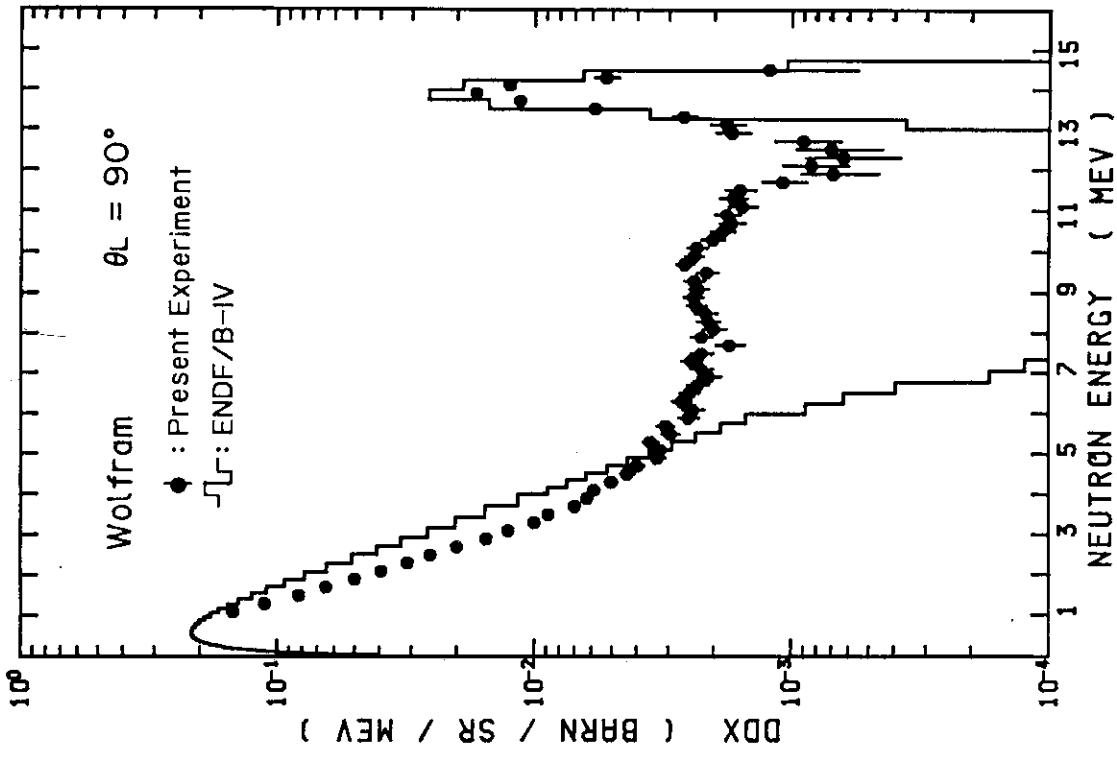

Fig. 56 Double differential neutron emission cross section at 90 deg with En = 14.1 MeV, for W

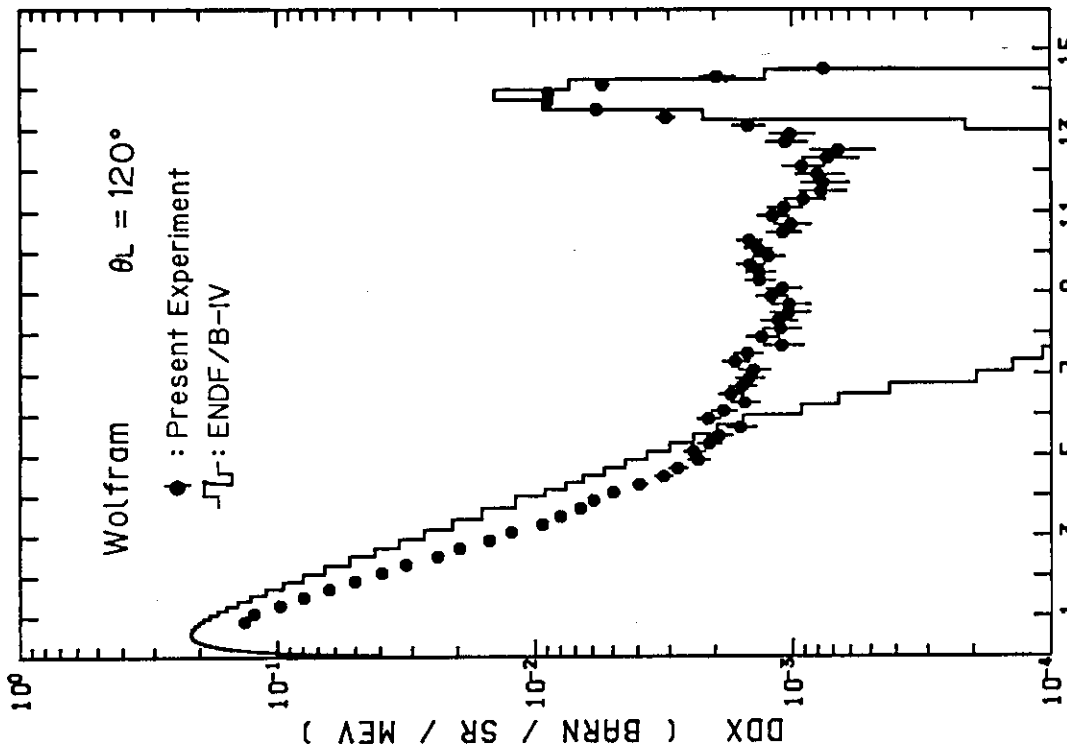

Fig. 59 Double differential neutron emission cross section at 120 deg with En = 14.1 MeV, for W

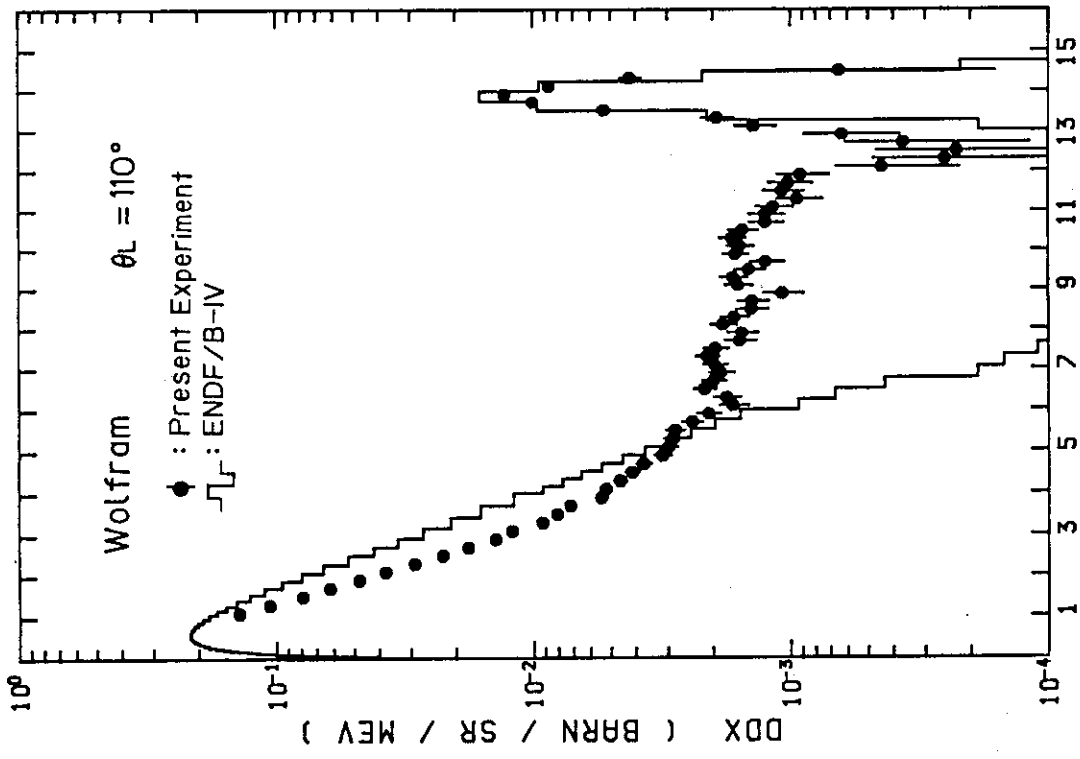

Fig. 58 Double differential neutron emission cross section at 110 deg with En = 14.1 MeV, for W

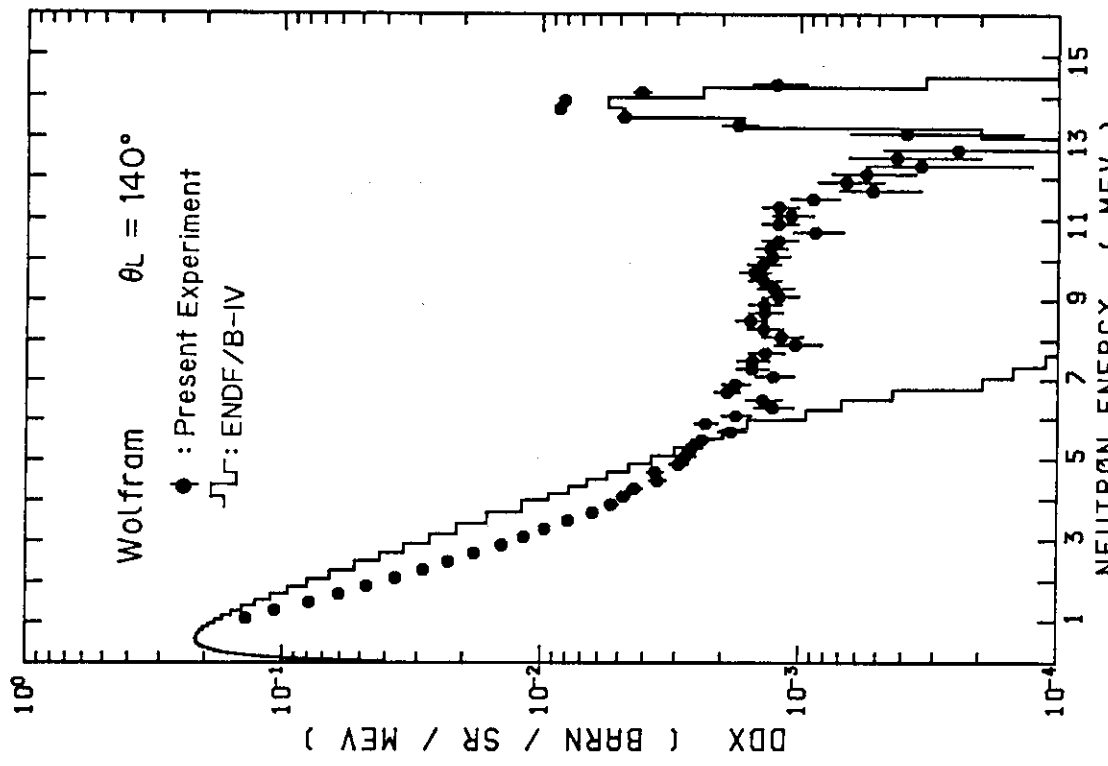

Fig. 61 Double differential neutron emission cross section at 140 deg with En = 14.1 MeV, for W

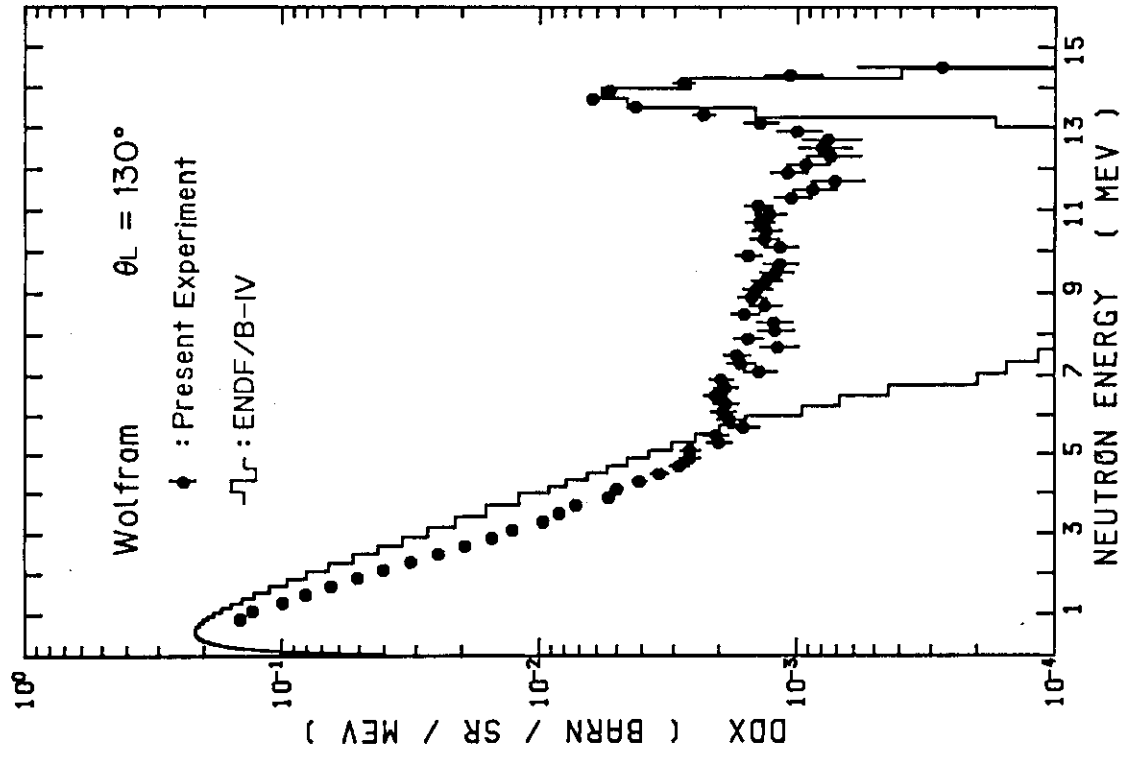

Fig. 60 Double differential neutron emission cross section at 130 deg with En = 14.1 MeV, for W

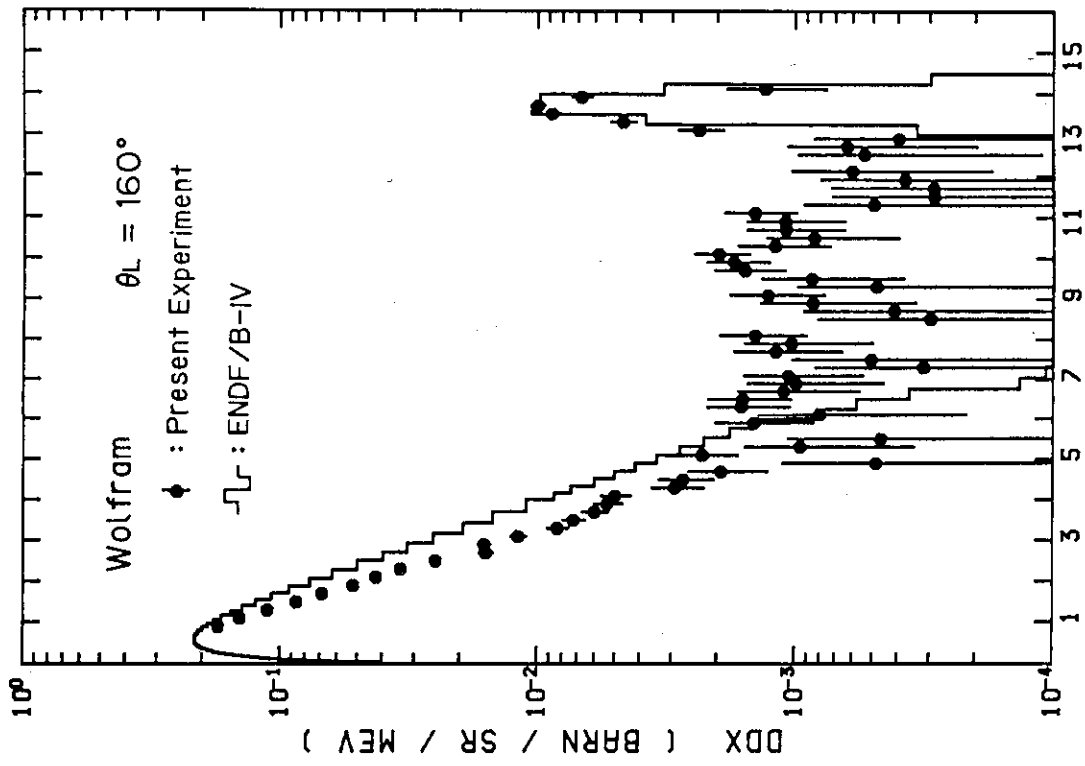

Fig. 63 Double differential neutron emission cross section at 160 deg with En = 14.1 MeV, for W

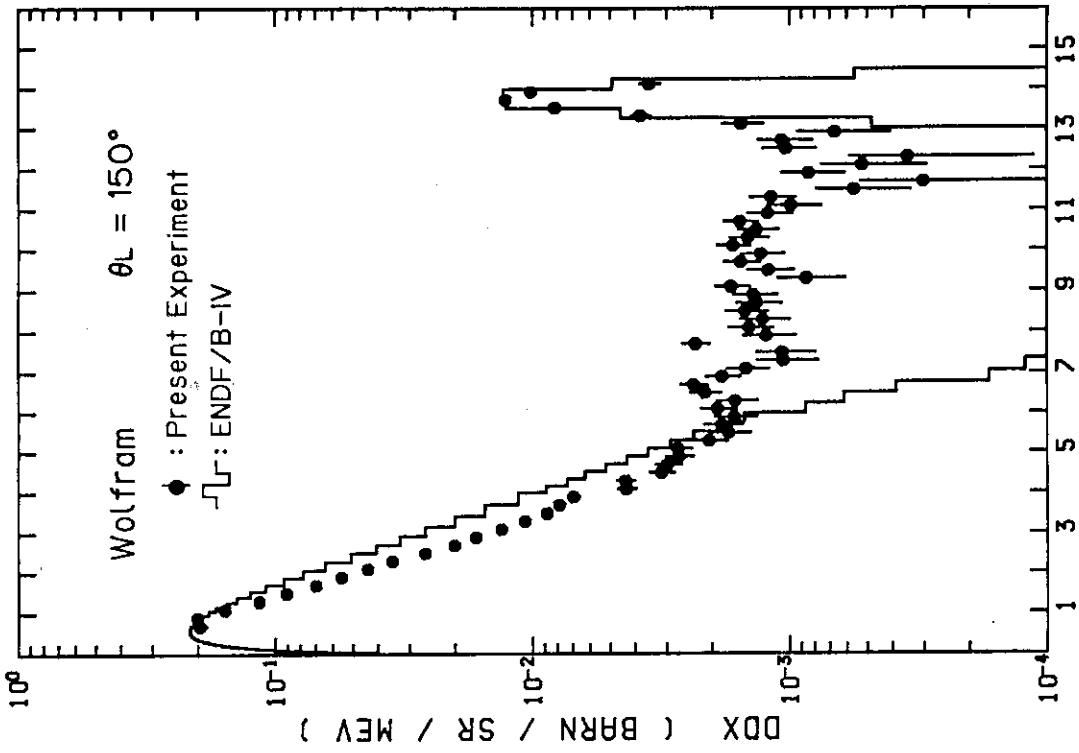

Fig. 62 Double differential neutron emission cross section at 150 deg with En = 14.1 MeV, for W

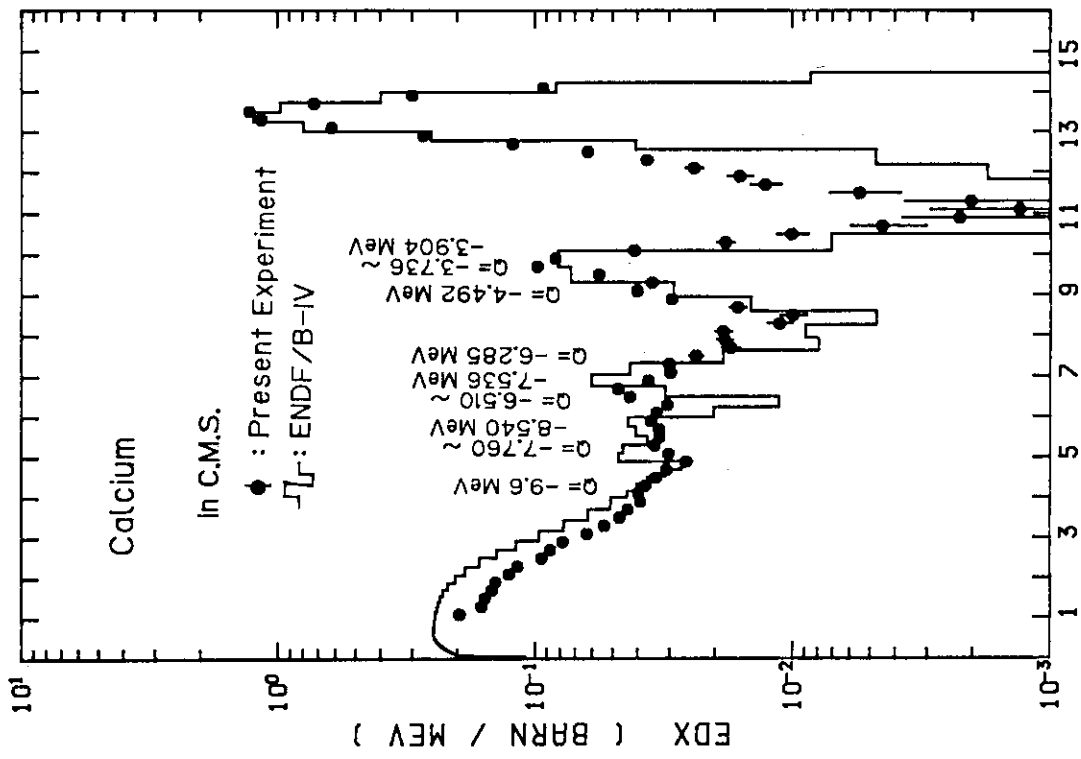

Fig. 65 Angle-integrated neutron emission spectrum in the CM system with En = 14.1 MeV, for Ca

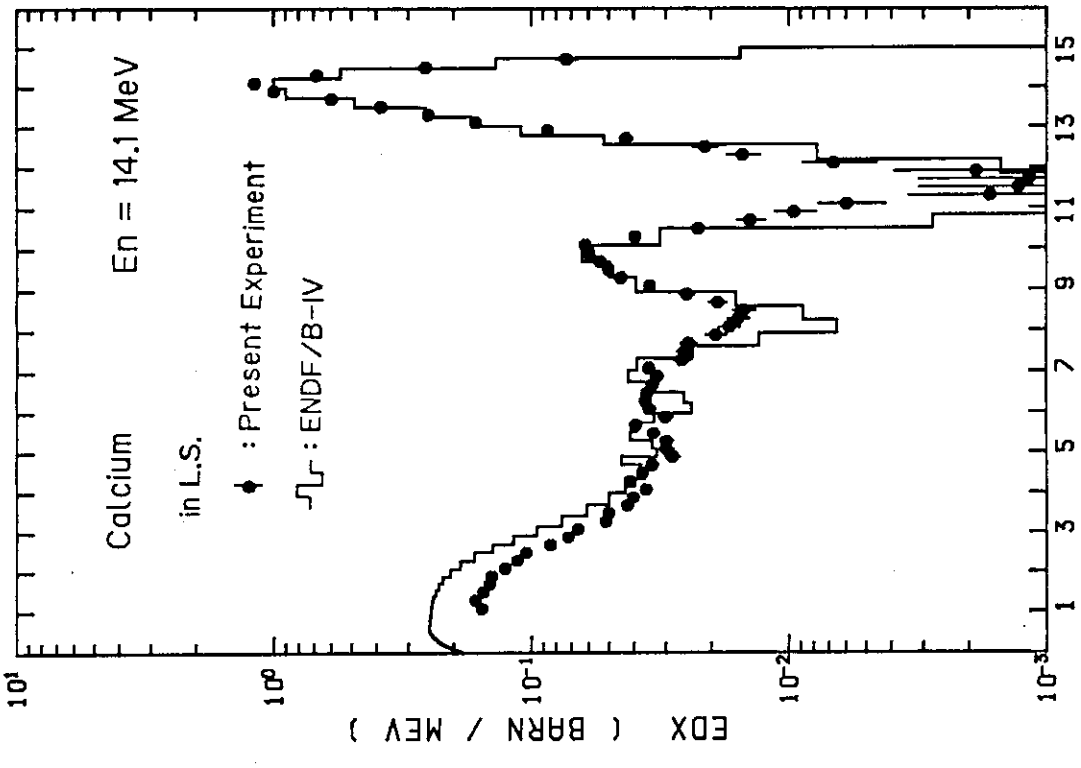

Fig. 64 Angle-integrated neutron emission spectrum in the LAB system with En = 14.1 MeV, for Ca

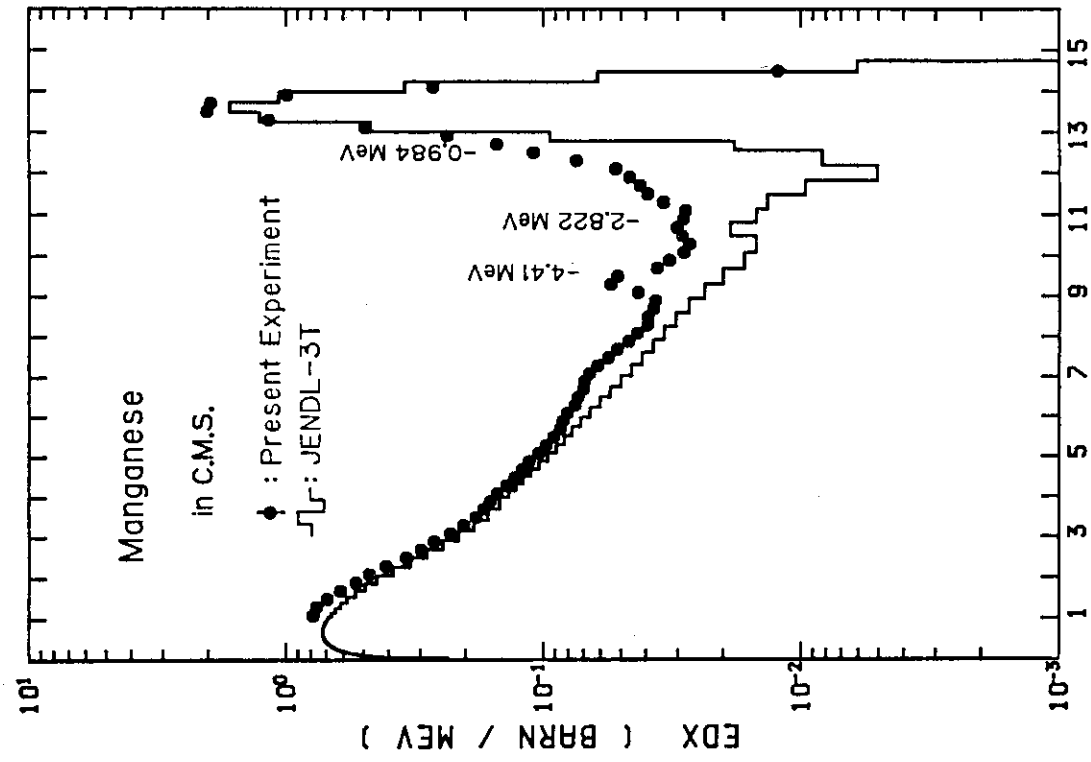

Fig. 67 Angle-integrated neutron emission spectrum in the CM system with En = 14.1 MeV, for Mn

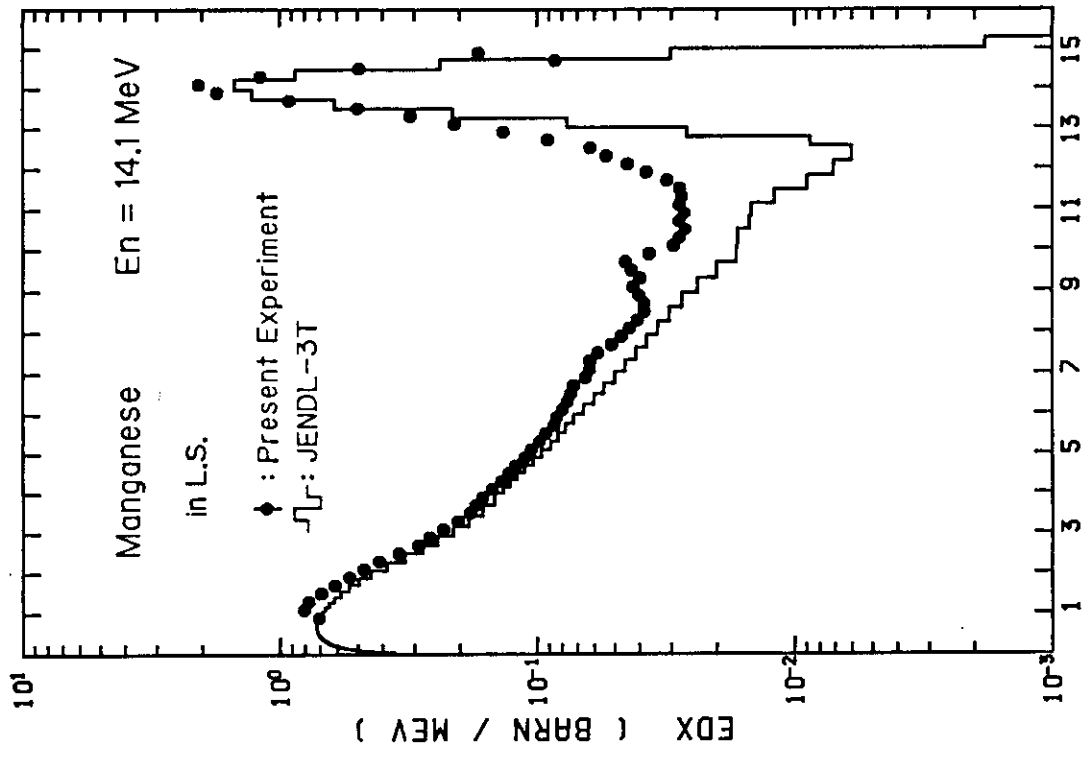

Fig. 66 Angle-integrated neutron emission spectrum in the LAB system with En = 14.1 MeV, for Mn

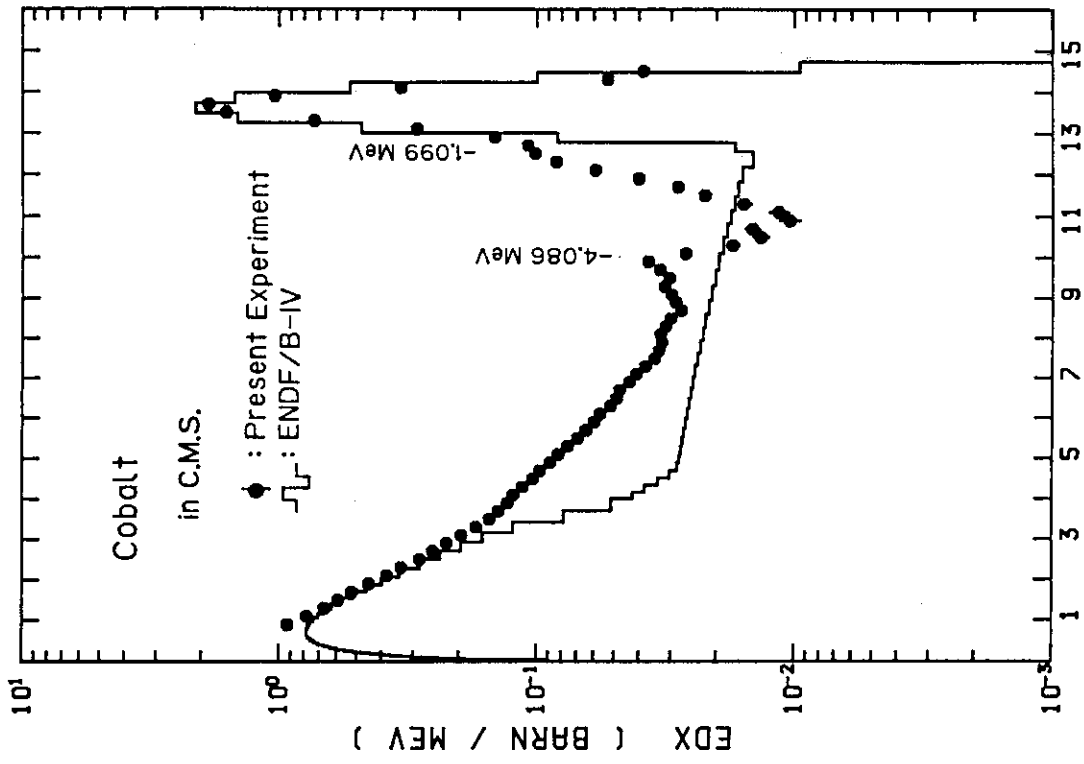

Fig. 69 Angle-integrated neutron emission spectrum in the CM system with En = 14.1 MeV, for Co

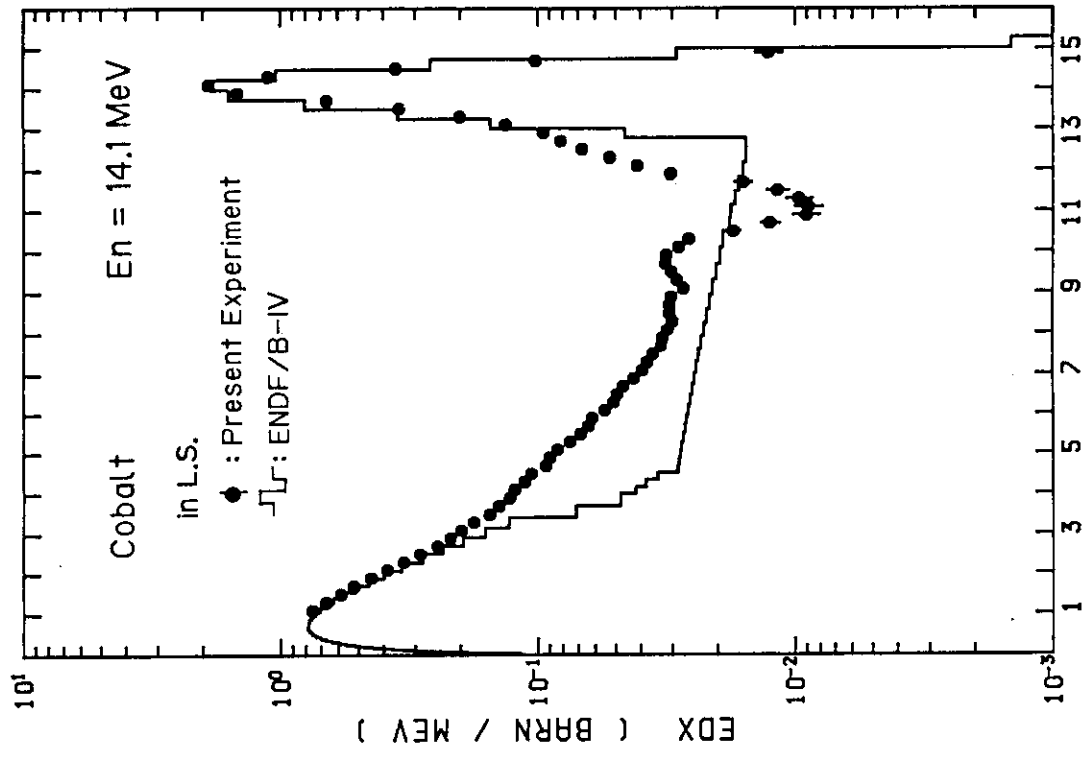

Fig. 68 Angle-integrated neutron emission spectrum in the LAB system with En = 14.1 MeV, for Co

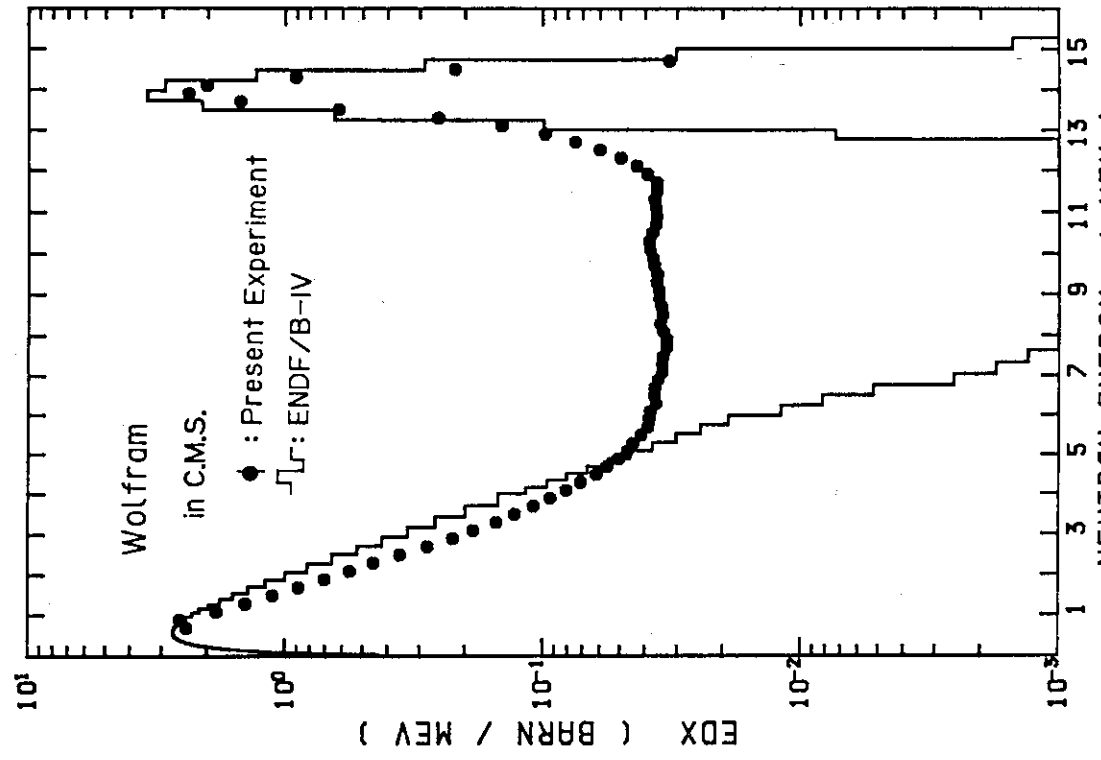

Fig. 71 Angle-integrated neutron emission spectrum in the CM system with En = 14.1 MeV, for W

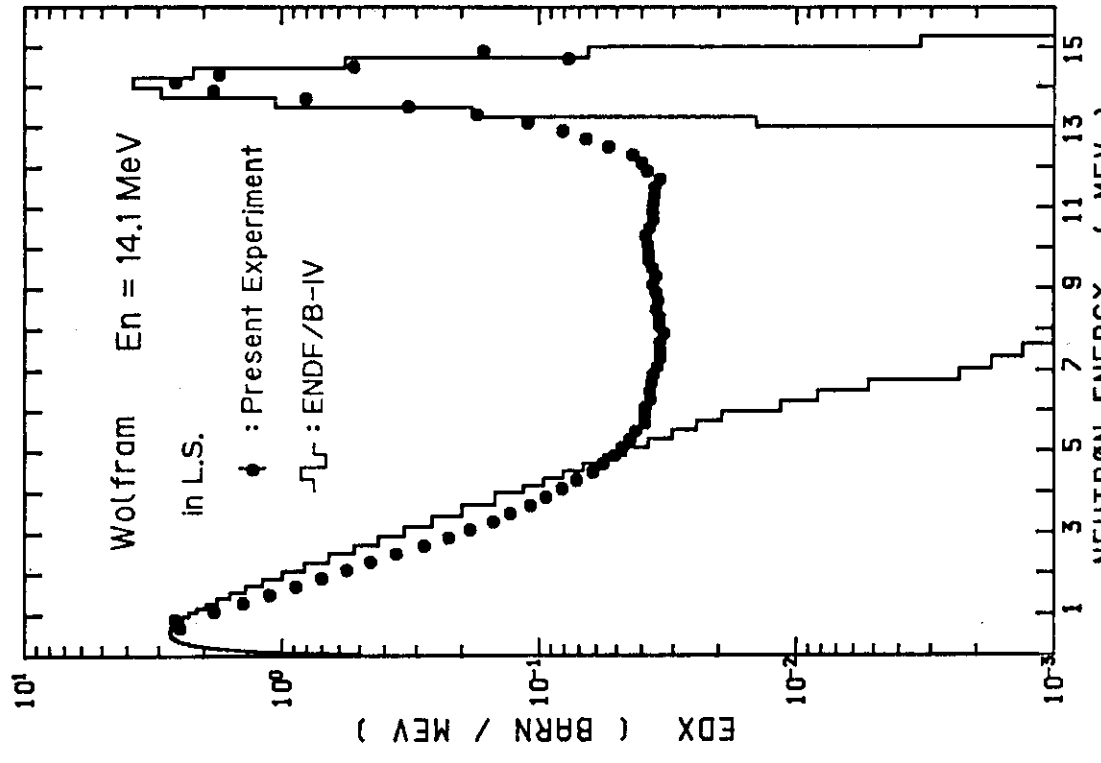

Fig. 70 Angle-integrated neutron emission spectrum in the LAB system with En = 14.1 MeV, for W

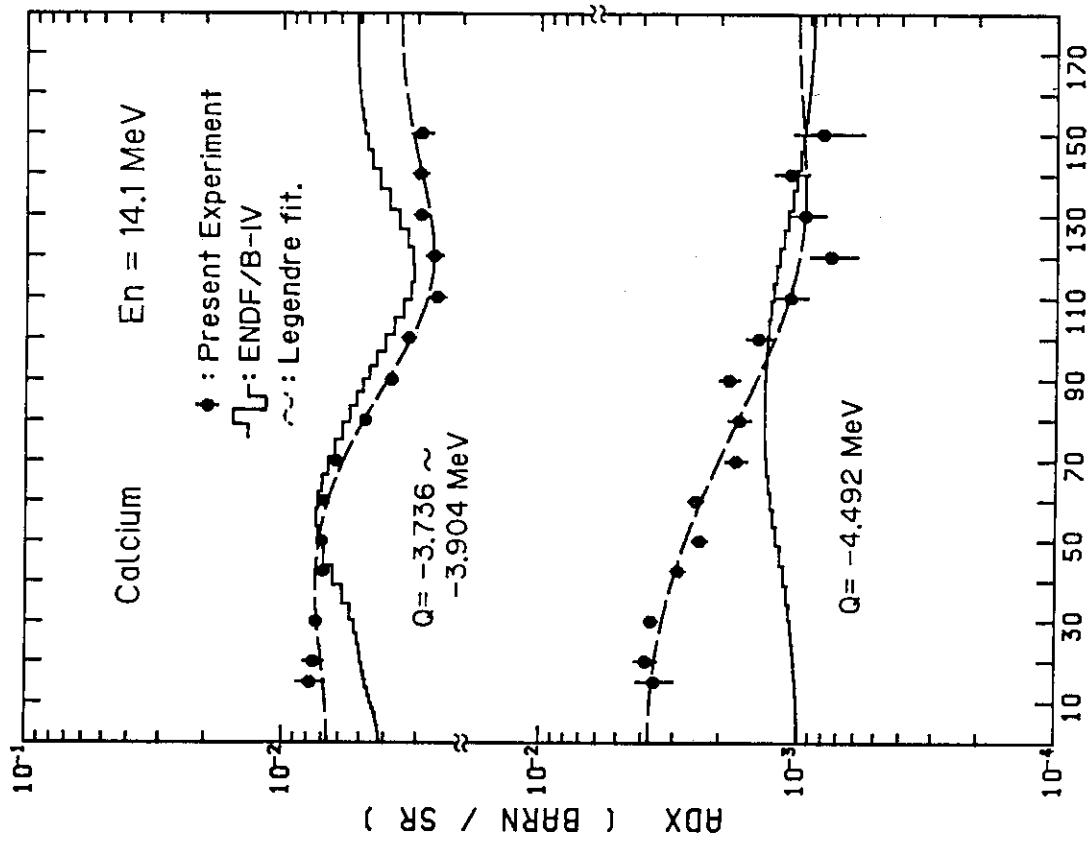

Fig. 73 Differential cross sections of discrete inelastic scattering at En = 14.1 MeV, for Ca

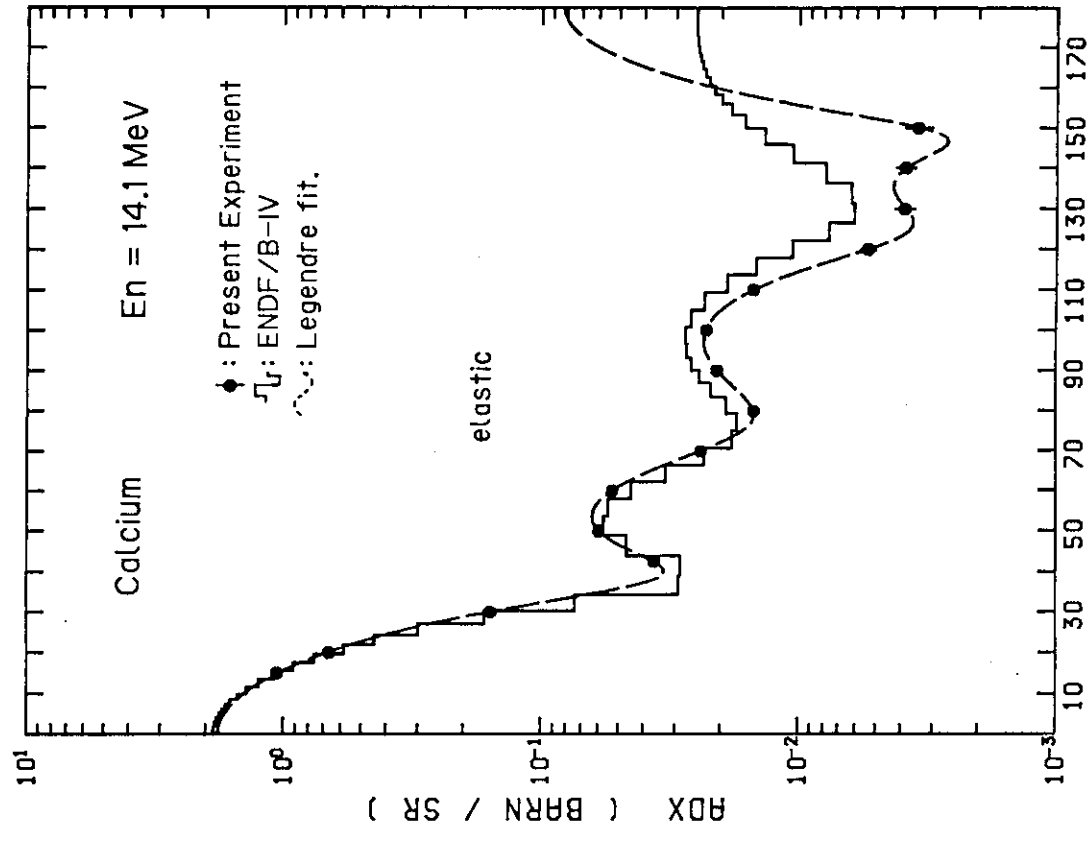

Fig. 72 Differential elastic scattering cross sections at En = 14.1 MeV, for Ca

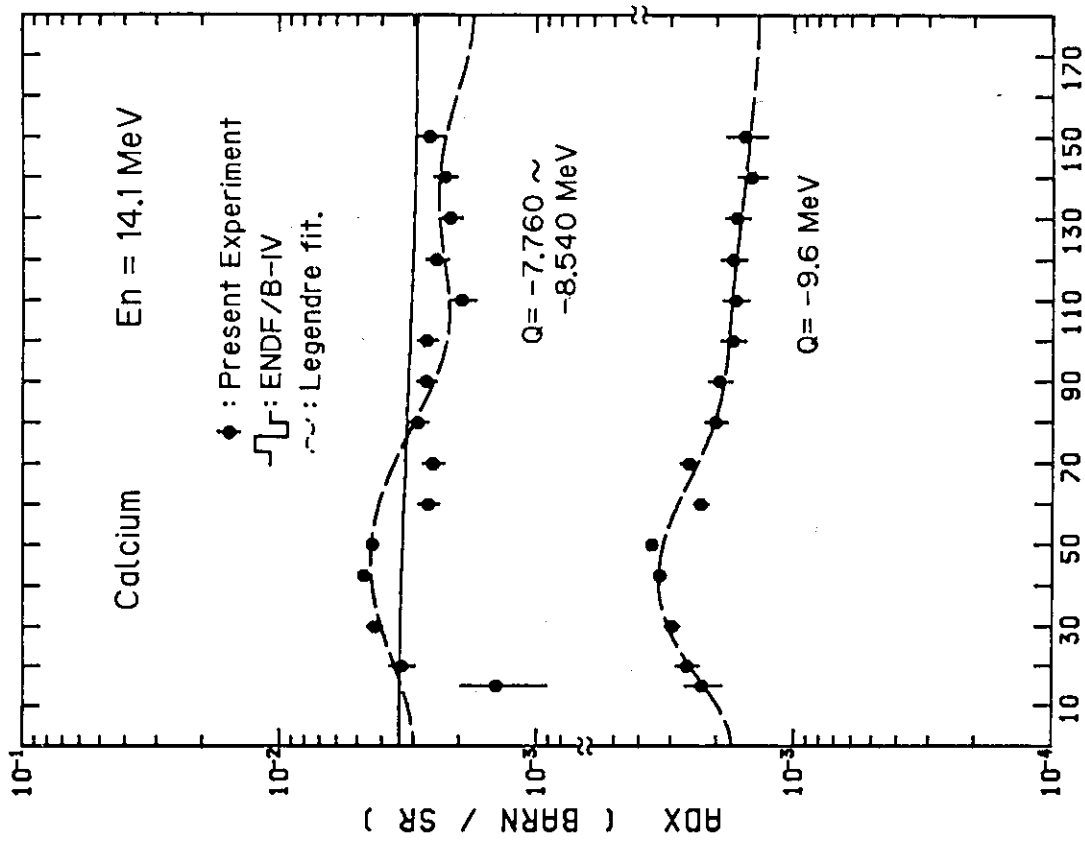

Fig. 75 Differential cross sections of discrete inelastic scattering at En = 14.1 MeV, for Ca

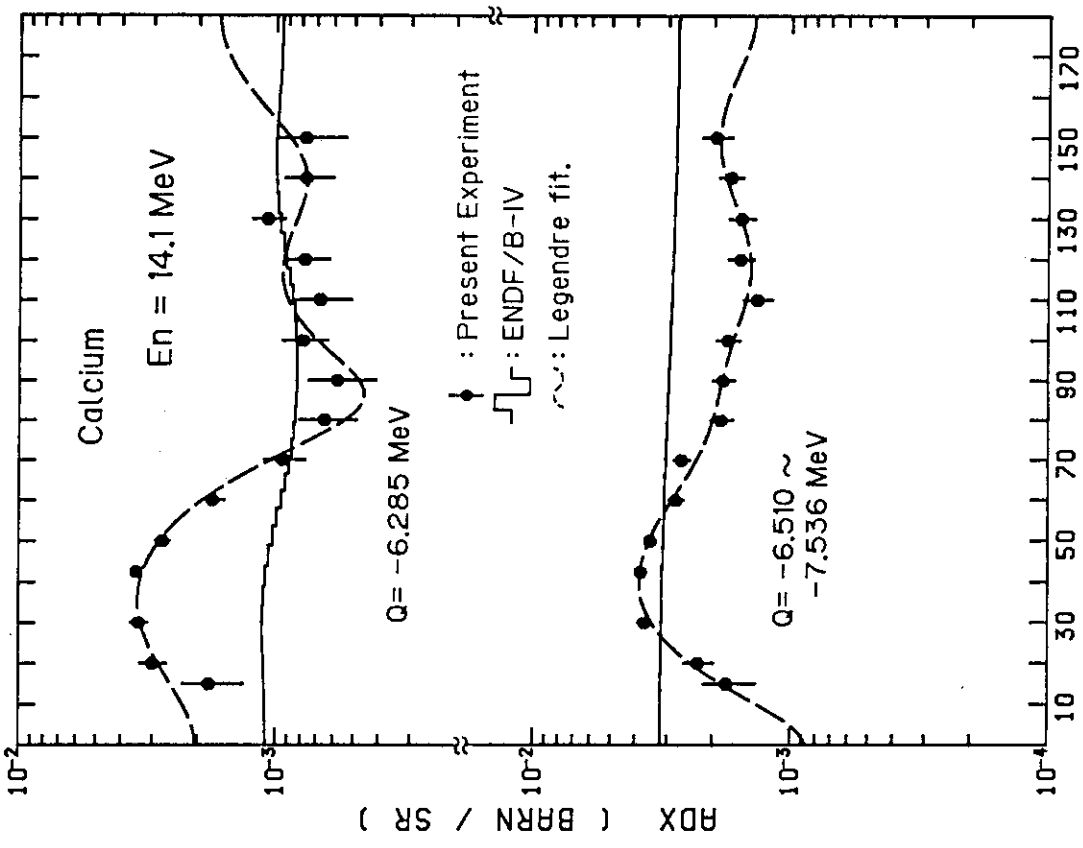

Fig. 74 Differential cross sections of discrete inelastic scattering at En = 14.1 MeV, for Ca

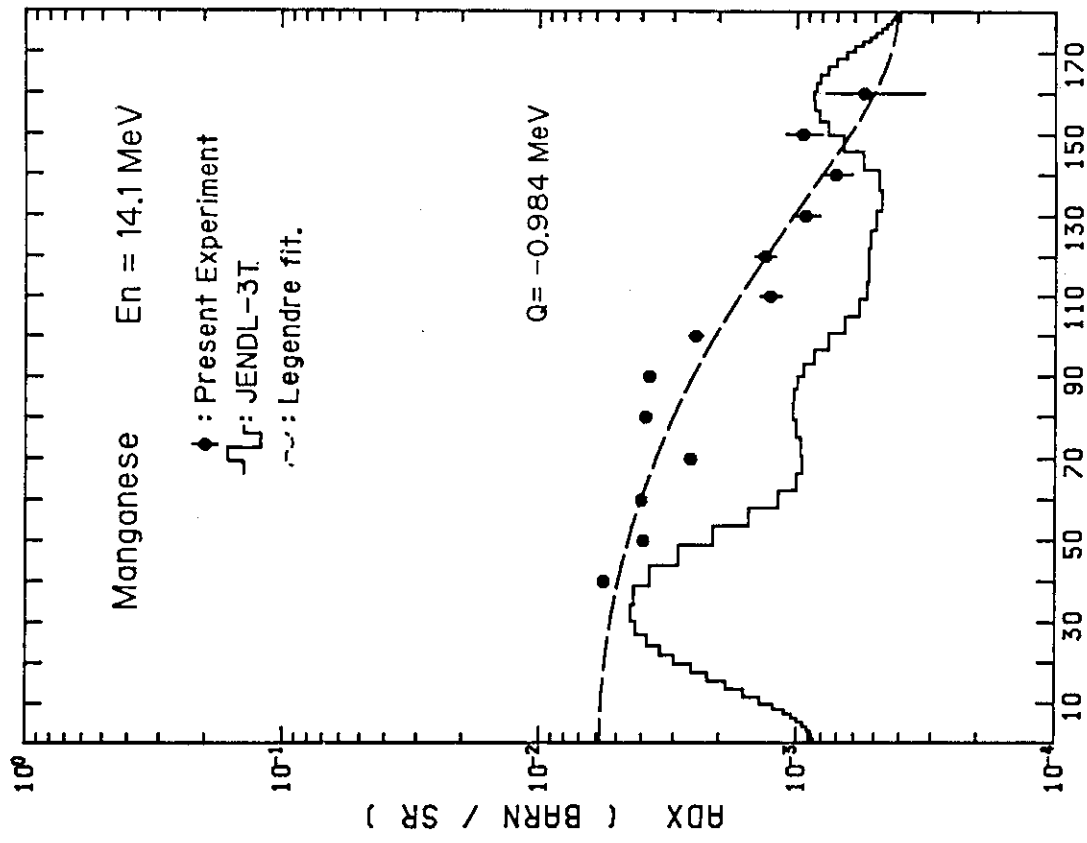

Fig. 77 Differential cross sections of discrete inelastic scattering (0.984 MeV level) at En = 14.1 MeV, for Mn

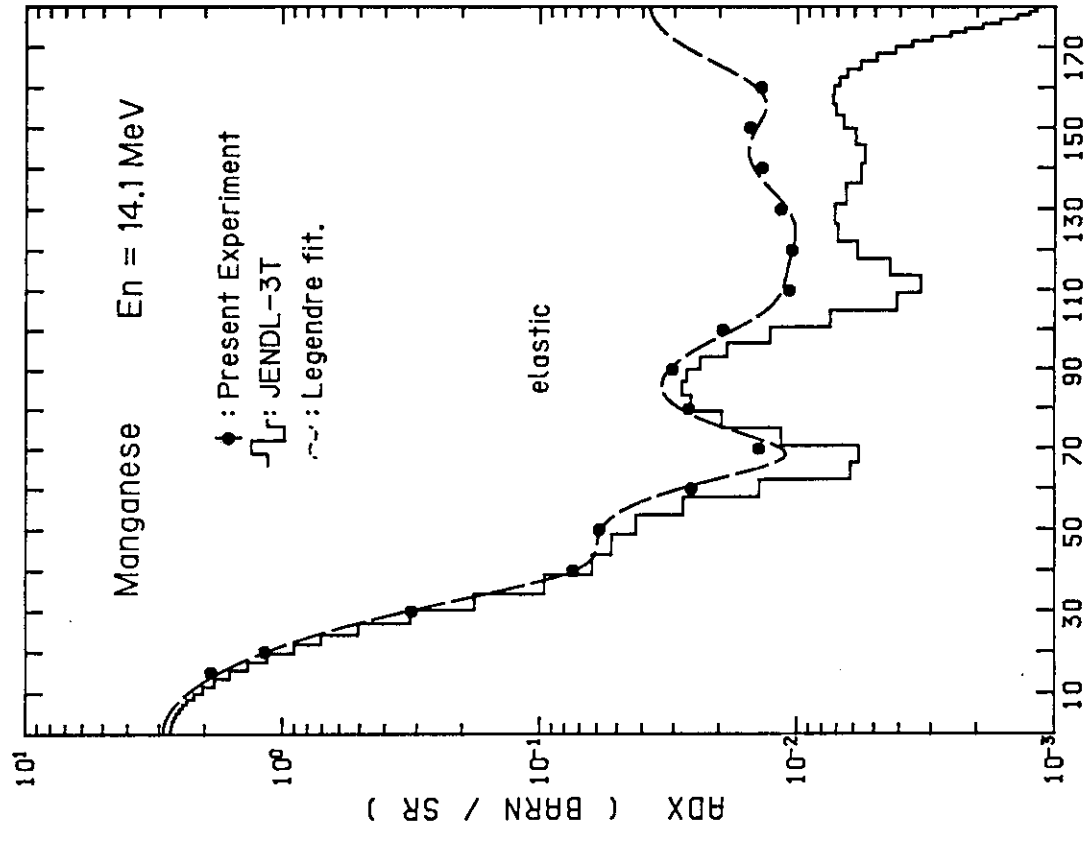

Fig. 76 Differential elastic scattering cross sections at En = 14.1 MeV, for Mn

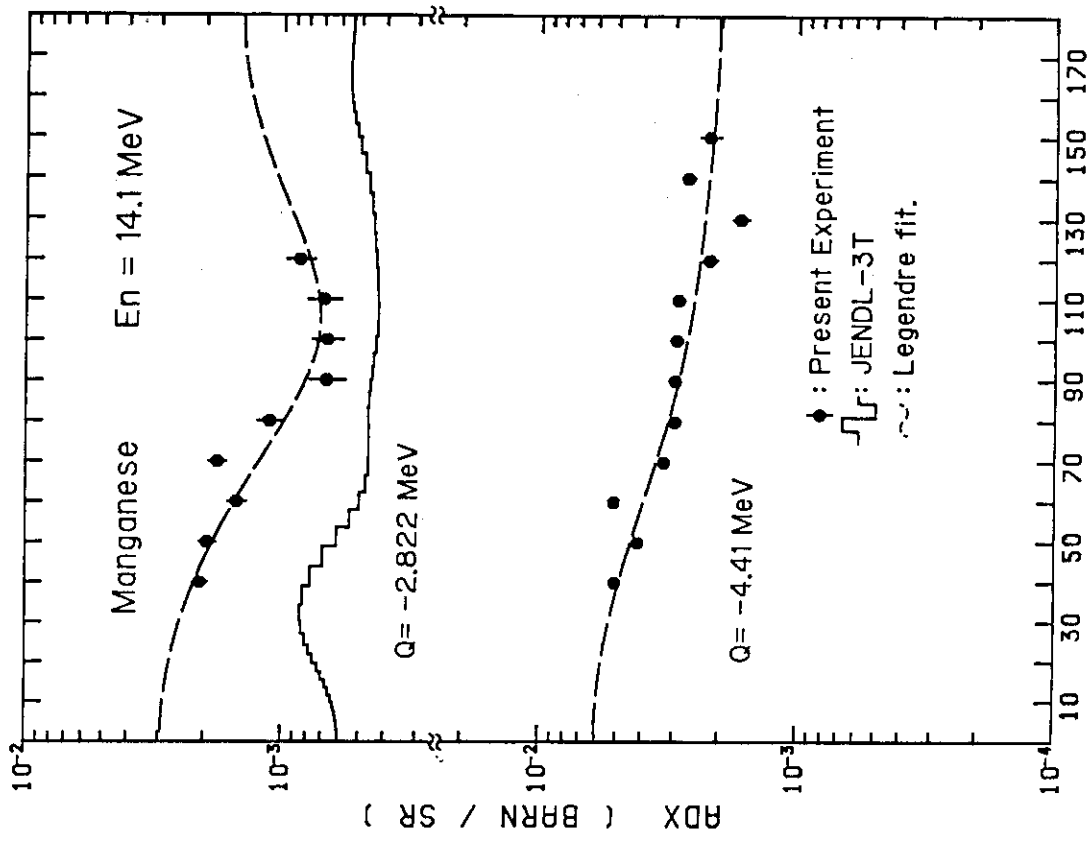

Fig. 78 Differential cross sections of discrete inelastic scattering at En = 14.1 MeV, for Mn

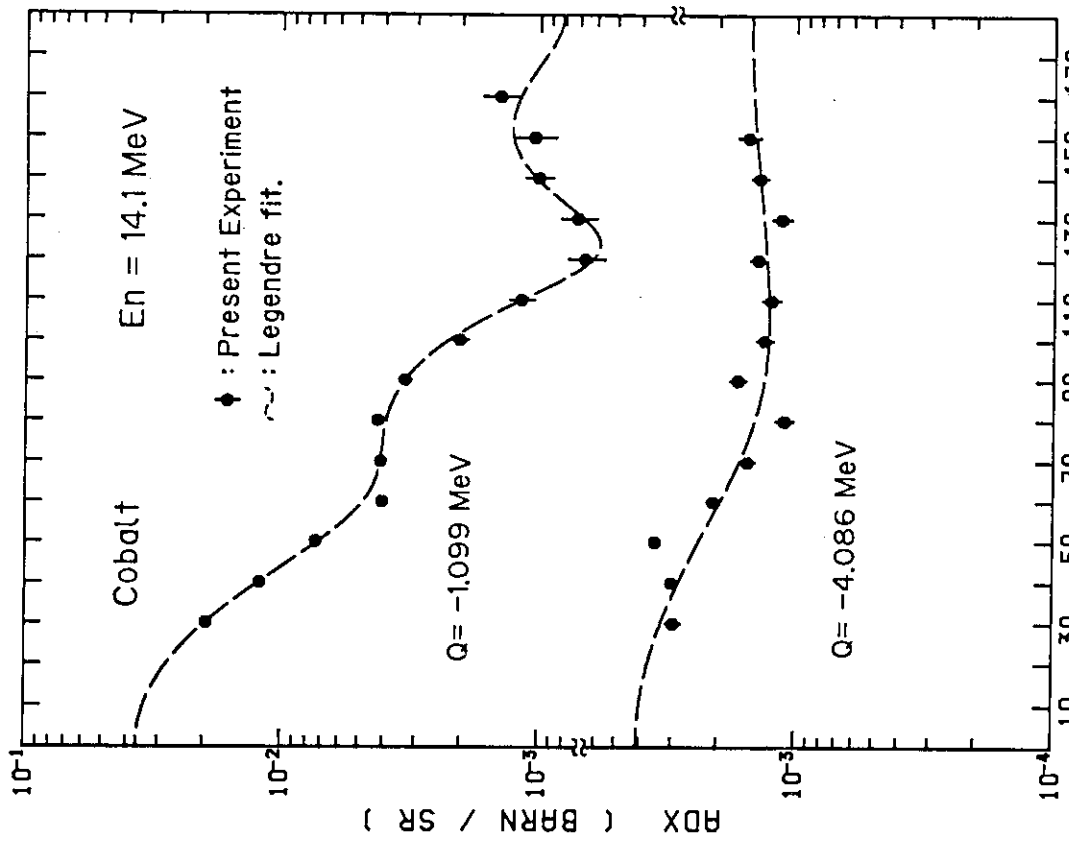

Fig. 80 Differential cross sections of discrete inelastic scattering at En = 14.1 MeV, for Co

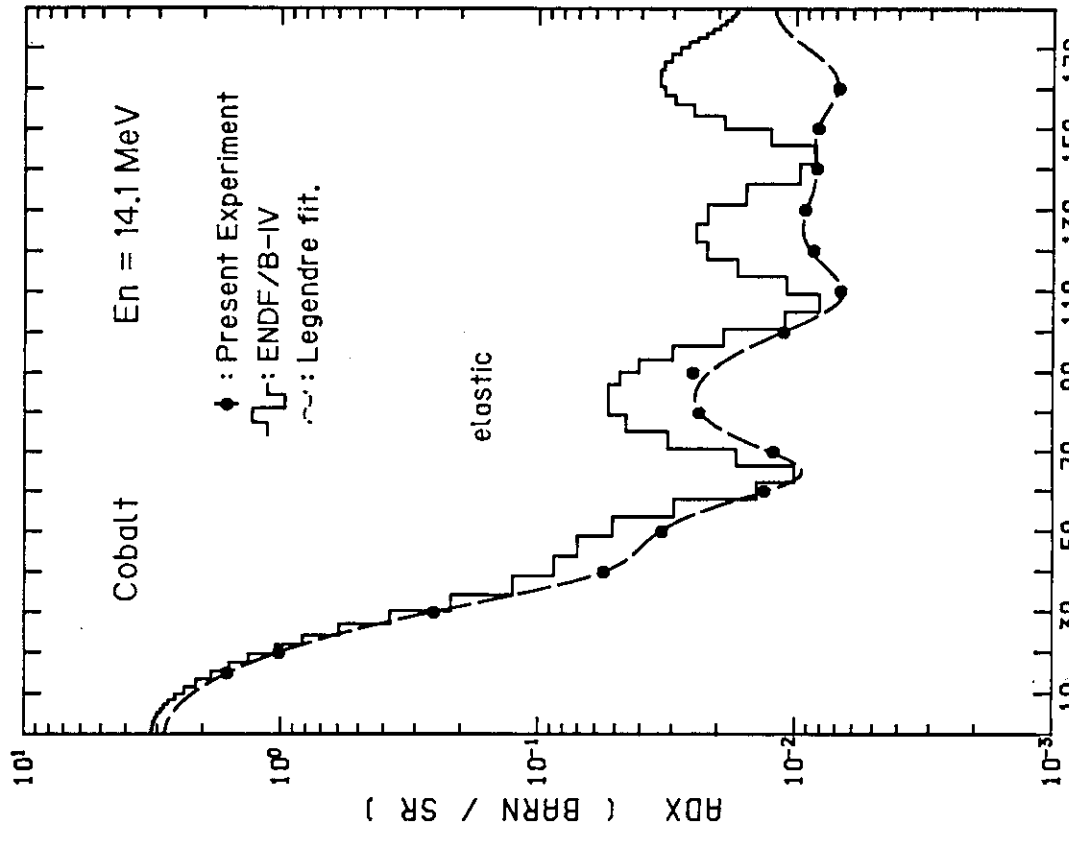

Fig. 79 Differential elastic scattering cross sections at En = 14.1 MeV, for Co

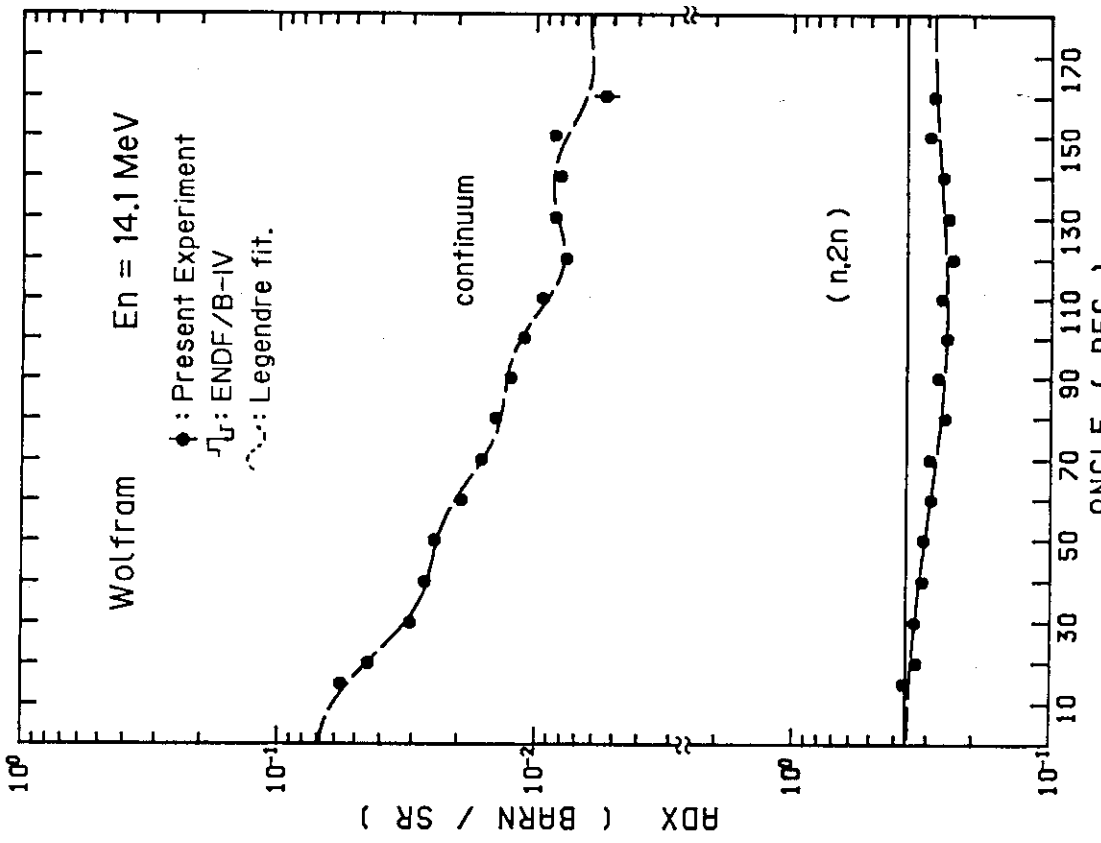

Fig. 82 Angular distributions of continuum-inelastic and (n, 2n) channels with En = 14.1 MeV, for W

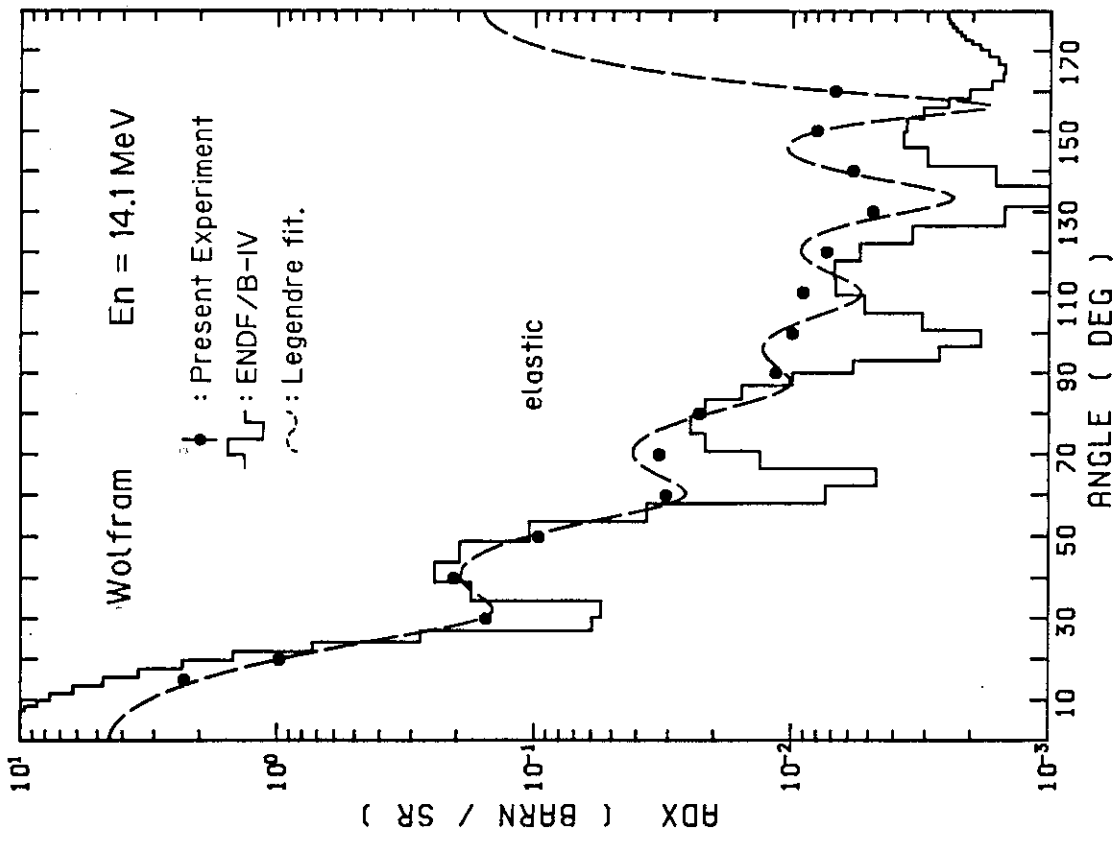

Fig. 81 Differential elastic scattering cross sections at En = 14.1 MeV, for W